Functional analysis of ICAD-S protein and the development of a novel technology for site-specific protein cleavage in vertebrate cells

ALEXANDER VALERY AGEICHIK

A THESIS PRESENTED FOR THE DEGREE OF DOCTOR OF PHILOSOPHY

UNIVERSITY OF EDINBURGH

July 2007

Acknowledgements

I would like to thank Professor Sir Kenneth Murray and the Darwin Trust of Edinburgh for the generous funding of my PhD study.

I am grateful to my supervisor, Professor William C. Earnshaw, for giving me an opportunity to study in his laboratory, his suggestions and advice on my PhD project.

My kind regards are extended to my second supervisor, Dr. Kumiko Samejima, for her dedicated support and advice throughout my PhD study.

I would like to thank all past and presents members of our lab for creating a nice environment in which to work and study: Ana, Damien, Daniel, Fan, Fiona, Hiromi, Liz, Mafalda, Mar, Marcella, Paola, Reto, Sandrine, Sarah, Shinya, Stefano, Susana, Zhenjie and Zuojun.

I am very grateful to Lauren Simpson for proofreading my thesis.

My special thanks go to my mother and father and my two younger brothers, Misha and Yura, for their encouragement and support.

Abbreviations

°C	degrees Celsius
aa	amino acid
AIF	apoptosis-inducing factor
Apaf-1	apoptosis protease-activating factor 1
ASC	apoptosis-associated speck-like protein
ATP	adenosine-5′-triphosphate
BID	BH3 Interacting Domain Death agonist
BH	bcl-2 homology domain
bp	base pairs
BSA	bovine serum albumin
bs	blasticidin
cDNA	complementary DNA
C. elegans	*Caenorhabditis elegans*
c-FLIP	cellular-FLIP
CAD	caspase activated DNAse
cCAD	chicken CAD
cICAD	chicken ICAD
caspase	cysteine-containing, aspartate-specific proteinase
CIDE	cell death inducing DFF45-like effector
CIP	calf intestinal alkaline phosphatase
CPAN	caspase-activated nuclease
DAPI	4′6′-diamidino-2-phenylindole
DD	death domain
DED	death effector domain
DFF	DNA fragmentation factor
DISC	death-inducing signalling complex
DNA	deoxyribonucleic acid
Dox	doxycycline
dNTPs	deoxyribonucleotide-5′-triphosphate
DR	death receptor
DTT	1,4-dithiothreitol
E. coli	*Escherichia coli*
EDTA	ethylenediaminetetraacetic acid
EGTA	ethylene-bis(oxyethylenenitrilo)tetraacetic acid
ERK	extracellular signal-related kinase
ER	endoplasmic reticulum
FADD	Fas associated death domain
FBS	fetal bovine serum
FITC	fluorescein isothiocyanate
FLICE (caspase 8)	FADD-like interleukin-1 converting enzyme
FLIP	FLICE (caspase-8)-inhibitory protein
g	gravity
GFP	green fluorescent protein
GST	glutathione S transferase

h	hour(s)
hCAD	hCAD
HeLa	Henrietta Lacks
HEPES	*N*-[2-Hydroxyethyl]piperazine-*N'*-[2-ethanesulfonic acid]
hICAD	human ICAD
hICAD-L^{2TEV}	human ICAD-L with two TEV protease cleavage sites
hICAD-S^{2TEV}	human ICAD-S with two TEV protease cleavage sites
hICAD-L^{2PRE}	human ICAD-L with two Prescission protease cleavage sites
His	histidinol
His tag	hexa-histidine tag
HMG	high-mobility group
HMW	high molecular weight
IAP	inhibitor of apoptosis protein
ICAD	inhibitor of caspase activated DNAse
ICAD-L	ICAD-Long
ICAD-S	ICAD-Short
JNK	jun N-terminal kinase
kb	kilobase pairs
kDa	kilo Dalton(s)
LB	Luria-Bertani medium
M	Molar, (moles/litre)
MBP	maltose-binding protein
MAP kinases	mitogen-activated protein kinases
min	minutes
mRNA	messenger RNA
mTEV	mutant TEV
NF-κB	nuclear factor kappaB
neo	neomycin
NLS	nuclear localisation signal
NMR	nuclear magnetic resonance
Opa1	optic atrophy 1
ORF	open reading frame
PAGE	polyacrylamide gel electrophoresis
PARL	presenilin-associated rhomboid-like
PARP	poly (ADP-ribose) polymerase
PBS	phosphate buffered saline
PCR	polymerase chain reaction
PIPES	1,4-piperazinediethanesulfonic acid
PTP	permeability transition pore
Puro	puromycin
RIP	receptor interacting protein
RNA	ribonucleic acid
RNAi	RNA interference
RNAse	ribonuclease
RT-PCR	reverse transcriptase PCR
SDS	sodium dodecyl sulphate

SDS-PAGE	SDS-polyacrylamide gel electrophoresis
Smac/DIABLO	second mitochondria-derived activator of caspase/direct IAP binding protein with low pI
TAE	tris-acetate EDTA
tBID	truncated BID
TEV protease	tobacco etch virus protease
tk	thymidine kinase
TNF	tumour necrosis factor
TNFR	tumour necrosis factor receptor
TRADD	TNFR-associated death domain
TRAF2	TNFR-associated Factor 2
TRAIL	TNF-related apoptosis-inducing ligand
Tris	tris (hydroxymethyl) aminomethane
TRIzol	total RNA isolation reagent
UV	ultraviolet
V	volt
v-FLIP	viral-FLIP
wt	wild-type
XIAP	X-chromosome-linked inhibitor of apoptosis protein

List of figures

List of tables

Table of contents

1. Abstract

1. Abstract

Caspases are the main initiators and executors of apoptosis, cleaving more than two hundred different targets in apoptotic cells. The activation of caspases results in the activation of multiple pathways leading to apoptotic cell death.

CAD (Caspase Activated DNAse) exists in a complex with its inhibitor, ICAD, in living cells. The cleavage of ICAD by caspase-3 causes the release of CAD from ICAD. Activated CAD causes internucleosomal (about 200 bp) and large-scale (about 50-200 kb) DNA fragmentation. In addition, CAD is required for the completion of the final chromatin condensation stage, involving the formation of apoptotic bodies.

To study the role of ICAD splice forms ICAD-S and ICAD-L *in vivo* I constructed DT40 cell lines in which the entire coding regions of ICAD or ICAD plus CAD had been deleted. *ICAD*$^{-/-}$ and *ICAD*$^{-/-}$/*CAD*$^{-/-}$ double knockouts lacked both DNA fragmentation and nuclear fragmentation after the induction of apoptosis. I constructed a humanized system in which hICAD-L and hCAD expressed in DT40 *ICAD*$^{-/-}$/*CAD*$^{-/-}$ double knockouts could rescue both DNA fragmentation and stage II chromatin condensation. hICAD-S could not replace hICAD-L as a chaperone for hCAD in these cells. However, caspase-resistant hICAD-S^{2TEV}, where the two caspase-3 cleavage sites were replaced for two TEV sites, did inhibit hCAD activation upon induction of apoptosis *in vivo* and *in vitro*. hICAD-L^{2TEV} was functional as a chaperone for hCAD, which was activated after hICAD-L^{2TEV} cleavage by TEV protease *in vitro* under non-apoptotic conditions. Thus no other inhibitors of CAD exist in these cell-free extracts. Taken together, these observations indicate that ICAD-S may function together with

ICAD-L to prevent inappropriate CAD activation, particularly in cells where ICAD-S is the dominant form of ICAD protein.

Because CAD is a nuclease, it is an attractive potential target for the induction of cell death. This could have a practical application as a strategy for killing cancer cells. The use of CAD as a drug target could be particularly advantageous since CAD is situated at the end of apoptotic pathway, and thus, once activated, CAD may avoid upstream regulatory mechanisms that protect cells against apoptotic stimuli involved in caspase-dependent apoptosis. I constructed a model system based on the ICAD/CAD double knockout to study the possibility that CAD can cause cell death. This system included hICAD-L^{2TEV}:hCAD and TEV protease under the control of an inducible promoter. However, it was not possible to cleave the hICAD-L^{2TEV} protein *in vivo* with TEV protease, despite the fact that it was possible to do so *in vitro*. As an alternative strategy, I used PreScission protease, whose active part is 3C protease originating in human rhinovirus. A cleaved fragment of hICAD-L^{2PRE} protein was detected in DT40 cells expressing PreScission protease. Preliminary data suggest that CAD contributes to cell death in cells expressing hICAD-L^{2PRE}:hCAD and transfected with PreScission protease.

2. General introduction

2.1 Different forms of cell death

Cell death can occur accidentally, or it can be tightly regulated. The process of cell death can be encoded in programmes responsible for controlled execution of the cell a process known as programmed cell death. There are two main pathways in cells operating a programmed cell death mechanism: apoptosis and autophagy (Fig. 2.1). In contrast to programmed cell death, cells can sometimes die as a result of accidental physical or chemical damage, and this is termed necrosis.

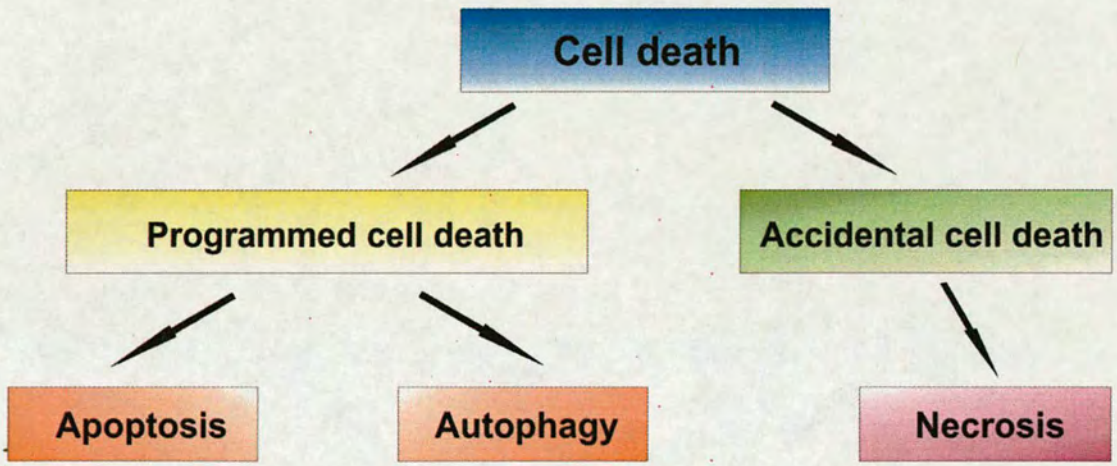

Fig. 2.1. The cell death pathways. Programmed cell death can be accomplished through apoptosis and autophagy mechanisms.

2.1.1 Apoptosis

Apoptosis, a term originating in the Greek word describing leaves falling off a tree (Kerr et al., 1972), is a form of programmed cell death leading to the elimination of useless, damaged or harmful cells in metazoans. It is required to eliminate unnecessary cells during the organism's development and adult life. Apoptosis is used during development to eliminate cells of the immune system that react with the organism's own

antigens (Jacobson et al., 1997; Krammer, 2000). Apoptosis is also activated in cells that have suffered too much damage to continue their function. In addition, cytotoxic T-lymphocytes can induce apoptosis in cancer cells and in virus-infected cells to help eliminate cells that may cause harm to the whole organism. Defects in the apoptotic process can be the cause of cancer, autoimmune and neurodegenerative diseases (Thompson, 1995).

The components of the apoptosis pathway were first identified in the nematode *Caenorhabditis elegans*, where genetic studies revealed the existence of genes required for programmed cell death (Ellis and Horvitz, 1986; Yuan et al., 1993). The genes involved in apoptosis were then identified in mammals and in a wide range of multicellular organisms, including humans (Vaux and Korsmeyer, 1999).

The process of apoptosis can be achieved by the activation of extrinsic & intrinsic pathways that regulate and accomplish the cell death. Apoptosis is defined by characteristic morphological and biochemical features. Morphological features include separation from neighbouring cells, cell shrinkage, loss of microvilli, membrane blebbing, chromatin condensation and formation of apoptotic bodies (Hacker, 2000; Kerr, 1971; Kerr et al., 1972; Wyllie et al., 1980). Inflammation, however, is absent during apoptosis due to the anti-inflammatory interaction between apoptotic cells and macrophages (Gregory and Devitt, 2004).

In addition, distinct biochemical changes occur in cells undergoing apoptosis. A family of cysteine-containing, aspartate-specific proteinases called caspases is a key component of the programmed cell death pathway (Earnshaw et al., 1999; Nicholson and Thornberry, 1997). Activation of the caspase cascade results in the cleavage of

multiple caspase substrates. Caspases directly or indirectly cleave more than two hundred intercellular targets (Degterev et al., 2003; Earnshaw et al., 1999), which results in the degradation of cell components responsible for the maintenance and regulation of homeostasis. Protein degradation, loss of plasma membrane asymmetry, the mitochondrial transmembrane potential dissipation and accumulation of reactive oxygen species plus large-scale and oligonucleosomal DNA fragmentation, are the characteristic biochemical features of apoptosis (Grimsley and Ravichandran, 2003; Hacker, 2000; Wyllie, 1980; Ziegler and Groscurth, 2004). Interestingly, apoptosis can occur without caspases (Lorenzo and Susin, 2004), and caspases can work without apoptosis (Zeuner et al., 1999).

2.1.2 Autophagy

Autophagy is a process of destruction of cellular organelles and parts of cytoplasm in specialized vesicles using the cellular lysosomal system. The destruction of cell organelles can either be a process of organised cellular components turnover, or it can lead to cell death (Levine and Yuan, 2005). Autophagy is characterised by the formation of autophagosomes, large cytoplasmic vesicles bounded by a double membrane (Klionsky and Emr, 2000) that cause the destruction of engulfed cellular components once fused with lysosomes. The process is regulated by multiple molecular mechanisms (Eskelinen, 2005). The destruction allows for the release of the molecules for macromolecular synthesis or for their further processing as an energy source. If the cell is starved for structural components or energy, autophagy can be a survival strategy, as cells with mutations in autophagy-linked genes die early under starvation conditions

(Tsukada and Ohsumi, 1993). Autophagy can also allow for the elimination of damaged organelles or of organelles not required for further cell development (Levine and Klionsky, 2004; Rusten et al., 2004).

In addition to the biochemical features, morphological characteristics of autophagic cell death include multiple vacuolisation and chromatin condensation. In the end, the cells are engulfed by macrophages, and no inflammation develops (Bursch, 2001; Clarke, 1990).

2.1.3 Necrosis

By contrast to the programmed cell death mechanisms described above, necrosis is an accidental event of cellular damage by physical or chemical factors. Necrosis is characterised by the rupture of cell and organelle membranes, mitochondrial swelling and disintegration of the nucleus, sometimes with initial chromatin condensation. Unlike programmed cell death, necrosis leads to an inflammatory response. (Wyllie et al., 1980; Ziegler and Groscurth, 2004). Interestingly, even if necrotic cell death is accidental, under specialised circumstances, some molecular mechanisms shared with the programmed cell death pathways can be involved in necrosis once it is initiated (Festjens et al., 2006).

2.2 Cellular pathways of apoptosis

Apoptosis can be activated in cells in response to outside stimuli through the death receptor pathway, or, alternatively, it can be initiated as a result of intrinsic cellular signals through the mitochondrial pathway (Hengartner, 2000). Modulation

exists between both pathways to ensure that the cell death activation mechanism is under tight control.

2.2.1 Death Receptor pathway of caspase activation

The death receptor pathway can activate apoptosis in response to extracellular ligands (Ashkenazi and Dixit, 1998). Death receptors (DR) belong to the Tumour Necrosis Factor (TNF) superfamily (Smith et al., 1994), which has eight members (Lavrik et al., 2005). They are situated in the cell membrane and have extracellular and cytoplasmic domains (Smith et al., 1994); appropriately, a portion of the cytoplasmic domain is also termed the "death domain" (Tartaglia et al., 1993). The two most extensively characterized receptors are Fas/CD95 (DR2) and Tumour Necrosis Factor Receptor 1 TNFR1/DR1 (Ashkenazi and Dixit, 1998; Krammer, 2000) (Nagata, 1997); their ligands are FasL and TNF, respectively. Other death receptors include: DR3, TRAILR1 (DR4), TRAILR2 (DR5), DR6, EDAR and NGFR (Lavrik et al., 2005).

Fas receptor signalling

FasL/CD95 is a protein, which was initially identified to be expressed on the surface of cytotoxic T-lymphocytes after their activation to initiate the killing of target cells (Li et al., 1998b). Upon FasL binding, Fas receptor forms stable trimeric aggregates (Fig. 2.2). This results in the aggregation of its cytoplasmic death domains (DD), which in turn bind to the death domains of the Fas-associated Death Domain (FADD) protein (Boldin et al., 1995; Chinnaiyan et al., 1995; Kischkel et al., 1995), triggering the formation of the Death-Inducing Signalling Complex (DISC) (Medema et al., 1997). FADD, in addition to having a death domain, also has death effector domains (DED).

During the DISC complex formation, FADD's DED unmasks and recruits the DED of procaspase-8/FLICE (FADD-like interleukin-1 converting enzyme) (Medema et al., 1997; Muzio et al., 1996).

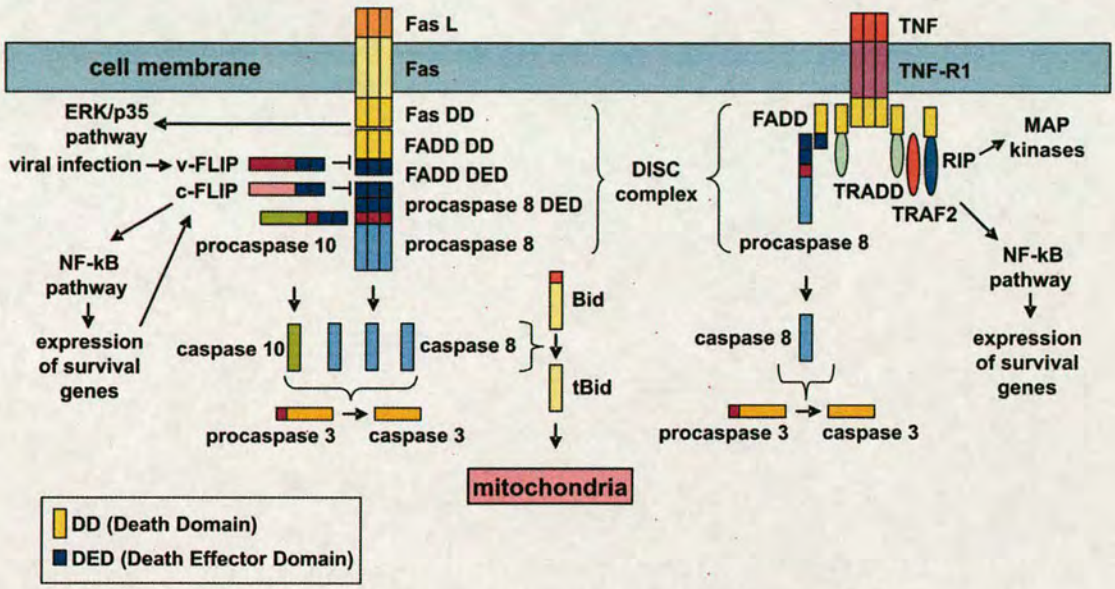

Fig. 2.2. Death receptor pathway of apoptosis activation in mammalian cells. Activation of death receptors Fas or TNF-R1 occurs through trimerization by their ligands, FasL or TNF, respectively. This results in the formation of the DISC complex, which consists of death receptor, FADD, procaspase 8 or adaptor molecule TRADD. The involvement of procaspase-10 is debatable. The dimer of procaspase-8 or procaspase-10 cleaves and activates itself in the DISC complex. Caspase-8 or caspase-10 then cleaves procaspase-3 leading to its activation. tBid transfers apoptotic signals from the cell surface to the mitochondria. In addition to their apoptotic function, death receptors can modulate survival pathways and genes.

In the DISC, procaspase-8 molecules are grouped together. The key element of procaspase-8 activation is a dimer formation in the DISC complex (Boatright et al., 2003; Chen et al., 2002), which results in the cross-cleavage of procaspase-8 molecules (Chang et al., 2003). Once a small amount of procaspase-8 is cleaved, the activated caspase-8 amplifies the signal by cleaving the rest of the procaspase-8 molecules (Muzio et al., 1998; Salvesen and Dixit, 1999). Activation of caspase-8 causes the cleavage of

procaspase-3 and other downstream targets, thereby amplifying pathways leading to apoptotic cell death. In addition to caspase-8, caspase-10 has been also proposed to have a role in initiating cell death receptor pathways. Caspase-10 is homologous to caspase-8 and can be activated in a DISC complex (Kischkel et al., 2001; Wang et al., 2001). While caspase-10 can initiate apoptosis in the absence of caspase-8 (Milhas et al., 2005), the extent of caspase-10 activation in the absence of caspase-8 and its functional role remains controversial (Sprick et al., 2002).

In addition to its apoptotic function, CD95/Fas can also modulate survival signals (Lavrik et al., 2007). Expression of CD95 and CD95L was found during brain development (Park et al., 1998; Shin et al., 2002). Fas signalling can activate the extracellular-signal regulated kinase ERK/p35 pathway and promote branching of growing neurons (Desbarats et al., 2003; Zuliani et al., 2006). The modulation of survival signals can be also operated through c-FLIPs proteins, as described below.

TNFR signalling

TNFR1, following binding by its ligand TNF, operates in a way similar to Fas/FasL through trimerization to activate caspase-8, or alternatively, the NF-κB signalling cascade. TRADD (TNFR-associated Death Domain) is an adaptor molecule used in the TNFR1 pathway (Hsu et al., 1995); it associates with the death domains of TNFR1 upon its activation, and also with FADD, TRAF2 (TNFR-associated Factor 2) (Hsu et al., 1996b) and RIP (Receptor interacting protein) (Hsu et al., 1996b; Ting et al., 1996). TRADD facilitates the binding of FADD to form the DISC complex and activation of the caspase cascade. Alternatively, it can also bind TRAF2, which, together with RIP, activates the NF-κB signalling cascade and promotes cell survival (Hsu et al.,

1996b) (Hsu et al., 1996a). The NF-κB pathway induces proinflammatory and immunomodulatory genes following TNF stimulation (Tartaglia and Goeddel, 1992), and regulates the expression of molecules involved in the immune response, immune cell development and apoptosis (Ghosh and Karin, 2002; Karin and Lin, 2002). The RIP family of kinases can also activate MAP (Mitogen-activated protein) kinases (Meylan and Tschopp, 2005), which are involved in the regulation of gene expression in response to extracellular stimuli (Turjanski et al., 2007).

Inhibiting death receptor activation

c-FLIPs (cellular FLICE inhibitory proteins) can inhibit the activation of apoptosis at the DISC complex (Krueger et al., 2001; Tschopp et al., 1998). Three c-FLIP splice forms have been identified: c-$FLIP_S$, c-$FLIP_L$ and c-$FLIP_R$ (Golks et al., 2005; Irmler et al., 1997). These proteins have two DED domains and structurally resemble procaspase-8. Their DED domains allow c-FLIPs to interact with the DED domains of FADD and procaspase-8 and disrupt their association, thus preventing apoptosis (Tschopp et al., 1998). c-FLIPs can inhibit a wide range of death receptor signalling receptors, including Fas and TNFR1 (Irmler et al., 1997). Interestingly, c-FLIPs have viral counterparts, v-FLIPs, which interact with FADD to prevent procaspase-8 activation. They work to inhibit apoptosis during viral infection, thus providing viruses an opportunity to escape the host's defence mechanisms (Thome et al., 1997). Finally, beyond their anti-apoptotic function, c-FLIPs can stimulate the activation of the NF-κB signalling cascade (Golks et al., 2006; Hu et al., 2000), thus providing one more mechanism for cells to use external stimuli either to induce cell death or to modulate their development. In addition, activation of the NF-κB signalling pathway results in the

expression of more c-FLIP, thus providing a greater anti-apoptotic effect (Kreuz et al., 2001).

Transferring of apoptotic signals from the cell surface to the mitochondria

The death receptor pathway can induce apoptosis in cooperation with the mitochondria through the action of caspase-8 and tBID (truncated BH3 Interacting Domain Death agonist) (Li et al., 1998a; Wang et al., 1996). This shunt can be initiated by small amounts of caspase-8 becoming active during membrane receptor stimulation. After its activation by FADD, caspase-8 can cleave BID, causing the formation of tBID. BID has a cytoplasmic localization, but after cleavage, tBID is associated with mitochondria (Gross et al., 1999b; Li et al., 1998a). As a result, the mitochondrial pathway of apoptosis is activated, leading to the release of cytochrome c. This pathway can be utilised if the stimulation of death receptors is insufficient for the direct activation of the caspase cascade (Scaffidi et al., 1998; Scaffidi et al., 1999).

2.2.2 Mitochondrial pathway of caspase activation

Internal and external stimuli converge on the mitochondria, causing the activation of caspase-dependent or caspase-independent apoptotic cell death pathways. These are thought to operate through apoptogenic factors released from the mitochondria to the cytoplasm, a process controlled by pro-apoptotic and anti-apoptotic proteins (Fig. 2.3).

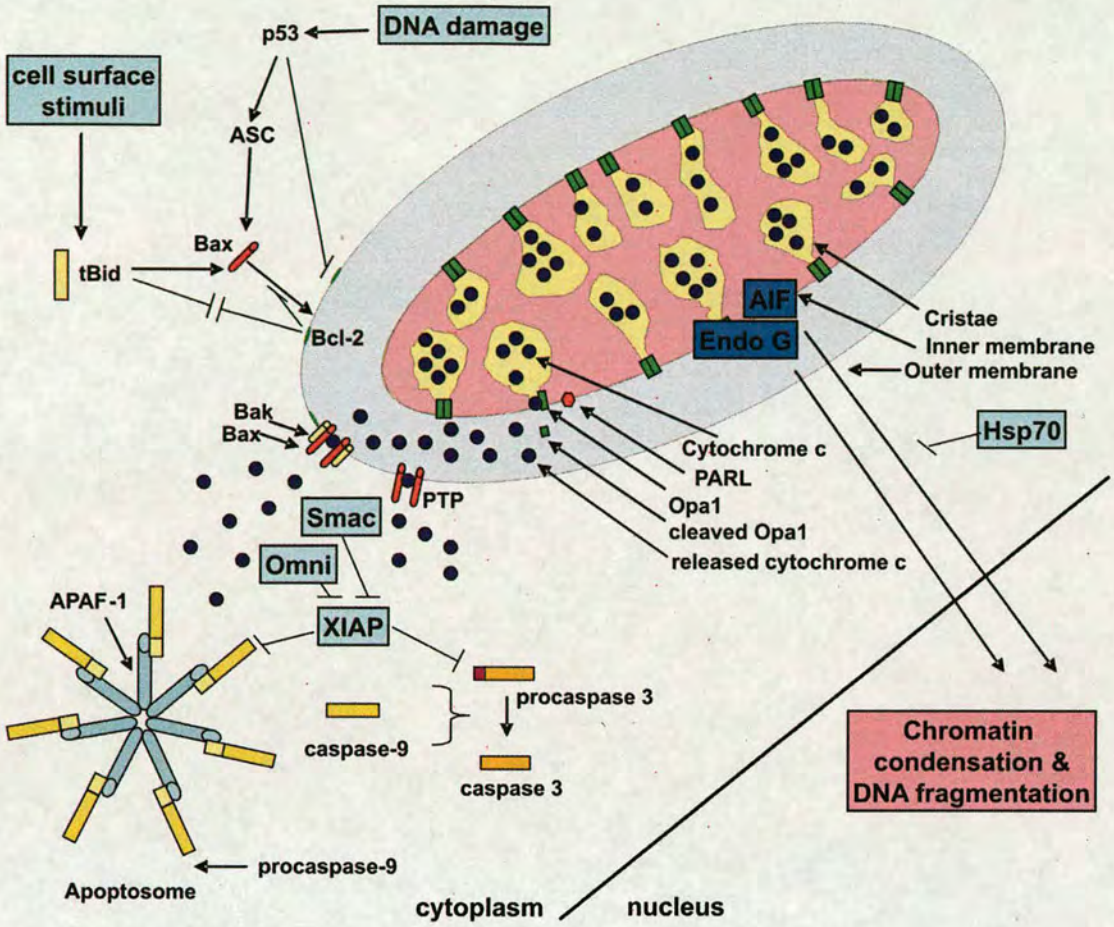

Fig. 2.3. Mitochondrial pathway of cell death. Multiple stimuli, including DNA damage and signals from the outer surface, can activate the mitochondrial pathway of cell death. This activation is modulated by pro-apoptotic and anti-apoptotic proteins. These have been proposed to control mitochondrial pathway activation through the formation of a pore complex containing Bax and Bak, which are required for the release of apoptogenic factors from the mitochondria. Alternatively, apoptogenic factors can be released through the PTP (permeability transition pore). Cytochrome c resides in the intra-cristae compartment, where its release is controlled by the cleavage of Opa1. Once released from the cristae and the mitochondrial outer membrane, cytochrome c initiates the formation of apoptosome consisting of seven Apaf-1 and procaspase-9 molecules. Activation of caspase-9 occurs in apoptosome. Active caspase-9 then cleaves and activates procaspase-3. XIAP can prevent the activation of caspases, and therefore, either Smac or Omni is required to eliminate XIAP function. Caspase-independent apoptosis can occur without caspases through the release of AIF and endonuclease G from the mitochondria and their subsequent translocation to the nucleus.

The key component of caspase-dependent apoptosis, which involves the activation of the caspase cascade, is the release of cytochrome c from mitochondria. To leave the mitochondria, cytochrome c needs to get through the outer mitochondrial membrane, a process regulated by pro-apoptotic and anti-apoptotic proteins. Mitochondria also control caspase-independent apoptosis through the release of Apoptosis inducing factor (AIF) and other factors.

Mitochondria possess Bcl-2 family proteins that can modulate the release of apoptogenic factors through the outer mitochondrial membrane, and thus the initiation of apoptosis. They share a different number of conserved motifs termed BH (Bcl2 homology) domains, and according to this and to their functions, are classified as pro-apoptotic, anti-apoptotic and BH3 only pro-apoptotic proteins (Adams and Cory, 1998; Letai et al., 2002).

Pro-apoptotic proteins

Pro-apoptotic proteins have three BH domains (1-3). Pro-apoptotic proteins Bax and Bak could cause the release of apoptogenic factors by forming a pore complex in the outer mitochondrial membrane (Wei et al., 2001). To form a pore complex, Bax is transported from cytosol into the mitochondrial outer membrane (Wolter et al., 1997). The hypothesis of pore formation is still controversial, however, as it has also been suggested that Bax can modulate outer mitochondrial membrane permeability by destabilising lipid bilayers (Basanez et al., 2002) (Lucken-Ardjomande and Martinou, 2005; Zamzami and Kroemer, 2003).

Interestingly, in the Bax/Bak double knockout, it was still possible to induce apoptosis after certain apoptotic stimuli (De Marchi et al., 2004; Scorrano et al., 2003).

In this case, mitochondrial membrane permeability appears to be regulated via the permeability transition pore (PTP). Ca^{2+} modulates the PTP opening in response to apoptotic stimuli (Crompton, 1999; Szalai et al., 1999).

Anti-apoptotic proteins

Anti-apoptotic proteins have four BH domains (1-4). The most well characterised anti-apoptotic proteins are Bcl-2 and Bcl-x_L (Gross et al., 1999a; Yang et al., 1997). Anti-apoptotic proteins can prevent the release of cytochrome c and the initiation of apoptosis, possibly by preventing the formation of the Bax and Bak pore complex (Yi et al., 2003). The exact nature of how anti-apoptotic proteins prevent the release of cytochrome c remains unclear, but one possible mechanism may involve the sequestering of pro-apoptotic proteins and other components required for the formation of the pore complex (Cheng et al., 2001; Yi et al., 2003).

BH3-only pro-apoptotic proteins

BH3-only pro-apoptotic proteins share a homology in the BH3 domain. One of the proteins from this family is tBid, discussed in the previous section. Transferring tBID to the mitochondria causes the release of cytochrome c by inducing oligomerization of the pro-apoptotic proteins Bax and Bak through direct interactions (Gross et al., 1999b; Korsmeyer et al., 2000; Li et al., 1998a). BH3-only proteins can also interact and neutralise the action of anti-apoptotic proteins (Letai et al., 2002).

One more step in the regulation of cytochrome c release from the mitochondria

To leave the mitochondria, cytochrome c needs to get through the outer mitochondrial membrane, which is regulated by pro-apoptotic and anti-apoptotic proteins. According to recent studies, however, before it can accomplish this, it first

needs to leave the intra-cristae compartment where it is localised (Cipolat et al., 2006; Frezza et al., 2006).

Opa1 (Optic Atrophy 1) is a protein that controls the release of cytochrome c from the intra-cristae compartment into the mitochondrial intermembrane space (Frezza et al., 2006). PARL (Presenilin-associated rhomboid-like) is a protease that can either directly or indirectly cause Opa1 cleavage to produce a soluble form (Cipolat et al., 2006). The cleavage of Opa1 results in channel remodelling and cytochrome c release into the intermembrane space. Interestingly, the tBid protein can induce cytochrome c release from intra-cristae compartments (Scorrano et al., 2002), possibly through action on Opa1 (Frezza et al., 2006).

Stimuli converging on the mitochondria and inducing apoptosis

DNA damage, cellular stress and oncogene expression can promote apoptosis through p53 activation. Phosphorylation activates p53 by increasing its stability, which then leads to either the arrest of the cell cycle or apoptotic cell death (Rich et al., 2000; Schuler and Green, 2001). p53 can induce apoptosis by activating the transcription of the mitochondrial pro-apoptotic proteins Bax, Noxa and Puma (Schuler and Green, 2001) and preventing the transcription of anti-apoptotic proteins (Wu et al., 2001), or by activating Bax through ASC (apoptosis-associated speck-like protein) (Ohtsuka et al., 2004). p53 can also antagonise the action of mitochondrial anti-apoptotic proteins, such as such as Bcl-2 and Bcl-x_L (Mihara et al., 2003).

Proteins released from the mitochondria

The main proteins released from the mitochondria during caspase-dependent apoptosis are cytochrome c, IAP, Smac/DIABLO and Omi/HtrA2. The factors released in caspase-

independent apoptosis are AIF and endonuclease G (Saelens et al., 2004), which are discussed in a later section.

Cytochrome c

Once released, cytochrome c initiates Apaf1 (Apoptotic protease activating factor 1) (Zou et al., 1997) and procaspase-9 assembly in a complex that causes caspase-9 activation in the presence of ATP (Li et al., 1997). This complex is called the apoptosome (Cain et al., 2000). Seven Apaf-1 molecules oligomerize into a complex that recruits seven procaspase-9 molecules (Acehan et al., 2002). Activated caspase-9 then causes the cleavage of procaspase-3.

IAPs, Smac/DIABLO and Omi/HtrA2

IAPs (inhibitor of apoptosis proteins) can bind procaspase-9 and block its activation, as well inhibiting active caspase-9 and caspase-3 (Deveraux et al., 1998). Smac/DIABLO (Second mitochondria-derived activator of caspase/Direct IAP binding protein with low pI) has been found to inactivate IAPs (Du et al., 2000; Verhagen et al., 2000). Smac/DIABLO is localized in the mitochondria and released into the cytosol during apoptosis activation. However, apoptosis proceeds normally in Smac knockout mice (Okada et al., 2002). It is therefore possible that an alternative pathway exists for inactivating IAPs. This could operate through Omni/HtrA2, which, like Smac, is released from the mitochondria during apoptosis and is able to inhibit IAPs (Martins, 2002; Martins et al., 2002; Suzuki et al., 2001).

2.2.4 Caspase cascade

Caspases exist in healthy cells in an inactive (zymogen) procaspase. Once activated by upstream regulatory pathways, they form the key element of a signal transduction cascade during apoptosis (Thornberry and Lazebnik, 1998).

In general, 13 caspases have been identified in mammalian cells (Zhang et al., 2003b; Koenig et al., 2001). Human caspase-4 and -5 do not have counterparts in mice, while mouse caspase-11 and -12 do not have counterparts in human (Lamkanfi et al., 2002). To activate procaspases, at least two cleavages must occur to separate the prodomain, large and small subunits (Earnshaw et al., 1999). After their cleavage, caspases form heterotetramers consisting of two large and two small subunits (Wilson et al., 1994). Based on their structure, regulation and targets, caspases can be divided into initiator and effector caspases. In addition, some caspases can perform additional specialised functions.

Initiator caspases

Initiator caspases work at the beginning of the caspase cascade. They contain long prodomains that take part in interactions with upstream regulatory molecules that activate the caspase cascade (Earnshaw et al., 1999). Caspase-2, -8, -9, -10 and -12 are initiator caspases involved in apoptosis (Degterev et al., 2003). As discussed in previous sections, caspase-8, -9 and possibly -10 are thought to be the key regulators of the caspase signal transduction cascade.

Caspase-2 can initiate the mitochondrial pathway of apoptosis (Guo et al., 2002; Lassus et al., 2002). One of the possible mechanisms to achieve this is through the

cleavage of tBid. Caspase-2 can be activated as a result of heat-shock induced apoptosis (Tu et al., 2006). Once initiator caspases are activated, they cleave other initiator and effector caspases and amplify a positive feedback loop (Degterev et al., 2003).

Effector caspases

Effector caspases work downstream in the caspase cascade, and are processed by initiator caspases or by other effector caspases to amplify the apoptotic signal. Effector caspases include caspase-3, -6 and -7, all of which have short prodomains (Degterev et al., 2003; Earnshaw et al., 1999). The activation of effector caspases causes the cleavage of more than two hundred different cellular targets, which results in cell death. Caspase targets include apoptotic, cell cycle and inflammatory regulators, protein kinases, proteins involved in cell adhesion, nuclear membrane and cytoskeletal structural proteins, DNA synthesis and repair proteins, and proteins involved in transcription and translation (Fischer et al., 2003).

Other caspases

In addition to their role in apoptosis, some initiator caspases participate in the regulation of cytokine processing and inflammation processes. Caspase-1 is activated by caspase-5 in humans, or by the homologous caspase-11 in mice, in the intracellular complex termed the inflammasome (Degterev et al., 2003; Martinon and Tschopp, 2004). Caspase-1 takes part in the production of interleukin-1β and interleukin-18, which are the major mediators of inflammation (Creagh et al., 2003; Martinon and Tschopp, 2004).

Another caspase with a specialised function is caspase-14, which can be expressed in epithelial cells (Pistritto et al., 2002). It is known to be involved in the differentiation of keratinocytes (Fischer et al., 2005), but the exact role of caspase-14 requires further clarification.

2.2.4 Caspase-independent cell death

Apoptotic stimuli acting on mitochondria can initiate cell death without the activation of caspases (Susin et al., 2000; Susin et al., 1999). AIF has been proposed to be a major factor contributing to caspase-independent cell death (Cande et al., 2002; Cregan et al., 2002; Joza et al., 2001; Saelens et al., 2004; Susin et al., 2000). In normal cells, AIF is localised in the mitochondrial inner membrane and must be cleaved from the membrane in order to function in apoptosis (Otera et al., 2005). Once apoptosis is induced, AIF is then transferred to the nucleus (Daugas et al., 2000). The release of AIF from the mitochondria is antagonised by Bcl-2 proteins (Susin et al., 1996), and its transport to the nucleus is prevented by Hsp70 (Ravagnan et al., 2001). AIF triggers DNA condensation, large-scale DNA fragmentation and phosphatidylserine exposure on the plasma membrane. (Cande et al., 2002; Susin et al., 2000; Susin et al., 1999).

Potentially, multiple pathways can converge on the mitochondria and cause the release of AIF (Yu et al., 2003). Most of these are still obscure. As one possible mechanism, caspase-2 can induce the release of AIF after p53 activation (Seth et al., 2005). It has been shown that the release of AIF from the mitochondria can be initiated by poly (ADP-ribose) polymerase-1 (PARP-1) in response to DNA damage and cell stress (Koh et al., 2005; Yu et al., 2002).

2.3 Proteins involved in apoptotic DNA fragmentation and chromatin condensation

DNA fragmentation and chromatin condensation are two characteristic features of apoptosis in most cells (Kerr et al., 1972; Wyllie, 1980). DNA fragmentation is a two-step process that usually occurs in tandem with chromatin condensation. Large-scale or high molecular weight (HMW) DNA fragmentation (50-300 kb) precedes internucleosomal (oligonucleosomal) DNA fragmentation, which produces fragments that are multiplex of 180-200 bp (Cohen, 1997; Wyllie, 1980). Apoptotic chromatin condensation can be divided into two stages. At stage I, chromatin condenses against the nuclear periphery. Later, chromatin condensation proceeds to the formation of apoptotic bodies, termed stage II chromatin condensation (Samejima et al., 2001; Susin et al., 2000).

The degradation of cellular DNA was the first biochemical marker of apoptosis to be discovered, and it was proposed that an endonuclease is involved in the process of DNA fragmentation (Wyllie, 1980). Nearly 20 years passed, however, before the apoptotic endonuclease was identified and named CAD (caspase-activated DNAse)/DFF40/CPAN (Enari et al., 1998; Halenbeck et al., 1998; Liu et al., 1998; Sakahira et al., 1998). In cells, CAD nuclease is associated with its inhibitory chaperone, ICAD/DFF45 (Liu et al., 1998; Liu et al., 1997; Sakahira et al., 1998), which is now known as ICAD-L.

CAD has been shown to be the main enzyme responsible for apoptotic internucleosomal DNA fragmentation and stage II chromatin condensation. It has also

been suggested that CAD participates in large-scale DNA fragmentation. The CAD knockout in chicken DT40 cells results in the loss of oligonucleosomal DNA fragmentation, while the high molecular weight fragmentation remains normal in cells exposed to etoposide (Samejima et al., 2001). Stage I DNA condensation occurs in the CAD knockout, while stage II DNA condensation, characterised by the formation of apoptotic bodies, is absent (Samejima et al., 2001). Similar data has been obtained in mouse ICAD and CAD knockouts, except that the large-scale DNA fragmentation was also abolished in the mouse CAD or ICAD knockout (Zhang et al., 2000) (Kawane et al., 2003). CAD and ICAD will be discussed in greater detail in the next section.

It has been noted that peripheral or stage I chromatin condensation still occurs during apoptosis even if caspases are inhibited, or in caspase-3 knockout cells, which fail to undergo CAD activation (Susin et al., 2000). It was shown that AIF can contribute to stage I chromatin condensation (Susin et al., 1999; Yuste et al., 2005), though the data on AIF involvement in high molecular weight DNA cleavage with the production of 50 kb DNA fragments is more controversial. HMW DNA cleavage was observed if AIF was microinjected into HeLa cells (Susin et al., 1999). However, the depletion of AIF by RNAi did not prevent HMW DNA cleavage in apoptotic cells (Yuste et al., 2005), although the experimental data of this study showed that the depletion of AIF was incomplete.

AIF's three-dimensional structure shows that it is associated with chromatin during the initiation of apoptosis and has a positive potential, which allows it to bind to negatively charged DNA (Ye et al., 2002). AIF can also interact with cyclophilin A and

cooperate to cause plasmid DNA cleavage or DNA degradation in isolated nuclei (Cande et al., 2004).

Endonuclease G is a nuclease transported into the nucleus from the mitochondria during apoptosis (Li et al., 2001). In mouse embryonic fibroblast cells during the induction of apoptosis by ultraviolet irradiation and TNF, DNA fragmentation was noticed in wild type cells and in cells with the ICAD knockout (Li et al., 2001). However, in other studies, no clear DNA fragmentation was seen in ICAD knockout fibroblasts induced by TNF, etoposide, staurosporine or actinomycin D (Zhang et al., 1998) (Zhang et al., 2003a; Zhang et al., 2000). It has been proposed, though, that endonuclease G acts in addition to CAD to cause internucleosomal DNA fragmentation (Li et al., 2001), and endonuclease G was also shown to be involved in DNA fragmentation in *C. elegans* (Parrish et al., 2001). Recent data render this claim is highly controversial, at least for mammalian cells.

Two mouse endonuclease G knockouts show different phenotypes (Zhang et al., 2003a) (Irvine et al., 2005). In one, the mouse develops normally and endonuclease G depletion does not interfere with apoptotic DNA fragmentation upon the induction of apoptosis with etoposide and actinomycin D (Irvine et al., 2005). In the other, the mouse dies during early embryonic development and the heterozygote is partly resistant to apoptotic cell death (Zhang et al., 2003a). Importantly, in the latter case, a part of the DNA adjacent to the endonuclease G gene was removed during knockout construction (Zhang et al., 2003a). This DNA encodes another gene with an unidentified function, whose disruption could potentially confound the endonuclease G depletion phenotype (Irvine et al., 2005). No oligonucleosomal DNA fragmentation was observed during the

activation of apoptosis by etoposide in the DT40 CAD knockout (Samejima et al., 2001). This, however, does not exclude the possibility that different apoptotic stimuli, could activate different nucleases – particularly UV treatment for endonuclease G. Alternatively, the nuclease activated by UV irradiation in mouse ICAD knockout fibroblasts (Li et al., 2001) may not be endonuclease G.

DNase II has been identified as an enzyme causing DNA fragmentation in thymocytes engulfed by macrophages (Kawane et al., 2003). In thymocytes, both DNAse II and CAD contribute to DNA fragmentation, and function cooperatively in this process. In addition to DNase II, DNase I had also been reported to take part in apoptotic DNA fragmentation in the human Jurkat cell line (Oliveri et al., 2001). However, this conclusion was not supported by the data from DNAse I knockout mice (Nagata et al., 2003). DNAse gamma (Shiokawa and Tanuma, 1998) is another of the company of controversial apoptotic DNAses, and can induce oligonucleosomal DNA fragmentation in isolated nuclei *in vitro* (Mizuta et al., 2006). Whether DNAse gamma can function *in vivo* remains to be determined.

In addition, the Acinus (apoptotic chromatin condensation inducer) protein has also been identified as the basis for chromatin condensation activity, as it can induce chromatin condensation *in vitro* on permeabillised HeLa cells (Sahara et al., 1999). Acinus has a nuclear localization and is activated by caspase-3 cleavage during the induction of apoptosis. Still, the involvement of Acinus in chromatin condensation is controversial; in one study, the depletion of Acinus by RNAi led to a decrease in chromatin condensation (Hu et al., 2005). However, these results are not supported by

another study, which suggests that Acinus depletion by RNAi does not interfere with chromatin condensation, but does reduce DNA fragmentation. (Joselin et al., 2006).

2.4 The role and function of ICAD and CAD

CAD and its inhibitor, ICAD, are broadly conserved across different species, from insects to humans, with orthologs even in cnidaria (Eckhart et al., 2007). Their prevalence may indicate their importance in apoptosis, DNA fragmentation and chromatin condensation. Most of the studies on ICAD and CAD proteins have been done on the mouse, human, chicken and rat proteins.

2.4.1 ICAD-L, ICAD-S and CAD

CAD is an endonuclease that is present throughout the cell cycle in a complex with ICAD (Enari et al., 1998; Sakahira et al., 1998). CAD is activated after the cleavage of ICAD by caspase-3 (Fig. 2.4). Activation of CAD during apoptosis causes the fragmentation of chromosomal DNA, and CAD, together with ICAD, was previously identified in humans as DNA fragmentation factor 40 (DFF40) and DNA fragmentation factor 45 (DFF45), respectively (Liu et al., 1998; Liu et al., 1997).

One function of ICAD is to prevent the spontaneous activation of CAD. ICAD exists in cells in two splice forms: ICAD-L (long) and ICAD-S (short) (Kawane et al., 1999). ICAD-L plays a role as not only an inhibitor, but also as a chaperone for CAD during its synthesis on the ribosome, and this chaperone function of ICAD-L is absolutely necessary for CAD to achieve its active conformation (Enari et al., 1998). If ICAD-L is added to CAD after CAD synthesis, the subsequent cleavage of ICAD-L by caspase-3 does not activate CAD. ICAD-L, but not ICAD-S, has also been shown to

promote CAD renaturation under reducing conditions *in vitro* (Sakahira et al., 2000). Chaperone Hsc70 and its co-chaperone, Hsp40, take part in this process (Sakahira and Nagata, 2002). When CAD is released from ICAD, its activity is stimulated by the presence of Hsp70 *in vitro* (Liu et al., 2003). ICAD-L was shown not only to be required for the synthesis of active CAD, but also for its stability in solution. CAD incubated without ICAD-L *in vitro* aggregates and becomes insoluble (McCarty et al., 1999b).

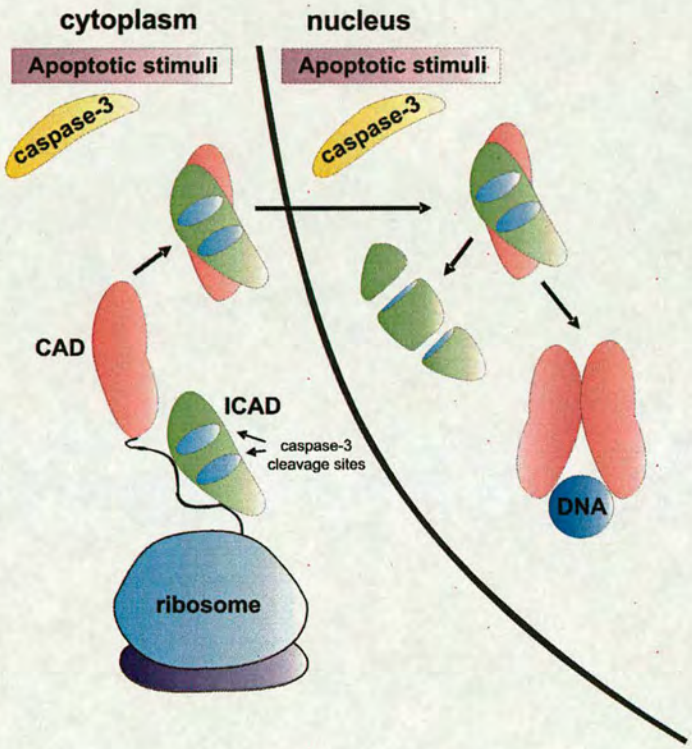

Fig. 2.4. ICAD and CAD function. ICAD acts as a chaperone for CAD, promoting its folding to an active conformation on the ribosome. ICAD also functions as an inhibitor of CAD. After the activation of caspases during apoptosis, the ICAD is cleaved and active CAD is released. Active CAD dimer causes DNA cleavage.

In contrast to ICAD-L, the role of ICAD-S is obscure. The ICAD-S form is formed by alternative splicing (Kawane et al., 1999). Both ICAD forms are able to inhibit CAD *in vitro* (Gu et al., 1999; Sakahira et al., 1999), though ICAD-L has been found in many cases to be the main form associated with CAD *in vivo*. The co-expression of mouse ICAD-L and ICAD-S together with CAD in insect Sf-9 cells

demonstrated that CAD is principally associated with ICAD-L, while ICAD-S exists as a free form (Sakahira et al., 1999). However, in an *in vitro* transcription and translation system, human GST-ICAD-S can pull down more CAD than full-length ICAD (Gu et al., 1999). Moreover, in rat neurons, ICAD-S is the form associated with CAD in the nucleus, and ICAD-L has not been detected (Chen et al., 2000). ICAD-S is also the dominant form of ICAD detected in the rat, mouse and human central nervous systems (Chen et al., 2000). Therefore, determining which form of ICAD is mostly associated with CAD and the functional role of such association remains controversial.

In recent research, it was reported that mouse and human ICAD-S does not have a chaperone function (Gu et al., 1999; Nagase et al., 2003; Sakahira et al., 1999). Nevertheless, low chaperone activity has been claimed for ICAD-S (Scholz et al., 2002). In one study ICAD-S promoted the formation of active CAD in *E. coli*, but its activity was, however, 40- to 50-fold lower than that produced with ICAD-L. Therefore, the actual ICAD-S function *in vivo* required further clarification during my study.

2.4.2 ICAD and CAD regulation

The main mechanism of CAD regulation is provided through the cleavage of ICAD by caspase-3 after the induction of apoptosis (Fig. 2.5). ICAD-L and ICAD-S are cleaved by caspase-3 at two sites, releasing three polypeptides (Sakahira et al., 1998). Mutation of the caspase-3 cleavage sites in ICAD-L demonstrated that the cleavage of both sites is necessary for the release of CAD from ICAD-L. The cleavage of the first caspase-3 site of ICAD-S is enough to release and activate CAD, however, even if the second caspase-3 site is not cleaved (Sakahira et al., 1998).

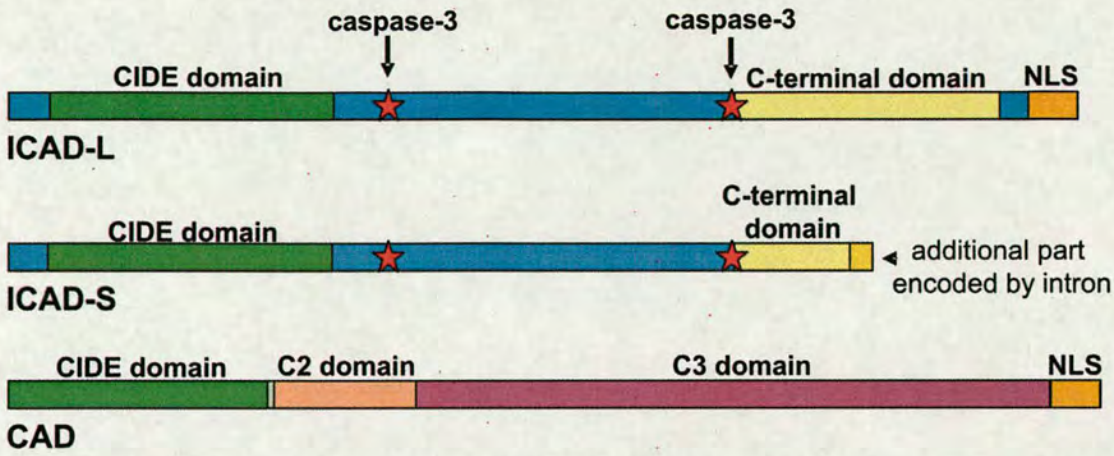

Fig. 2.5. ICAD and CAD proteins. ICAD-L and ICAD-S proteins have two cleavage sites for caspase-3. Also, ICAD-L has a nuclear localization signal (NLS) on the C-terminal end. ICAD-L C-terminal domain is disrupted in ICAD-S. However, ICAD-S has a small fragment with unidentified function encoded by alternatively spliced mRNA. ICAD and CAD proteins share a homologous CIDE N-terminal domain. In addition, CAD has C2 and C3 domains and an NLS on its C-terminus.

Another effector caspase, caspase-7, has been shown to cleave both ICAD sites if added to reactions *in vitro* (Liu et al., 1999; McIlroy et al., 1999). However, an endogenous caspase-7 activity from MCF7 cell line extracts lacking caspase-3, was not able to cause ICAD cleavage nor DNA fragmentation on isolated nuclei (Wolf et al., 1999).

ICAD can be also cleaved *in vitro* and *in vivo* by the serine proteinase granzyme B, with subsequent CAD activation and DNA fragmentation (Thomas et al., 2000). Granzyme B is released from granules of cytotoxic T-lymphocytes as one mechanism of killing target cells. ICAD cleavage by granzyme B can be done either by activating the apoptotic pathway through caspase-3 cleavage or by direct ICAD cleavage, as was shown in the presence of caspase inhibitors (Sharif-Askari et al., 2001). Granzyme B can

also initiate other pathways independent of ICAD and leading to cell death (Thomas et al., 2001).

2.4.3 Additional putative CAD inhibitors

B23/Nucleophosmin has been reported to inhibit CAD. B23 is a protein involved in ribosome biogenesis in the nucleolus (Savkur and Olson, 1998), and has chaperone, ribonuclease and nucleic acid binding activity (Hingorani et al., 2000). B23 was shown to inhibit CAD *in vitro*, and, if overexpressed, *in vivo*. The inhibitory action of B23 was in response to a second messenger, phosphatidylinositol 3,4,5-triphosphate (Ahn et al., 2005).

However, B23 can bind NLS containing peptides with high affinity and participate in nuclear importation (Szebeni et al., 1995). This, and the fact that B23 has chaperone activity (Szebeni and Olson, 1999), may mean that the association of B23 with CAD via its NLS might have implications for nuclear transport or chaperoning.

A protein named CIIA has also been identified as a CAD interactor (Cho et al., 2003). CIIA was shown to interact with CAD *in vitro* and in the ICAD:CAD complex, but not with ICAD alone. CIIA was also found to inhibit CAD activity after ICAD destruction *in vitro* and during overexpression in 293T cells.

2.4.4. Modulators of ICAD and CAD function

Histone H1 and high mobility group (HMG) proteins 1 and 2 can stimulate the cleavage of naked plasmid DNA by CAD *in vitro* (Liu et al., 1998; Toh et al., 1998). These proteins bind to nucleosomal linker DNA (Schroter and Bode, 1982). It was proposed that histone H1, HMG-1 and HMG-2 may target CAD to nucleosomal linkers

and stimulate its catalytic activity (Liu et al., 1998; Liu et al., 1999), but it has been noticed that the degree of CAD stimulation was significantly lower on chromatin than on naked DNA *in vitro* (Widlak et al., 2000).

CAD can also interact with topoisomerase IIα (Durrieu *et al*, 2000), and was shown to stimulate CAD activity on naked DNA, though not on chromatin. Topoisomerase IIα also contributes to chromatin condensation during apoptosis (Durrieu et al., 2000).

2.4.5 Proteins with CIDE domain

ICAD and CAD proteins have a homologous N terminal domain, the CIDE domain (cell death inducing DFF45-like effector). Interestingly, a homologous N-terminal domain has also been found in three other human proteins: CIDE-A, CIDE-B and CIDE-C/CIDE-3/FSP-27 (Danesch et al., 1992; Inohara et al., 1998; Liang et al., 2003). In addition to the N-terminal domain, CIDE proteins also contain a C-terminal domain different to that of ICAD or CAD. The expression of these proteins can be tissue-specific (Da et al., 2006; Inohara et al., 1998). CIDE proteins have been found to stimulate apoptosis and cause DNA fragmentation and condensation upon overexpression in 293T cells (Inohara et al., 1998). Their CIDE domain can interact with the similar domain of ICAD and CAD *in vitro* (Lugovskoy et al., 1999). Interestingly, hepatitis C virus NS2 protein can inhibit apoptosis through action on CIDE-B's C-terminal domain (Erdtmann et al., 2003). Whether interaction of CIDE proteins with ICAD and CAD has a physiological role remains to be determined.

CAD splice variants have also been reported in a variety of human and mouse tissues (Bayascas et al., 2004). The three CAD splice forms identified correspond to the N-terminal CIDE domain of CAD alone or to the CIDE domain with approximately thirty additional amino acids on its C-terminus. These short CAD forms were shown to interact with ICAD *in vitro* (McCarty et al., 1999a). This interaction, therefore, has a structural basis, but it is not clear whether CAD splice forms have a physiological function *in vivo*.

2.4.6 Additional putative mechanisms of ICAD and CAD regulation

It has been claimed that there is less ICAD-L protein in cell tissues that express less CAD protein, though the amount of ICAD-S remains unchanged (Nagase et al., 2003). Moreover, in CAD knockout cells, the amount of ICAD-L protein was reduced as compared to wild–type cells. While the amount of ICAD-L protein was reduced in the CAD knockout, the amount of ICAD-L mRNA was not affected. This study therefore suggests that the regulation of ICAD-L protein levels may occur at the post-transcriptional level (Nagase et al., 2003). The reduced amount of ICAD-L protein in the CAD knockout may be explained by the possibility that ICAD-L, if not in complex with CAD, is a more likely target for protein degradation.

In addition to possible ICAD posttranslational modifications, some data propose that CAD be can down-regulated and degraded once apoptosis is induced and ICAD is cleaved (Lui and Kong, 2006; Yuste et al., 2001). The disappearance of CAD shortly after caspase-3 cleavage of ICAD has been noticed in the human neuroblastoma IMR-5 cell line (Yuste et al., 2001). Apoptosis proceeded in this cell line without characteristic

DNA fragmentation. It must, however, be noted that there is a cell line variability on the presence of DNA fragmentation in different neuroblastoma cell lines (Boix et al., 1997). The DNA fragmentation was restored in the IMR-5 cell line after the overexpression of CAD (Yuste et al., 2001).

Caspase-3 could be involved not only in apoptosis, but also in erythropoiesis (Carlile et al., 2004). Caspase-3 activation can also cause a partial cleavage of ICAD during erythroid development (Lui and Kong, 2006), though no DNA fragmentation was observed. Interestingly, it was noticed that the levels of both CAD mRNA and protein were decreased by an unknown mechanism in these cells.

2.4.7 ICAD and CAD localization

To participate in DNA fragmentation, CAD must have access to the DNA in the nucleus. A nuclear localization signal has been identified on the C-terminus of ICAD and CAD (Enari et al., 1998; Liu et al., 1998; Samejima and Earnshaw, 1998), but the nuclear localisation signal is absent in ICAD-S, which is distributed diffusely in cells (Lechardeur et al., 2000; Samejima and Earnshaw, 2000).

The localisation of ICAD-L and CAD is controversial. The papers assessing ICAD and CAD localisation by immunostaining of tagged ICAD and CAD proteins make claims for ICAD and CAD nuclear localisation (Lechardeur et al., 2000; Liu et al., 1998; Samejima and Earnshaw, 2000). In contrast, the data from the experiments in which the cytoplasmic and nuclear fractions were analysed for the presence of ICAD and CAD shows that these proteins have mostly cytoplasmic localisation (Durrieu et al., 2000; Enari et al., 1998; Mitamura et al., 1998). However, the occurrence of ICAD and

CAD in the cytosolic extracts may be the result of their leakage from the nuclei during the biochemical purification procedure (Liu et al., 1998).

2.4.8 The three-dimensional structure of ICAD and CAD

The structure of CAD had been solved first for its N-terminal domain (Uegaki et al., 2000; Zhou et al., 2001), and then for the rest of the protein (Woo et al., 2004). The N-terminal CIDE domain, which is homologous in ICAD and CAD (Fig. 2.6), consists of one α-helix and five β-strands organised in a β-sheet with two hydrophobic clusters situated on opposite sides (Uegaki et al., 2000).

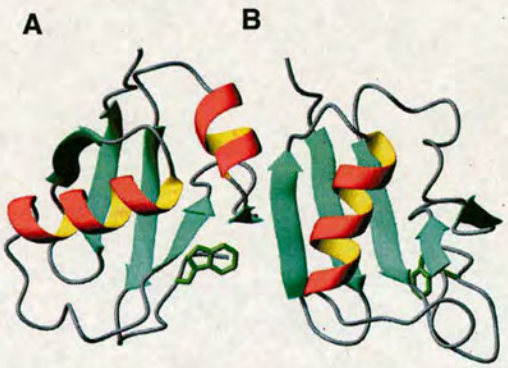

Fig. 2.6. The three-dimensional structure of ICAD and CAD N-terminal (CIDE) domains solved by NMR. **(A)** CIDE domain of ICAD has a structure consisting of one α-helix and one β-sheet from five β strands. **(B)** CAD CIDE domain. The difference between ICAD and CAD CIDE domains is in a short helical element present in ICAD and disrupted in CAD. CAD and ICAD CIDE domains also differ in the angle between α-helix and β strands (Adapted from (Zhou et al., 2001)).

The middle and C-terminal part of the CAD protein was crystallised (Woo et al., 2004) and is shown on Fig. 2.7. ICAD blocks the ability of CAD to bind DNA (Sakahira et al., 2001). After ICAD cleavage, CAD protein is liberated and forms a homodimer. Zinc was shown to be crucial for homodimer formation and stability. The CAD homodimer has a crevice formed between two C-terminal (C3) domains of CAD protein, which accommodates and cleaves double-stranded DNA (Woo et al., 2004). This crevice is thought to be inaccessible to DNA packaged into nucleasomes, which could allow

only the free internucleosamal DNA to be cleaved. As a result, the characteristic oligonucleosomal DNA cleavage of about 200 bp would be produced.

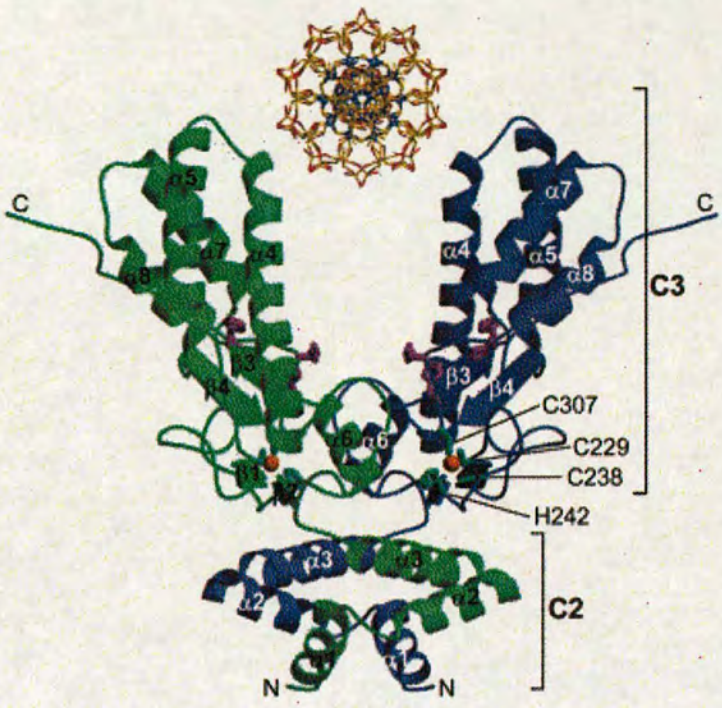

Fig. 2.7. The three-dimensional structure of mouse CAD middle (C2 domain) and C-terminal part (C3 domain). The C2 domain consists of three α-helixes, while the C3 domain consists of five α-helixes and four β-strands in addition to a long C-terminal loop with a nuclear localization signal. In a homodimer form, two CAD C3 domains form a crevice surrounding DNA (Adapted from (Woo et al., 2004)).

The ICAD protein CIDE domain structure (Fig. 2.6A) is similar to that of CAD (Otomo et al., 2000; Zhou et al., 2001). While the structure of the ICAD middle part remains to be determined, the ICAD C-terminal domain (Fig. 2.8) has a unique structure of four α-helixes, one of which (α1) is situated perpendicularly to the other three α-helixes (Fukushima et al., 2002). It was suggested that in ICAD-S the unique organisation of the C-terminal domain is disrupted (Fukushima et al., 2002), and as a result, human ICAD-S cannot completely provide its chaperone function for human CAD (Fukushima et al., 2002).

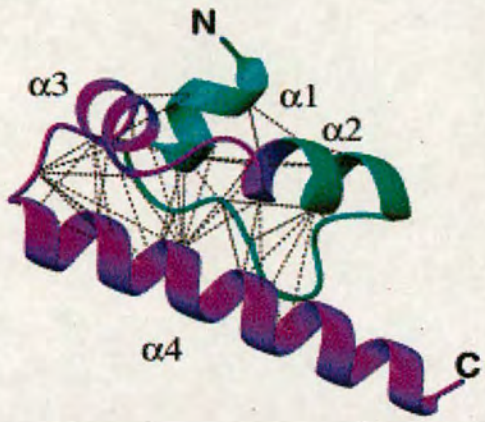

Fig. 2.8. The structure of the human ICAD C-terminal domain. It has a unique structure of four α-helixes. (Adapted from Fukushima et al., 2002)

2.4.9 Physiological role of the DNA cleavage by CAD for an organism

Pathways leading to CAD activation and DNA fragmentation were shown to be specific to cells dying by apoptosis. Several reasons have been suggested to explain the importance of this pathway for an organism.

Cleavage of DNA into smaller pieces may be an important step to reduce the influence of the dead cells' DNA uncoiling on the neighbouring cells (Wyllie, 1998). DNA fragmentation can also eliminate viral DNA in the case of viral infection. In transformed cells undergoing apoptosis, the degradation of DNA may also prevent the potential releasing of DNA containing oncogenes and its transformation to healthy cells. Macrophages can be particularly sensitive to foreign DNA, as they engulf cells that contain viruses or transformed cells with oncogenes. That can partly explain why macrophages have an alternative to the CAD pathway for causing DNA fragmentation with DNAse II in engulfed cells (Kawane et al., 2003). In addition, DNA produced during massive cell death can act as an autoimmunogen. Therefore, the cleavage of

DNA to oligonucleosomal fragments may prevent an autoimmune reaction (Nagata, 2000).

2.4.10 CAD role in cell death.

CAD does not appear to be essential for apoptotic cell death. *Caspase-3*$^{-/-}$, *ICAD*$^{-/-}$ or *CAD*$^{-/-}$ cells still die after the activation of apoptosis (Janicke et al., 1998; Samejima et al., 2001; Woo et al., 1998; Zhang et al., 1999). This implies that CAD is dispensable for cell death, but does not explain CAD's role in cell death. Therefore, I am interested in investigating the particular role of CAD in this process.

Indirect data has been obtained to support the hypothesis that CAD activation can lead to cell death. Mouse thymocytes and fibroblasts lacking the *ICAD*$^{-/-}$ gene were reported to be more resistant to a number of proapoptotic stimuli than were cells with the intact *ICAD*$^{+/+}$ gene (Boulares et al., 2001; Thomas et al., 2000; Zhang et al., 1999). A delay in cell death in the fibroblasts of *ICAD*$^{-/-}$ mice could imply the contribution of CAD to this process.

Cleavage of DNA by CAD produces double-strand breaks that can act as apoptotic signals (Liu et al., 1999). DNA breaks can be detected by PARP. It has been noticed that after the induction of apoptosis by TNF in *ICAD*$^{-/-}$ fibroblasts, a significant delay occurs in PARP activation relative to what is seen in wild type fibroblasts (Boulares et al., 2001). This is also supported by the fact that DNA cleavage by CAD can facilitate apoptosis in a positive feedback loop (Ben-Yehudah et al., 2003). In addition, it has been shown that a chimeric CAD protein consisting of CAD linked to gonadotropin-releasing hormone can cause cell death in adenocarcinoma cells through

DNA damage, which causes the subsequent activation of apoptosis (Ben-Yehudah et al., 2003). After targeting cells with chimeric CAD protein, cytochrome c was shown to be released from the mitochondria with the subsequent activation of caspase-9 and caspase-3. However, this experiment did not use native CAD protein, and therefore the question of whether this process takes places *in vivo* under physiological conditions is still uncertain.

CAD is activated at the end of the apoptotic signalling pathway. Therefore, if it could be directly activated to kill the cell, it might escape regulation by the complex apoptosis machinery. CAD activation *in vivo* could be done by discovering compounds that disrupt the interactions between ICAD and CAD. In addition, ICAD could be destroyed in model system *in vivo* if specially targeted for disruption. Therefore, a part of my PhD project aim was to create a model system for ICAD destruction and discover if *in vivo* activation of CAD is enough to kill the cell.

2.4.11. Project aims.

The specific questions I wished to address in my PhD study are:

1) Can CAD activation *in vivo* cause cell death in the absence of initial apoptosis?
2) To answer this question, it was necessary to create a model system for the specific destruction of ICAD in DT40 cells. The development of such a system involving site-specific protease, which has not been done before in vertebrate cells, was another aim of my study.
3) What is the role of the ICAD-S splice form *in vivo* and can it work as a chaperone and inhibitor for CAD in the absence of ICAD-L?

3. Materials and Methods

3.1 Chemicals and common solutions

All chemicals used in this study were from Sigma-Aldrich, unless otherwise indicated. Restriction enzymes and other enzymes for molecular cloning were from New England Biolabs (NEB). Luria-Bertani medium (LB) pH 7.0 is 1 % tryptone, 0.5 % yeast extract, 1% NaCl. Low-salt LB (1 % tryptone, 0.5 % yeast extract, 0.5% NaCl) was used for the selection of zeocin resistance plasmids in *E. coli*. Phosphate-buffered saline (PBS) is 137 mM NaCl, 2.7 mM KCl, 10 mM Na_2HPO_4, and 2 mM KH_2PO_4.

3.2 Molecular biology

3.2.1 Molecular cloning

DNA for molecular cloning was digested with the appropriate restriction enzyme for one to four hours at 37°C, following the manufacturer's instructions. Vectors were treated with 10 units of calf intestine phosphatase for one hour at 37° C to prevent self-ligation. The DNA fragments in gel loading buffer (0.04% Bromophenol Blue, 5% glycerol) were separated on 0.8 – 2.5 % agarose gels, depending on the product size. The agarose gels contained 0.5 μg/ml ethidium bromide in TAE buffer (40 mM Tris-acetate, pH 8 ; 1 mM EDTA). DNA ladders 1 kb (Invitrogen) and 100 bp (NEB) were used as size markers. The gels were visualised on a UV transilluminator, and the DNA fragments were purified from the agarose gels using a QIAquick Gel Extraction Kit (Qiagen). The DNA products were ligated with 400 U of T4 DNA ligase (NEB), either for one hour at room temperature for cohesive end termini or at 16° C overnight for blunt end ligations. The ligation products were transformed into competent *E. coli* and selected with the appropriate antibiotic: ampicillin (100 μg/ml), kanamycin (50 μg/ml),

or zeocin (25 μg/ml). The list of vectors used and constructed in this study is summarised in Table 1.

Table 1. Cloning of coding sequences and construction of targeting vectors

Construct	Coding sequence	Vector	Restriction sites insert vector	Source, PCR or cloning, comments
AA4.1	loxP-neo-loxP	pLoxNeo		(Arakawa et al., 2001)
AA4.2	CAD targeting vector backbone	pBluescript II KS (+)		(Samejima et al., 2001)
AA4.3	CAD targeting vector	pBluescript II KS (+)	*Bam*HI/*Bam*HI *Bam*HI	Cloning from AA4.1 into AA4.2
AA4.4		pBluescript II KS (+)		Stratagene
AA4.5	ICAD genomic region	λ FIX II		Dr. Kumiko Samejima
AA4.6	3' ICAD arm	pBluescript II KS (+)	*Spe*I/*Not*I *Spe*I/*Not*I	PCR: KS23/KS24 from AA4.5 and digest Cloning into AA4.4
AA4.7	5' ICAD arm	pBluescript II KS (+)	*Bam*HI/*Bam*HI *Kpn*I/*Nco*I* *Kpn*I/*Hinc*II*	Cloning of AA4.5 into AA4.4
AA4.8	5'-3' ICAD Arms	pBluescript II KS (+)	*Spe*I/*Not*I *Spe*I/*Not*I	Cloning of AA4.6 into AA4.7
AA4.9	Tk	pBT/SP-TK		Prof. Adrian Bird
AA4.10	loxP-puro-loxP	pLoxPuro		(Arakawa et al., 2001)
AA4.11	loxP-puro-tk-loxP	pLoxPuro	*Xba*I/*Xba*I *Nhe*I	Cloning of AA4.9 into AA4.10
AA4.12	ICAD targeting vector loxP-puro-tk-loxP	pBluescript II KS (+)	*Bam*HI/*Bam*HI *Bam*HI	Cloning from AA4.11 into AA4.8
AA4.13	ICAD targeting vector loxP-puro-loxP	pBluescript II KS (+)	*Bam*HI/*Bam*HI *Bam*HI	Cloning from AA4.10 into AA4.8
AA4.14		pGEM-T-Easy		Promega
AA4.15	hICAD-L	pGEM-T-Easy	Direct PCR product cloning	PCR: KS5/KS6 from HeLa RNA
AA4.16		pZeoSV2+		Invitrogen
AA4.17	hICAD-L	pZeoSV2+	*Not*I/*Not*I *Not*I	Cloning from AA4.15 into AA4.16

AA4.18	hCAD	pGEM-T-Easy	Direct PCR product cloning	PCR: KS7/KS8 from HeLa RNA
AA4.19		pCAGGS-Cre		(Araki et al., 1995)
AA5.1	hICAD-L with *Eco*RV site	pGEM-T-Easy	Site-directed mutagenesis	PCR: Sa11/Sa12
AA5.2	hICAD-L with 1st TEV site	pGEM-T-Easy	*Eco*RV/*Bgl*II	Klenow polymerase synthesis: Sa25/Sa18 and digest with cloning into AA5.1
AA5.3	hICAD-L with 1st TEV site	pZeoSV2+	*Not*I/*Not*I *Not*I	Cloning from AA5.2 into AA4.16
AA5.4	hICAD-L fragment with 2nd TEV site	pGEM-T-Easy	Direct reaction product cloning	Klenow polymerase synthesis: Sa21/Sa22 and treatment with TaKaRa LA Taq
AA5.5	hICAD-L fragment with 2nd TEV site extension	pGEM-T-Easy	Direct PCR product cloning	PCR: Sa26/Sa27 from AA5.4
AA5.6	hICAD-L^{2TEV}	pZeoSV2+	*Ear*I/*Blp*I *Ear*I/*Blp*I	Cloning from AA5.5 into AA5.3
AA5.7		pECE		(Ellis et al., 1986)
AA5.8		His-cassette		(Hartman and Mulligan, 1988)
AA5.9		pECE-His	*Bam*HI/*Bam*HI *Bam*HI (incomplete digest)	Cloning from AA5.7into AA5.7
AA5.10	hCAD	pECE-His	*Not*I/*Not*I *Not*I	Cloning from AA4.18 into AA5.9
AA5.11	rtTA	pTet-On		Clontech
AA5.12	TEV	Yip204		(Uhlmann et al., 2000)
AA5.13		pUHD10.3		(Manfred Gossen-unpublished, ZMBH, Heidelberg)
AA5.14	TEV	pUHD10.3	*Eco*RI/*Xba*I *Eco*RI/*Xba*I	PCR: Sa36/Sa37 from AA5.12 and digest into AA5.13
AA5.15	MBP-mTEV	pRK793		(Kapust et al., 2001)
AA5.16	MBP-mTEV with 2NLS	pGEM-T-Easy	Direct PCR product cloning	PCR: Sa115/Sa116 from AA5.15
AA5.17		pUHD10.3-RFP		Dr Kumiko Samejima
AA5.18	MBP-mTEV with 2NLS	pUHD10.3-RFP	*Eco*RI/*Eco*RI *Eco*RI	Cloning from AA5.16 into AA5.17
AA5.19	PreScission	pGEX-1N		(Leong et al., 1992)
AA5.20	PreScission	pGEM-T-Easy	Direct PCR product cloning	PCR: Sa184/Sa185 from AA5.19
AA5.21	PreScission	pECE-His	*Not*I/*Not*I *Not*I	Cloning from AA5.20 into AA5.9

AA5.22		PTracer-SV40		Invitrogen
AA5.23	PreScission	PTracer-SV40	*NotI*/*NotI* *NotI*	Cloning from AA5.21 into AA5.22
AA5.24	hICAD-L^{2PRE} fragment	pGEM-T-Easy	Direct PCR product cloning	PCR step1:Sa178/Sa179 PCR step2:Sa181/Sa183
AA5.25	hICAD-L^{2PRE}	pGEM-T-Easy	*EarI*/*BlpI* *EarI*/*BlpI*	Cloning from AA5.24 into AA5.1
AA5.26	hICAD-L^{2PRE}	PZeoSV2+	*NotI*/*NotI* *NotI*	Cloning from AA5.25 into AA4.16
AA6.1	cICAD-L incomplete cDNA	pBluescript		Dr. Kumiko Samejima
AA6.2	cICAD-L	pGEM-T-Easy	Direct PCR product cloning	PCR: Sa72/Sa54 from AA6.1
AA6.3	cICAD-L no stop codone	pGEM-T-Easy	Direct PCR product cloning	PCR: Sa72/Sa56 from AA6.1
AA6.4	double tag (S-TEV-SBP)	pcDNA3.1/ Hygro (+)		Dr. Sandrine Ruchaud
AA6.5	SATH tag C-terminal (S-TEV-SBP-His)	pcDNA3.1/ Hygro (+)	*XhoI*/*XhoI* *XhoI*	Cloning of annealed *XhoI* cut primers Sa75/Sa76 into AA6.4
AA6.6	cICAD-L-SATH tag	pcDNA3.1/ Hygro (+)	*NotI*/*NotI* *NotI*	Cloning of AA6.3 into AA6.5
AA6.7	cICAD-S	pGEM-T-Easy	Direct PCR product cloning	PCR: Sa150-Sa132 from cICAD fragment
AA6.8	cICAD-S	pZeoSV2+	*NotI*/*NotI* *NotI*	Cloning from AA6.7 into AA4.16
AA6.9	cCAD	pTracer-SV40		Dr Kumiko Samejima
AA6.10	hICAD-S	pGEMT-Easy	Direct PCR product cloning	PCR: Sa81/Sa121 from into AA4.15
AA6.11	hICAD-S	pZeoSV2+	*NotI*/*NotI* *NotI*	Cloning from AA6.10 into AA4.16
AA6.12	hICAD-S^{2TEV}	pGEM-T-Easy	Direct PCR product cloning	PCR: Sa81/Sa121 from AA5.6
AA6.13	hICAD-S^{2TEV}	pZeoSV2+	*NotI*/*NotI* *NotI*	Cloning from AA6.12 into AA4.16
AA6.14	hICAD-S	pcDNA3.1/ Hygro (+)	*HindIII*/*XhoI* *HindIII*/*XhoI*	Cloning of AA6.11 into AA6.5
AA6.15	hICAD-S^{2TEV}	pcDNA3.1/ Hygro (+)	*HindIII*/*XhoI* *HindIII*/*XhoI*	Cloning of AA6.13 into AA6.5

*-indicates that the site was blunt-ended before ligation

3.2.2 Partial digestions

To isolate a DNA product with a single cut from a plasmid containing two restriction sites, partial digestion was used. The restriction enzyme was diluted at

different concentrations (0.25, 0.5, 1, and 2 U) per 1 μg of plasmid DNA. The reaction was incubated for 30 minutes at 37° C. The reaction products were separated on agarose gels and gel purified using a QIAquick Gel Extraction Kit (Qiagen).

3.2.3 Blunting the end of DNA fragments

T4 DNA polymerase (NEB) was used to create blunt ends after restriction digestion. 1.5 U per 1 μg of DNA was used in a reaction supplemented with 100 μM of dNTP mix. The reaction was carried out for 15 minutes at 37° C, then the T4 DNA Polymerase was heat inactivated for 20 minutes at 70° C. The reaction products were separated on agarose gels and gel purified using a QIAquick Gel Extraction Kit (Qiagen).

3.2.4 Preparation of competent E. coli and transformation

E. coli strains Top10 and DH5α were used to make competent cells. The *E. coli* culture (5 ml) was grown overnight in LB medium with ampicillin. The culture was then diluted 1:200 in LB medium with ampicillin and incubated with shaking at 37° C until OD_{600} 0.48 was reached. The cells were chilled on ice for 10 minutes and then pelleted by centrifugation for five minutes at 2700 × g at 4° C. Then the pellet was resuspended in 40 ml of TfbI buffer (30 mM CH_3COOK; 100 mM $RbCl_2$; 10 mM $CaCl_2$; 50 mM $MnCl_2$; 15% Glycerol; pH adjusted to pH 6.5 using KOH) per 100 ml of bacterial culture. The cells were incubated on ice for five minutes, then centrifuged at 1000 × g for 10 minutes. The supernatant was discarded and the cells were resuspended in 4 ml TbfII buffer (10 mM MOPS; 75 mM $CaCl_2$; 10 mM $RbCl_2$; 15 % (w/v) glycerol; pH was adjusted to 6.5 with KOH). The 100–200 μl aliquots were snap frozen in liquid nitrogen for storage at -80° C. The TfbI and TfbII buffers were filter sterilised before use.

To transform *E. coli* cells, the aliquots of competent cells were thawed on ice and mixed with the ligation mixture. The samples were left incubated on ice for 30 minutes, and the the mixture was heat shocked at 42° C for two minutes and chilled on ice for three minutes. The cells were incubated with an additional 1 ml of LB medium on a shaker for one hour at 37° C, then spread on agar plates with the selection antibiotic.

3.2.5 Isolation of plasmid DNA

The colonies of *E. coli* cells after transformation were grown in LB medum with the appropriate antibiotic for 12 to 16 hours at 37° C. Plasmid DNA was isolated using the plasmid purification kits FastPlasmid Mini (Eppendorf), QIAfilter Midi (Qiagen), and QIAfilter Maxi (Qiagen), according to the amount of DNA required. Purifications were performed according to the manufacturers' instructions. The DNA concentration and quality was determined on a Beckman DU530 Spectrophotometer by reading the absorption at 260 and 280 nm.

3.2.6 PCR

Oligodeoxynucleotides for PCR reactions were synthesized by Sigma-Genosys (Table 2). The PCR reactions were performed with TaKaRa LA Taq (Takara Bio Inc.), Taq polymerase (Roche), or PfuTurbo (Stratagene) according to the manufacturers' instructions.

TaKaRa polymerase was used in a mixture (30:1) with PfuTurbo for PCR amplication of fragments over 1 kb where high fidelity was required.

Table 2. PCR primers employed in this study

Primer name	Primer sequence	Used to construct
KS5 hICAD s	fw 5'-AGCTCTAGAATGGAGGTGACCG-3'	AA4.15
KS6 hICAD a	rv 5'-AGCGAATTCCTATGTGGGATCCTG-3'	AA4.15

KS7 hCAD s	fw 5'-AGCTCTAGAATGCTCCAGAAGCCC-3'	AA4.18
KS8 hCAD a	rv 5'-AGCAAGCTTTCACTGGCGTTTCCG-3'	AA4.18
KS13 ICAD 5' probe s	fw 5'-ATCCAAACATAAGCATGT-3'	
KS14 ICAD 5' probe a	rv 5'-ATGTTGTGTTAGTATGGG-3'	
KS15 ICAD 3' probe s	fw 5'-CAAGAAAGCAAGTAGTGG-3'	
KS16 ICAD 3' probe a	rv 5'-TTATAAACATTTTCCTTT-3'	
KS23 cICAD 3arm s	fw 5'-ACTACTAGTGCATGCGACTATAGTTCTGCC-3'	AA4.6
KS24 cICAD 3arm a	rv 5'-ACTGCGGCCGCAAGTTCATGAGGCTTTGTG-3'	AA4.6
Sa11 TEV-EV	fw 5'-GGTACAGCTTGGATATCCCAAGAGTCC-3'	AA5.1
Sa12 TEV-EV	rv 5'-GGACTCTTGGGATATCCAAGCTGTACC-3'	AA5.1
Sa18 TEV1 a	rv 5'-TGGACAGATCTTCTTTCAGCTGCCTGGCCAC ATTCTTCCACTTCAACCCTGCCCCGC-3'	AA5.2
Sa21 TEV2 s	fw 5'-GCCTCTTGTCAAAGCAGGAAGAGTCCAAAGCT GCCTTTGGTGAGGAGGTGGAGAACCTCTACTTCCA GAGCGACACGGGTATCAGCAGAGAGACCTCCTC G-3'	AA5.4
Sa22 TEV2 a	rv 5'-CCTGACTAGATAAGCTCAGCTCTGGAGCCTGC TTCTCCCTCAGTGCAGTAAGGATGTGGCTCGCCAG CGCAACGTCCGAGGAGGTCTCTCTGCTG-3'	AA5.4
Sa25 TEV1 s	fw 5'-GCTTGGATATCCCAAGAGTCCTTTGATGTAGA GAACCTCTACTTCCAGAGCGACAGCGGGGCAGGGT TGAAGTGG-3'	AA5.2
Sa26 TEV2 short s	fw 5'-GCCTCTTGTCAAAGCAGGAAGAGTCCAAAGC TGCCTTTGG-3'	AA5.5
Sa27 TEV2 short a	rv 5'-CCTGACTAGATAAGCTCAGCTCTGGAGCCTG CTTCTCCCTCAG-3'	AA5.5
Sa36 TEV-Tet-On s	fw 5'-CCGGAATTCATGCCAAAGAAGAAGCGTAAGG-3'	AA5.14
Sa37 TEV-Tet-On a	rv 5'-GCTCTAGATTAATCAACTTTTCGTTTC	AA5.14
Sa54 cICAD cDNA a	rv 5'-TTA TTT TTT GCG TTT TGA ACT AAG CCC-3'	AA6.2
Sa56 cICAD-cDNA-no stop a	rv 5'-ATAGTTTAGCGGCCGCC TTT TTT GCG TTT TGA ACT AGC CC-3'	AA6.3
Sa72 cICAD s	fw 5'-ATGGCGGCGCGGCTGAAGCCGTGCGTGGT GCGGCGGGGCGACGGGCGCGAGCAGCACGGGCT GGCCGCC-3'	AA6.2 AA6.3
Sa75 6His s	fw 5'-ACCCGCTCGAGGGCATCACCATCACCATCA CCTCGAGCCACAC-3'	AA6.5
Sa76 6His a	rv 5'-GTGTGGCTCGAGGTGATGGTGATGGTGATG CCCTCGAGCGGGT-3'	AA6.5
Sa81 hICAD s	fw 5'-ATAAGAAGCGGCCGCATGGAGGTGACCGGG-3'	AA6.10 AA6.12
Sa115 MBP-TEV s	fw 5'-TCAGGGAATTCATGAAAATCGAAGAAGGTAAA CTGG-3'	AA5.16
Sa116 MBP-TEV a	rv 5'-TCAGGGAATTCTTATTATACTTTTCGTTTCTT TTTTGGTACTTTTCGTTTCTTTTTTGGATTCATGAG TTGAGTCGC-3'	AA5.16

Sa121 hICAD-S a	rv 5'-ATGGGCGGCCGC TCAGTGACC CTGGTTTCC GCCCACCTCCAAATCCTGACTAGATAAGCTC-3'	AA6.10 AA6.12
Sa132 cICAD-S a	rv 5'-CTGGGCGGCCGCTCAACCCCTTCTCCAGATAG GTGAGATTTGCCAGAACATGGTTGTATGATCCTCAC CCACCTCTAGAGTTTGACTGTCC-3'	AA6.7
Sa150 cICAD-S s	fw 5'-AACTAGCGGTACCATGGCGGCGCGGCTGAAG CCGTGCGTGG-3'	AA6.7
Sa178 ICAD-Pre s	fw 5'-GGATATCCCAAGAGTCCTTTGATGTACTCGAA GTTCTCTTTCAAGGACCCAGCGGGGCAGGGTTGAA GTGG-3'	AA5.24
Sa179 ICAD-Pre a	rv 5'-AGTGCAGTAAGGATGTGGCTCGCCAGCGCAAC GTCCGAGGAGGTCTCTCTGCTGATACCCGTGGGTC CTTGAAAGAGAACTTCGAGCACCTCCTCACCAAAGG CAG-3'	AA5.24
Sa181 ICAD-Pre-sm s	fw 5'-GGATATCCCAAGAGTCCTTTG-3'	AA5.24
Sa183 ICAD-Pre-sm a	rv 5'-AGCTCAGCTCTGGAGCCTGCTTCTCCCTCAGT GCAGTAAGGATGTGG-3'	AA5.24
Sa184 PreScission s	fw 5'-TCAGGGAATTCATGTCCCCTATACTAGGTTAT TGG-3'	AA5.20
Sa185 PreScission a	rv 5'-TCAGGGAATTCTCATTGTTTCTCTACAAAATA TTGTTTTTTAAGTTGAGCTG-3'	AA5.20

*3.2.7 Introduction of Eco*RV *site into hICAD-L by site-directed mutagenesis*

The QuikChange Site-Directed Mutagenesis Kit (Stratagene) was used to incorporate an *Eco*RV site into hICAD-L cDNA (construct AA5.1). The reaction was performed according to the manufacturer's instructions with primers Sa11 and Sa12.

3.2.8 Construction of hICAD-L^{2TEV}

To construct hICAD-L with two TEV sites (hICAD-L^{2TEV}), DNA Polymerase I, Large (Klenow) Fragment (NEB) was used (see chapter 5.2 and Fig. 5.2). Two long DNA oligos (2 µg each) were boiled for 10 minutes in Klenow buffer (0.01M Tris pH7.7; 0.05 M $MgCl_2$; 0.001M DTT; 1× BSA (NEB)). The reaction was cooled slowly to 37° C to allow oligo annealing. Klenow (40U) was added, together with 10 µl

of a 10 mM solution of each dNTP, bringing the total volume of the reaction to 50 µl. The reaction was incubated at 37° C for two hours, and then the reaction products were separated in a 2.5% agarose gel and purified. The hICAD-L fragment containing the first TEV site (from oligos Sa25 and Sa18) was digested with *Eco*RV and *Bgl*II enzymes and used to replace the corresponding fragment of hICAD-L, containing the caspase-3 site, yielding AA5.1 construct (Table 1). The hICAD-L fragment containing the second TEV site (from oligos Sa21 and Sa22) was cloned into the intermediate vector pGEM-T-Easy, which contains a single 3' T overhang for cloning of DNA products, which have a single 3' A overhang. To do this cloning it was first necessary to incorporate the 3' A overhang into the hICAD-L fragment containing the second TEV site. Therefore, it was incubated with TaKaRa LA Taq (Takara Bio Inc.). The reaction was performed at 68° C for 10 minutes, and then the product was gel purified and cloned into pGEM-T-Easy (construct AA5.4). A further extension was performed in a PCR reaction with oligos Sa26 and Sa27 (construct AA5.5), and fragments containing the first and the second TEV sites in the hICAD-L protein were combined (construct AA5.6).

3.2.9 Construction of hICAD-L^{2PRE}

To construct hICAD-L with two PreScission protease sites (hICAD-L^{2PRE}), a two-step PCR reaction was used (see chapter 5.6 and Fig. 5.7). The hICAD-L fragment containing two PreScission protease sites (Cordingley et al., 1990; Walker et al., 1994) was amplified with Sa178 and Sa179 primers during the first seven cycles of the PCR reaction. Then the product was diluted 100 times and used as a template for the second PCR reaction with primers Sa181 and Sa183, which was performed during the next

thirty cycles. The reaction was performed with TaKaRa LA Taq (Takara Bio Inc.). All other reaction conditions were as recommended by the manufacturer.

3.2.10 DNA sequencing

The BigDye Terminator v3.1 cycle sequencing kit (Applied Biosystems) was used for sequencing the plasmid constructs. Reactions were performed according to the manufacturer's instructions with 300 ng of plasmid DNA and 1.6 pM of the sequencing primer. The DNA sequencing reactions were analysed on the ABI 3100 sequencing machine by the School of Biological Sciences Sequencing Service, University of Edinburgh.

3.2.11 Isolation of total RNA and RT-PCR

Total RNA was prepared from DT40 or HeLa cells using the TRIzol reagent (Invitrogen). RNA isolations were performed according to the manufacturer's instructions. cDNA was synthesised from 5 μg of total RNA using SuperScript First–Strand Synthesis System for RT-PCR (Invitrogen). As a negative control, no reverse transcriptase was added during the first-stand synthesis. The first-strand cDNA was amplified in a PCR reaction with TaKaRa La Taq (Takara Bio Inc.) for full-length cDNAs, or Taq Polymerase (Roche) for cDNA fragments. The list of primers used in the RT-PCR reactions is summarised in Table 3.

Table 3. RT-PCR primers used in this study

Primer name	Primer sequence	Target mRNA	cDNA length (bp)	Description
KS7 hCAD s	same as in table 2	hCAD	1017	full-length
KS8 hCAD a	same as in table 2	hCAD	1017/ 307	full-length/ fragment
Sa64 hCAD RT s	fw 5'-CAAGACACTCCATC AACCCC-3'	hCAD	307	fragment
KS5 hICAD s	same as in table 2	hICAD-L	996	full-length

KS6 hICAD a	same as in table 2	hICAD-L	996/ 211	full-length/ fragment
Sa61 hICAD RT s	fw 5'-TGGTTACCAAGGAA GACCCC-3'	hICAD-L^{2PRE}	211	fragment
Sa164 cICAD-S RT s	fw 5'-TGGAACTCTACTTAG AGGCC-3'	cICAD-S	271	fragment
Sa161 cICAD-S RT a	rv 5'-TCAACCCCTTCTCCA GATAGGTGAG -3'	cICAD-S	271	fragment
Sa194 Pre RT s	fw 5'-CTAGAGCTTACAGTG TTGAC-3'	PreScission	304	fragment
Sa197 Pre RT a	rv 5'-GCTGAAAATCCTTGT CTTCC-3'	PreScission	304	fragment

3.3 Tissue culture

3.3.1 Tissue culture of DT40 cells

The chicken DT40 B cell lymphoma cell line was cultured at 39° C in RPMI 1640 medium with L-glutamine (Invitrogen) supplemented with 10% FBS (foetal bovine serum) (Sigma) and 1% chicken serum (Invitrogen). To transfect DT40 cells by electroporation, 10 µg of DNA was added to 5-10×10^6 cells and electroporated (950 microfarads, 300 V on a Bio-Rad Gene Pulser system) in OptiMEM I medium (Invitrogen). The cells were then incubated for 24 hours to recover after electroporation. For stable integration of plasmid DNA, the transfected cells were plated into 96 well dishes with the drug for selection, and after 7 to 10 days, individual clones were isolated. The list of stable cell lines constructed is summarized in Table 4. The following concentrations of drugs were used for selection of stable cell lines: Puromycin 0.5 µg/ml (Calbiochem), Zeocin 275 µg/ml (Invitrogen), Histidinol 1 mg/ml (Sigma), and Hygromycin B 1.75 mg/ml (Calbiochem). Doxycycline (Dox) 1 µg/ml (Calbiochem) was added to induce the Tet-On system in the DT40 cells.

Table 4. The list of stable cell lines

	Stable cell line name	Genotype	Stably expressed protein/ plasmid transfected	Made from
SC4.1	DT40 wt	($ICAD^{+/+}/CAD^{+/+}$)		(Winding and Berchtold, 2001)
SC4.2	CAD knockout	($ICAD^{+/+}/CAD^{-/-*}$)		(Samejima et al., 2001)
SC4.3	CAD knockout with loxP-neo-loxP cassette	($ICAD^{+/+}/CAD^{-/-**}$)	– /AA4.3	SC4.2
SC4.4	CAD knockout with removed loxP-neo-loxP cassette	($ICAD^{+/+}/CAD^{-/-}$)	– /AA4.19	SC4.3
SC4.5	ICAD heterozygote with loxP-puro-tk-loxP cassette	($ICAD^{+/-*}/CAD^{+/+}$) and ($ICAD^{+/-*}/CAD^{-/-}$)	– /AA4.12	SC4.1 and SC4.4
SC4.6	ICAD heterozygote with removed loxP-puro-tk-loxPcassette	($ICAD^{+/-}/CAD^{+/+}$) and ($ICAD^{+/-}/CAD^{-/-}$)	– /AA4.19	SC4.5
SC4.7	ICAD knockout (clones a and b)	($ICAD^{-/-}/CAD^{+/+}$)	– /AA4.13	SC4.6
SC4.8	ICAD/CAD double knockout (clones a and b)	($ICAD^{-/-}/CAD^{-/-}$)	– /AA4.13	SC4.6
SC4.9	hCAD	($ICAD^{-/-}/CAD^{-/-}$)	hCAD/AA5.10	SC4.8
SC4.10	hICAD-L:hCAD	($ICAD^{-/-}/CAD^{-/-}$)	hICAD-L/AA4.17 hCAD/AA5.10	SC4.9
SC5.1	hCAD (clones a and b)	($ICAD^{-/-}/CAD^{-/-}$)	hCAD/AA5.10 rtTA/AA5.11	SC4.8
SC5.2	hICAD-L^{2TEV}/hCAD (clones a and b)	($ICAD^{-/-}/CAD^{-/-}$)	hICAD-L^{2TEV}/AA5.6 hCAD/AA5.10 rtTA/AA5.11	SC5.1
SC5.3	TEV, hICAD-L^{2TEV}/hCAD, (clones a and b)	($ICAD^{-/-}/CAD^{-/-}$)	TEV/AA5.14 hICAD-L^{2TEV}/AA5.6 hCAD/AA5.10 rtTA/AA5.11	SC5.2
SC5.4	MBP-Tev^{site}-mTEV protease	($ICAD^{-/-}/CAD^{-/-}$)	MBP-TEV/AA5.18 hICAD-L^{2TEV}/AA5.6 hCAD/AA5.10 rtTA/AA5.11	SC5.1
SC5.5	PreScission/hICAD-L^{2PRE} (clones a, b, e)	($ICAD^{-/-}/CAD^{-/-}$)	PreScission/ AA5.21 hICAD-L^{2PRE} /AA5.26	SC4.8
SC5.6	PreScission/hICAD-L^{2PRE} (clones c and d)	($ICAD^{-/-}/CAD^{-/-}$)	PreScission/ AA5.21 – /AA5.26	SC4.8
SC5.7	hICAD-L^{2PRE}:hCAD (clones a and b)	($ICAD^{-/-}/CAD^{-/-}$)	hICAD-L^{2PRE} /AA5.26 hCAD/AA5.10	SC4.9

SC6.1	hICAD-S^{2TEV}:hICAD-L:hCAD	($ICAD^{-/-}$/$CAD^{-/-}$)	hICAD-S^{2TEV}/ AA6.15 hICAD-L/AA4.17 hCAD/AA5.10	SC4.10
SC6.2	hICAD-S:hICAD-L:hCAD	($ICAD^{-/-}$/$CAD^{-/-}$)	hICAD-S/ AA6.14 hICAD-L/AA4.17 hCAD/AA5.10	SC4.10
SC6.3	hICAD-S:hCAD	($ICAD^{-/-}$/$CAD^{-/-}$)	hICAD-S/ AA6.14 hCAD/AA5.10	SC4.9
SC6.4	cICAD-S (clones a, b, c)	($ICAD^{-/-}$/$CAD^{+/+}$)	cICAD-S/AA6.8	SC4.7
SC6.5	cICAD-L-SATH:cCAD	($ICAD^{-/-}$/$CAD^{-/-}$)	cICAD-L-3tag/ AA6.6 cCAD/AA6.9	SC4.8

$CAD^{-/-*}$ - CAD allele with blasticidin S resistance (bs) marker
$CAD^{-/-**}$ - CAD allele with loxP-neo-loxP cassette replaced for Bs resistance cassette
$ICAD^{+/-*}$ - ICAD allele with loxP-puro-tk-loxP cassette

3.3.2 Transfection of DT40 cells by nucleofection

DT40 cells (1×10^7) in the logarithmic growth phase were used for nucleofection. The cells were centrifuged at 1500×g for five minutes, then washed with PBS and centrifuged again at 1500×g for five minutes. The cells were resuspended in 100 µl of Nucleofector solution from the Cell Line Nuclefector Kit V (Amaxa Biosystems) with an additional 10 µg of plasmid DNA. The sample was nucleofected using programme B23 of the Nucleofector II (Amaxa Biosystems). After nucleofection, the cells were transferred to growth media.

3.3.3 Tissue culture of HeLa cells

HeLa cells were cultured attached in RPMI 1640 media with L-glutamine (Invitrogen) supplemented with 10% FBS (Sigma) at 37°C. The cells were detached from the flasks with 1% trypsin (Invitrogen).

3.4 Methods for the analysis of DT40 cells

3.4.1 Annexin V-staining

The progress of cells into apoptosis upon treatment with 10 μM etoposide was assessed with the Annexin-V-FLUOS Staining Kit (Roche Applied Science, Burgess Hill, UK) according to the manufacturer's instructions. Annexin V-stained cells were diluted in PBS and analysed using a Becton Dickinson Calibur flow cytometer. The Cell Quest software was used for data acquisition and analysis.

3.4.2 Living cell quantification analysis with trypan blue

DT40 cell suspensions were mixed with an equal amount of 0.4 % trypan blue solution (Sigma-Aldrich). After five minutes, the mixture was transferred to the chambers of a hemocytometer. Cells that excluded trypan blue were scored as living.

3.5 Targeted disruption of the *Gallus gallus* ICAD gene

To construct the ICAD knockout, a phage was isolated by Dr. Kumiko Samejima containing an approximately 18 kb fragment of the chicken ICAD genomic region through screening of a λ FIX II DT40 genomic library. A 9.2 kb fragment of this ICAD phage DNA was sequenced by Matthew A. Sims (GenBank accession number EF632343) and a 2.7 kb open reading frame (ORF) was identified (2614-5318 bp of the *Gallus gallus* genomic sequence), together with 2.6 kb 5' and 3.9 kb 3' non-coding regions (arms) flanking it. To construct the ICAD knockout, I completely removed the ORF using a targeting vector containing a 2.0 kb 5' arm (579-2612 bp) and a 3.4 kb 3' arm (5319-8710 bp) from the non-coding regions. This targeting vector was constructed

by PCR and direct cloning from the ICAD phage DNA into the pBluescript KS (+) vector.

A selection cassette was placed between the 5' and 3' ICAD non-coding regions. Drug resistance cassettes flanked with loxP sites (Arakawa et al., 2001) were used in the targeting vector. For the first targeting, a cassette consisting of the puromycin resistance gene (puro) and the thymidine kinase (tk) gene flanked by mutant loxP sites (loxP-puro-tk-loxP cassette) was used. This was constructed by cloning the Herpes simplex virus tk gene from the plasmid pBT/SP-TK (gift of Adrian Bird) into the loxP-puro-loxP cassette in the pLoxPuro vector (Arakawa et al., 2001). For the second targeting, a loxP-puro-loxP cassette lacking tk coding sequences was used.

The knockout constructs were linearized with restriction enzyme *Kpn*I before transfection into DT40 cells. Stable cell lines were selected with puromycin. After the first targeting, the loxP-puro-tk-loxP cassette was removed by Cre-recombinase expressed from transiently transfected vector pCAGGS-Cre (Araki et al., 1995). Following transfection, cells were diluted and grown for six to seven days to obtain individual colonies without drug selection. Next, cells were replica plated in media with and without the drug to identify clones that had lost the marker due to the removal of the loxP drug resistance cassette.

3.6 Southern Blotting

Throughout the knockout construction procedure, each step was confirmed by Southern blotting. Genomic DNA from DT40 cells was isolated using Tail buffer (50 mM Tris-HCl pH 8.8, 100 mM EDTA, 100 mM NaCl, 1% SDS) supplemented with 0.5

mg/ml proteinase K. The samples were mixed and incubated at 48°C for 12 hours, and then the mixture was shaken vigorously and 6 M NaCl was added (200 µl per 500 µl of Tail buffer). The products were mixed and centrifuged at 18,000 × g for 10 minutes. The supernatant was precipitated with an equal volume of isopropanol and washed with 70% ethanol. Genomic DNA (5 µg) was digested with the restriction enzyme *Bgl*II for 24 hours, then separated on a 0.8% agarose gel. The gel was then processed, and the DNA was transferred to Hybond N nylon membrane (Amersham). DNA hybridizations were performed at 65° C in phosphate buffer (0.5 M Na_2HPO_4/NaH_2PO_4 pH 7.2, 7% SDS) using an external 5'-probe. Following this, the membrane was washed with phosphate wash buffer (0.04 M Na_2HPO_4/NaH_2PO_4 pH 7.2, 1% SDS) at 65° C two or three times for five minutes each.

The 5' ICAD genomic DNA probe (0.5 kb) corresponding to the nucleotides 1-499 of the chicken genomic sequence was amplified in a PCR reaction with KS13 and KS14 primers from the ICAD phage DNA (construct AA4.5). The 3' ICAD genomic DNA probe (0.5 kb) corresponding to the nucleotides 8711-9210 of the chicken genomic sequence was amplified in a PCR reaction with KS15 and KS16 primers. The probes were labelled with ^{32}P (Amersham) using the Megaprime DNA labelling system (Amersham).

3.7 DNA fragmentation and DNA condensation assay

DT40 cells were grown to a concentration of 5×10^5/ml prior to the addition of etoposide (10 µM) to induce apoptosis. Aliquots of cells were harvested at zero, two and four hours, then used either to isolate genomic DNA or for microscopy analysis. To

isolate genomic DNA, cells (2.5×10^6) were disrupted in lysis buffer (500 mM Tris-HCl pH 8.0, 2 mM EDTA, 10 mM NaCl, 1% SDS) and incubated with proteinase K (1 mg/ml) overnight at 48° C. The DNA was extracted with phenol, precipitated with ethanol, resuspended in TE buffer with RNAse A (20 µg/ml), and analysed by gel electrophoresis. In addition, cells from the apoptosis reaction were analysed by fluorescence microscopy. DT40 cells were centrifuged at 63 × g for five minutes onto polylysine-coated microscope slides (BDH Laboratory Supplies) using a Cytospin 3 cytocentrifuge (Shandon). The cells were fixed for five minutes with 4% formaldehyde (Electron Microscopy Sciences) in PBS, washed in PBS, and stained with 1.5 µg/ml 4',6-diamidino-2-phenylindole (DAPI).

3.8 Fluorescence microscopy

Microscopy was performed using a DeltaVision system (Applied Precision, Issaquah, WA) based on an Olympus IX-70 with a Chroma Technology Sedat filter set, driven by the SoftWorx software under standard conditions. Images were deconvolved using the standard SoftWorx deconvolution algorithm.

3.9 SDS-PAGE and Immunoblotting

Protein samples were harvested from DT40 cells and resuspended in PBS at a concentration of 1-1.5 × 10^5 cell equivalents/µl. The samples were sonicated on ice once for 15 seconds using a MSE Soniprep 150 sonifier (Sanyo). Next, 3× SDS Gel-loading buffer (150 mM Tris-HCl pH 6.8; 6% SDS; 0.3% bromophenol blue; 30% glycerol; 300 mM DTT) was added and samples were heated for 6 to 10 minutes (depending on the

sample volume) at 100° C. SDS-PAGE was carried out using the Tris-glycine buffer system (Sambrook and Russell, 2001).

After separation by SDS-PAGE, proteins were transferred by electroblotting to nitrocellulose membranes (Amersham) using transfer buffer (25 mM Tris base; 0.2 M glycine; 0.1% SDS, 20% methanol). Transfers were performed at 220 mAmp for 140 minutes at 4° C. The membranes were rinsed with PBS for one minute, incubated for one hour in a blocking buffer (PBS; 5% milk; 0.05% Tween 20), and then incubated with the primary antibody in PBS supplemented with 1% milk and 0.05% Tween-20. After incubation, the membranes were washed three times for five minutes in the same solution and incubated with the secondary antibody. The membranes were then washed three times for five minutes in PBS with 0.05% Tween-20. The secondary antibody was visualised using ECL Western Blotting Detection reagents (Amersham).

Table 5. Antibodies used for immunoblotting (IB) and immunofluorescence (IF)

Antibody against	species	Source	dilution IB/ incubation time	dilution IF/ incubation time
human ICAD N-terminal	rabbit	Sigma-Aldrich	1:500/ over 12 hours at 4°C	not determined
human ICAD C-terminal	rabbit	Sigma-Aldrich	1:1000/ over 12 hours at 4°C	not determined
Myc	mouse	Cell Signalling	1:1000/ over 12 hours at 4°C	not determined
α-tubulin clone B512	mouse	Sigma-Aldrich	1:4000/ 1 hour at room temp.	not determined
MBP	rabbit	NEB	1:2000/ 3 hours at room temp. no Tween-20 added during the primary antibody incubation	not determined

SBP	mouse	Mayo Clinic Monoclonal antibody core facility	not determined	1:100/ 30 minutes at 37°C
anti-rabbit, HRP conjugated	donkey	Amersham	1:10000/ 1 hour at room temp.	not determined
anti-mouse, HRP conjugated	Sheep	Amersham	1:10000/ 1 hour at room temp.	not determined
anti-mouse, FITC conjugated	Goat	Jackson Laboratories	not determined	1:200/ 30 minutes at 37°C

3.10 Indirect immunofluorescence microscopy with anti-SBP monoclonal antibody

DT40 cells were centrifuged at 63 × g for five minutes onto polylysine-coated microscope slides (BDH Laboratory Supplies) using the Cytospin 3 cytocentrifuge (Shandon). The slides were then fixed for five minutes with 4% formaldehyde (Electron Microscopy Sciences) in PBS, washed with PBS for five minutes, then washed three times (one minute each) with 1 × TEEN buffer (1 mM Triethanolamine:HCl pH 8.5; 0.2 mM NaEDTA; 25 mM NaCl) supplemented with 0.1% Triton X-100 and 0.1% BSA. Anti-SBP monoclonal antibody was added in the TEEN buffer and incubated for 30 minutes at 37° C. After incubation, the slides were washed three times (two minutes, five minutes, and three minutes) with 1 × KB buffer (10 mM Tris:HCl pH 7.7; 0.15 M NaCl; 0.1 % BSA), then incubated with secondary mouse-FITC antibody (Jackson Laboratories) in KB buffer for 30 minutes at 37° C. Slides were then washed three times (two minutes, five minutes, and three minutes) with 1 × KB buffer, stained with DAPI (Vector Laboratories), and analysed using the DeltaVision system.

3.11 Assay for CAD activation *in vitro*

Cytosolic extracts were prepared from DT40 cell lines in exponential growth. The cells were washed once in PBS and then with KPM buffer (50 mM pipes pH 7.0, 50 mM KCl, 5 mM EGTA, 2 mM $MgCl_2$, 1 mM dithiothreitol). No protease inhibitors were added. The pellet was lysed by three cycles of freezing and thawing and subsequent sonication, then centrifuged at 55,000 x g for 30 minutes at 4°C. Each reaction used 75 μg of supernatant extract protein per 2 μg of plasmid DNA in CAD buffer (10 mM HEPES pH 7.4, 50 mM NaCl, 5 mM EGTA pH 8.0, 2 mM $MgCl_2$, 1 mM dithiothreitol) plus an ATP regenerating system (Wood and Earnshaw, 1990). Caspase-3 (200 U, Calbiochem) or TEV protease (20 U, Invitrogen) was added to the reaction mixture containing cell extract and plasmid DNA. After incubation for two hours at 37° C the reaction was terminated by isolating of the plasmid DNA by phenol extraction. The extracted DNA was then electophoresed on a 1.5% agarose gel.

TEV protease buffer (50 mM Tris-HCl, pH 8.0, 0.5 mM EDTA, 1 mM DTT) was used for quick assesement of hICAD-L^{2TEV} cleavage by TEV protease according to the manufacturer instructions. In this case, no plasmid DNA was added.

4. Constructing and characterizing ICAD and ICAD/CAD double knockouts in DT40 cells

4.1 Introduction

CAD is the main nuclease involved in apoptotic DNA fragmentation, while ICAD is its inhibitor and compulsory chaperone. It may be hypothesised that CAD can kill the cell once artificially dissociated from its inhibitor ICAD. This, however, can only be the case if there are no other proteins preventing CAD activation *in vivo* and if CAD can efficiently access the DNA upon its activation. Importantly, some proteins such as nucleophosmin/B23 (Ahn et al., 2005) and CIIA (Cho et al., 2003) have been suggested as potential CAD inhibitors. Therefore, one of the primary aims of my thesis was to activate CAD *in vivo* and to identify whether any constrains other than ICAD can interfere with this activation. This would allow research to shift from exploring the fundamental nature of the ICAD and CAD proteins to investigating their practical application based on the hypothesis that CAD as a nuclease can kill the cell and that such a property can be potentially useful in killing cancer cells.

To identify CAD role in cell death, it was necessary to construct a model system, to be described in Chapter 5. It was, however, first necessary to isolate an ICAD/CAD double knockout in DT40 cells, which are a part of the model system design. Also, in another project, the ICAD null background was used to test the function of ICAD-S and ICAD-L splice forms *in vivo*, either separately or together, in the absence of interference from the endogenous ICAD splice forms, as described in Chapter 6.

The current chapter is focused on the construction and characterisation of the ICAD and ICAD/CAD double knockouts in DT40 cells. The DT40 cell line was used because it is characterised by a high frequency of homologous recombination (Winding

and Berchtold, 2001). The two main features of CAD are its ability to form internucleosomal DNA fragmentation (Enari et al., 1998; Halenbeck et al., 1998; Liu et al., 1998; Liu et al., 1997; Sakahira et al., 1998) and stage II chromatin condensation (Samejima et al., 2001). Therefore, the ICAD and ICAD/CAD double knockouts were assessed for their phenotype in the absence of ICAD and CAD.

4.2 Removal of the puromycin resistance marker from the CAD knockout DT40 cell line

To construct an ICAD/CAD double knockout based on the CAD knockout in DT40 cells (Samejima et al., 2001), it was first necessary to modify a selection marker set of the CAD knockout cell line. The DT40 CAD knockout cell line (Tab. 4) obtained previously (Samejima et al., 2001) contained a blasticidin S resistance (bs) marker in place of one allele and a puromycin (puro) resistance marker in place of the second allele of the CAD gene (Fig. 4.1A). As the puro resistance marker has been proven to be highly effective in the selection of homologous recombinants in the DT40 cell line in Professor Earnshaw's lab, it was decided to remove this marker to allow its future use in the ICAD targeting vector for the construction of the ICAD knockout. Drug resistance cassettes flanked by mutant loxP sites were used for targeting and recycling (Arakawa et al., 2001).

A CAD targeting vector with a neomycin resistance cassette flanked by mutant loxP sites (construct AA4.3) was prepared from the CAD targeting vector made previously by Dr. Kumiko Samejima. This new CAD targeting vector was transfected into the chicken DT40 CAD knockout cell line (SC4.2) and four CAD knockout clones

(SC4.3) with the integrated loxP-neo-loxP cassette instead of the puro resistance marker were selected by resistance to Neomycin and sensitivity to Puromycin (Tab. 4). Isolated clones were analysed by Southern blotting to confirm the targeted removal of the puro resistance marker (Fig. 4.1B lanes 2-5). The targeting efficiency was 14.3%.

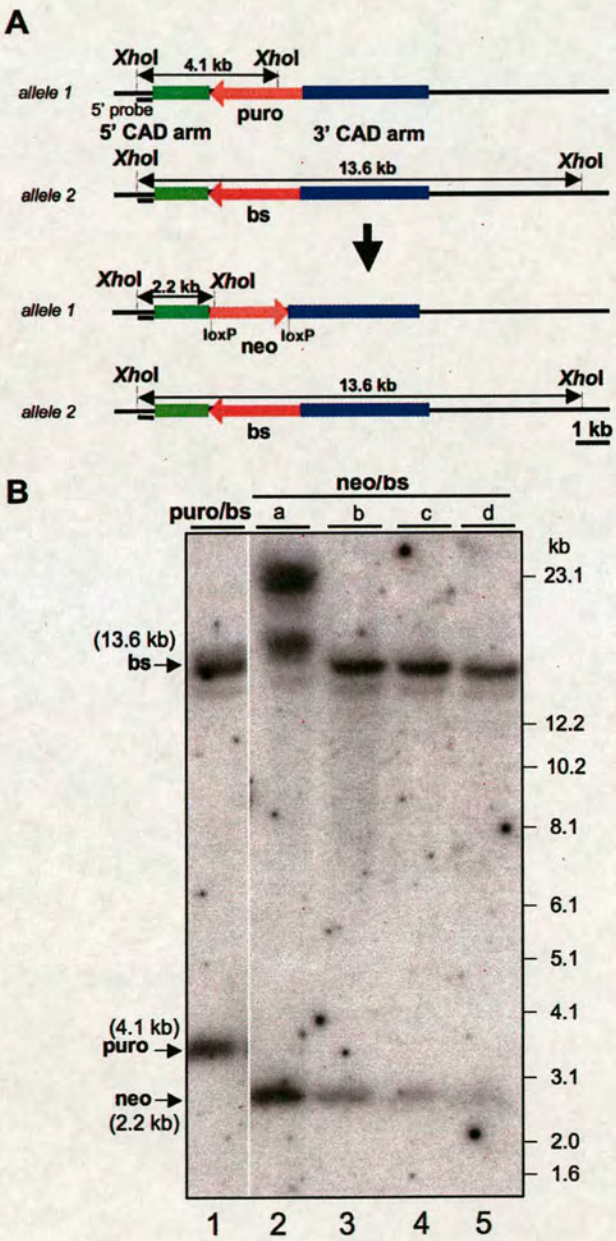

Fig. 4.1. Replacement of puro resistance cassette for loxP-neo-loxP cassette in CAD knockout cells. **(A)** Diagram of the two CAD alleles, which have puro and bs resistance markers. The puro resistance cassette was replaced with a neo resistance cassette flanked by mutant loxP sites. The CAD 5' radioactive probe is located outside the targeting vector. **(B)** Southern Blot. Genomic DNA was digested by *Xho*I.

To recycle the loxP-neo-loxP cassette (Fig. 4.2A) from the CAD knockout cell line (SC4.3 clone c), it was transiently transfected with a pCAGGS-Cre vector (Araki et al., 1995) containing the gene coding Cre recombinase. The clones picked up after the transfection were tested for the resistance to Neomycin by replica plating, and those that died after the addition of Neomycin were isolated (SC4.4). The removal of the neo resistance cassette with mutant loxP sites by Cre recombinase was confirmed by Southern blotting (Fig. 4.2B lanes 1-5). The efficiency of removal was 3.5%.

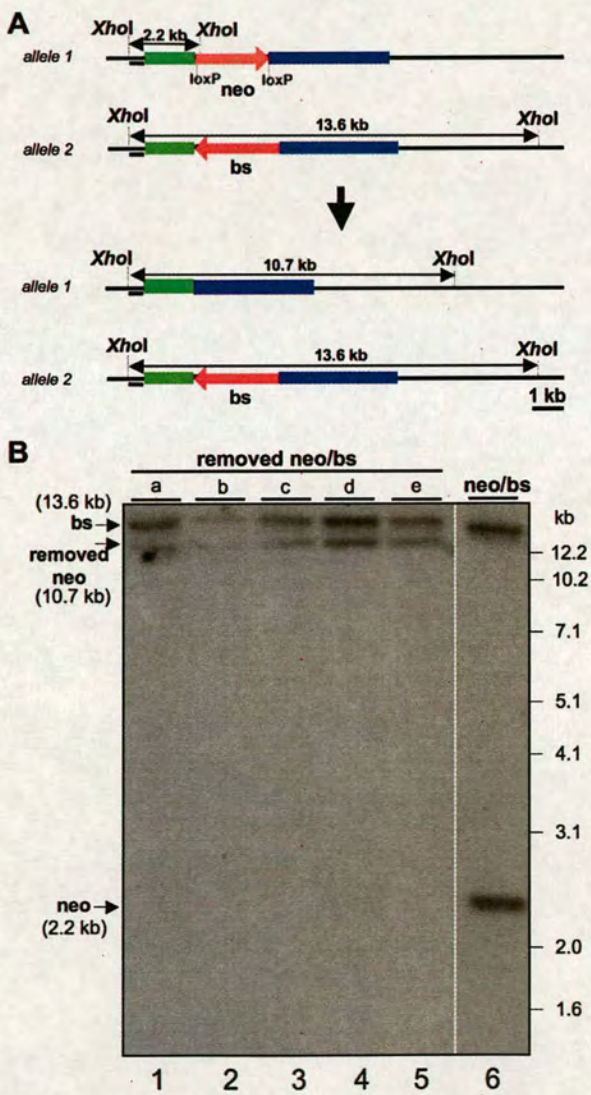

Fig. 4.2. Removal of loxP-neo-loxP cassette by Cre-recombinase. **(A)** Diagram of the loxP-neo-loxP cassette removal from the CAD genomic region. The CAD genomic locus contained bs resistance and neo resistance cassettes in two alleles. The loxP-neo-loxP cassette was removed by transient transfection with vector encoding Cre-recombinase. **(B)** Southern Blot. Genomic DNA was digested by *XhoI*.

4.3 Construction of ICAD and ICAD/CAD double knockouts in DT40 cells

To construct the *ICAD*$^{-/-}$ knockout a phage DNA containing a fragment of the chicken ICAD genomic region was isolated by Dr Kumiko Samejima (GenBank accession number EF632343). In this fragment a 2.7 kb ORF was identified encoding chicken ICAD (Fig. 4.3). ICAD knockout strategy results in complete removal of its ORF. This allowed me to study the function of ICAD-L and ICAD-S separately after their reintroduction into a knockout background in which no fragment of endogenous ICAD protein could be produced.

To delete the ICAD ORF, I constructed a targeting vector containing the 5' and 3' noncoding regions of ICAD but lacking the coding region. A selection cassette (loxP-puro-tk-loxP) was inserted between these non coding regions. A puromycin resistance gene was used for the positive selection of homologous recombinants. The cassette was flanked by mutant loxP sites to allow its removal by Cre-recombinase (Arakawa et al., 2001). The removal of the cassette allows marker recycling so that only a single knockout vector was required to disrupt both alleles. During removal of the cassette by Cre recombinase, two mutant loxP sites are joined to form a single non-functional site that does not interfere with the subsequent use of Cre-recombinase.

I originally planned to use the thymidine kinase (tk) gene for negative selection to detect cassette removal by Cre-recombinase. Such negative selection is achieved when thymidine kinase activates the pro-drug ganciclovir by phosphorylation (Cannon et al., 1999). As a result, clones could be selected in which the *ICAD*$^{-/-}$ knockout

occurred and then subsequently in which the puromycin resistance marker had been removed by Cre recombinase.

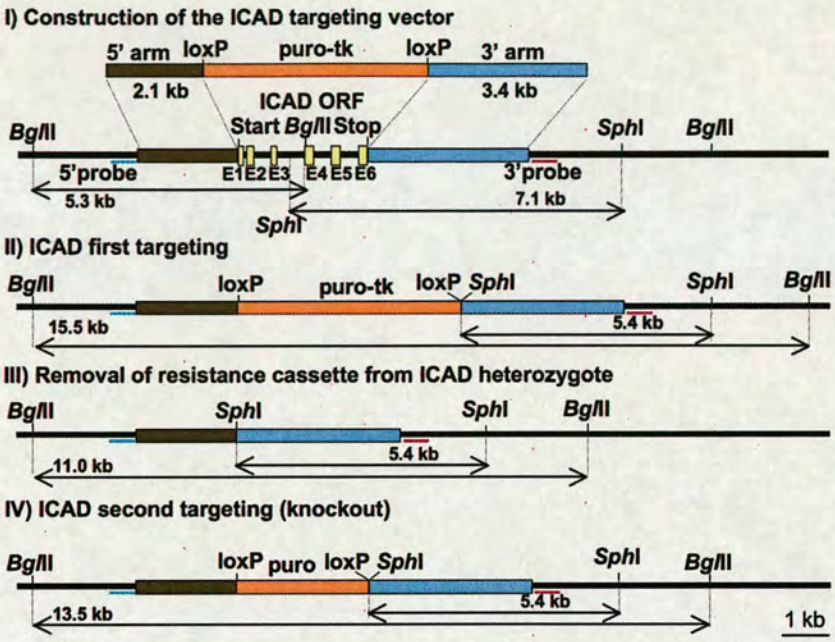

Fig. 4.3. Structure and targeting of the *Gallus gallus* ICAD gene. DT40 ICAD gene and the targeting strategy using a targeting vector with a resistance cassette flanked by ICAD 5' and 3' noncoding genomic regions. The location of 5' and 3' external radioactive probes for Southern Blot analysis is shown. The DNA fragments, which are formed after restriction digest with *Bgl*I and *Sph*I enzymes and recognized by radioactive probes, are shown with arrows.

The ICAD targeting vector (Fig. 4.3) with the loxP-puro-tk-loxP cassette (construct AA4.12) was used to transfect DT40 wild type cells and also DT40 cells with a complete deletion of the CAD gene (Tab. 4). After transfection, clones (SC4.5) were isolated using puro as a selectable marker. Correct targeting was recognized by Southern Blot analysis with a 5'-external probe, using *Bgl*II digested genomic DNA (Fig. 4.4A). The probe recognized a 5.3 kb band corresponding to a DNA fragment from the intact ICAD allele (Fig. 4.4A lanes 1-2) plus a 15.5 kb band corresponding to the integrated

loxP-puro-tk-loxP cassette (Fig. 4.4A lanes 3-4). The correct integration was further verified with an ICAD 3'-external probe (Fig. 4.4B). As a result, heterozygous clones with the genotype $ICAD^{+/-*}/CAD^{+/+}$ and $ICAD^{+/-*}/CAD^{-/-}$ were isolated (the * indicates alleles containing the tk gene). The total targeting efficiency of homologous recombination was 32% for isolating these $ICAD^{+/-}$ heterozygotes.

The use of thymidine kinase as a negative selection marker in DT40 was tested in cell lines containing the integrated ICAD targeting vector bearing the thymidine kinase gene. However, DT40 cells expressing HSV thymidine kinase demonstrated significant resistance to death in medium containing ganciclovir. Ganciclovir could block the growth of these cells over a wide range of concentrations (0.015 - 32 μM). However, after 10-14 days the cells incubated with 0.015 - 4 μM ganciclovir started to grow again, indicating that the drug had failed to kill the cells. The use of drug concentrations higher than 4 μM interfered with the growth rate of DT40 cells even without the exogenous thymidine kinase gene (data not shown). Therefore, ganciclovir appears not to be useful for negative selection in DT40 cells.

To remove the loxP-puro-tk-loxP cassette, $ICAD^{+/-*}/CAD^{+/+}$ and $ICAD^{+/-*}/CAD^{-/-}$ clones were transiently transfected with vector pCAGGS-Cre expressing Cre-recombinase. After transfection, the cells were grown without drug selection, diluted to obtain individual colonies, and then tested for their sensitivity to Puromycin by replica plating. Clones (SC4.6) in which removal of the loxP-puro-tk-loxP cassette had occurred had become sensitive to Puro.

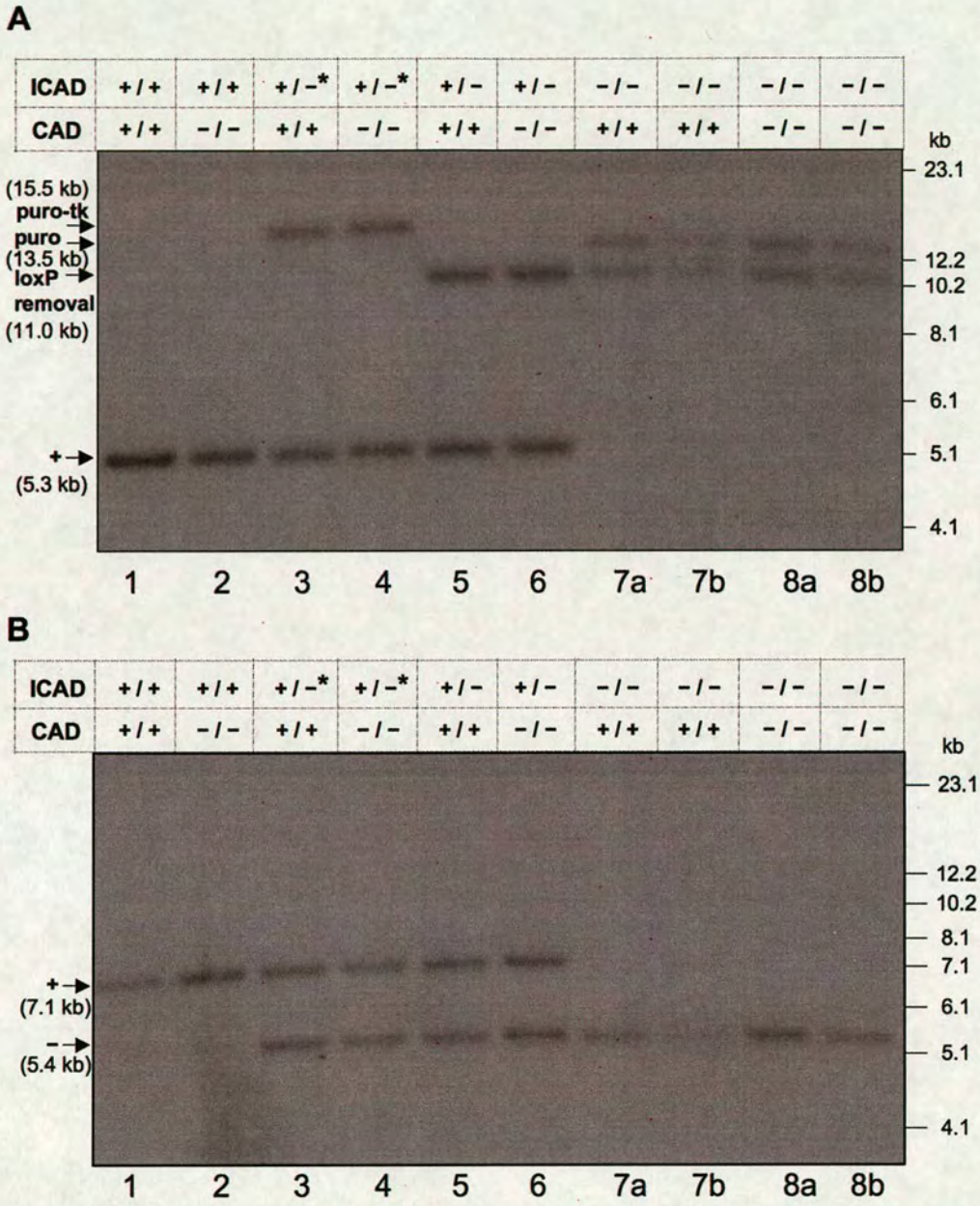

Fig. 4.4. Southern Blot analysis of genomic DNA prepared from the following: *ICAD*$^{+/+}$ (lanes 1-2); ICAD$^{+/-*}$ (ICAD heterozygote with puromycin/tk marker -lanes 3-4); ICAD$^{+/-}$ (ICAD heterozygote with puromycin/tk marker excised - lanes 5-6); and ICAD$^{-/-}$ (lanes 7-8). Genomic DNA (5 μg) was digested by *Bgl*II. The radioactive 5' probe was located outside of the targeting vector. The figure shows data from two independent *ICAD*$^{-/-}$ clones (lanes 7a and 7b) and two independent *ICAD*$^{-/-}$/*CAD*$^{-/-}$ clones (lanes 8a and 8b). **(A)** The genomic DNA was digested with *Bgl*II and analysed with 5' external radioactive probe. **(B)** The DNA was digested with *Sph*I and detected with 3' external radioactive probe.

These clones were further tested by Southern Blotting (Fig. 4.4A). The 5'-external probe recognized the shift from 15.5 kb to 11.0 kb that occurred as a result of the removal of the 4.5 kb loxP-puro-tk-loxP cassette (Fig. 4.4A lanes 5-6). As a result, clones with the genotype $ICAD^{+/-}/CAD^{+/+}$ and $ICAD^{+/-}/CAD^{-/-}$ were isolated. The removal efficiency of the loxP-puro-tk-loxP cassette was 11 %, so lack of the tk selection did not prove to be a significant impediment.

Once the puromycin marker had been removed from the $ICAD^{+/-}$ heterozygotes, it was possible to use the ICAD targeting vector to target the second ICAD allele. An ICAD targeting vector with a loxP-puro-loxP cassette (construct AA4.13) was used for this second targeting. The resulting drug-resistent clones were checked by Southern blotting (Fig. 4.4A). The 5'-external probe recognized the disappearance of the 5.3 kb band corresponding to the intact ICAD allele and appearance of the 13.5 kb band corresponding to the fragment bearing the integrated loxP-puro-loxP cassette (Fig. 4.4A lanes 7-8). The targeting efficiency for the second ICAD allele was 11%. The proper integration of the targeting vector by homologous recombination was confirmed for two clones SC4.7 (a and b) with a single $ICAD^{-/-}$ knockout ($ICAD^{-/-}/CAD^{+/+}$)(Fig. 4.4A lanes 7a-7b) and two clones SC4.8 (a and b) with the $ICAD^{-/-}/CAD^{-/-}$ double knockout (Fig. 4.4A lanes 8a-8b).

4.4. The pattern of apoptosis induction in ICAD and ICAD/CAD double knockouts

To determine whether apoptosis proceeds normally in the $ICAD^{-/-}$ and $ICAD^{-/-}/CAD^{-/-}$ double knockout cell lines, both were tested for the presence of

phosphatidylserine on the outer surface of the plasma membrane following treatment with etoposide. Exposure of phosphatidylserine on the outer leaflet of the plasma membrane reflects the loss of membrane asymmetry that occurs during apoptotic execution (Fadok et al., 1992), and can be detected using the binding of Annexin V (Koopman et al., 1994).

The percentage of Annexin V-positive cells was tested in the wt, *ICAD*$^{-/-}$ and *ICAD*$^{-/-}$/*CAD*$^{-/-}$ double knockouts after the induction of apoptosis with etoposide (Fig. 4.5). There was a small background amount of Annexin V positive cells at 0 time in all of the cell lines. The number of Annexin V-positive cells increased dramatically at 2 hours after apoptosis was induced by etoposide, with nearly half of the cells becoming apoptotic at this point. By 4 hours most of the cells were Annexin V-positive, with only minimal changes in the cultures thereafter. No difference in the kinetics of phosphatidylserine exposure was observed between the wild-type, *ICAD*$^{-/-}$ and *ICAD*$^{-/-}$ *CAD*$^{-/-}$ cells, indicating that deletion of the ICAD gene, either singly or in combination with CAD has no effect on the kinetics of cell death induction by etoposide in DT40 cells. In preliminary experiments the cell death rate measured by trypan blue exclusion appeared to be lower in ICAD and ICAD/CAD double knockouts (data not shown). That is consistent with another study in which mouse thymocytes lacking DFF45/ICAD-L were reported to be more resistant to several proapoptotic stimuli (Boulares et al., 2001; Thomas et al., 2000; Zhang et al., 1999)and suggests that CAD accelerates cellular demise after caspases have been activated.

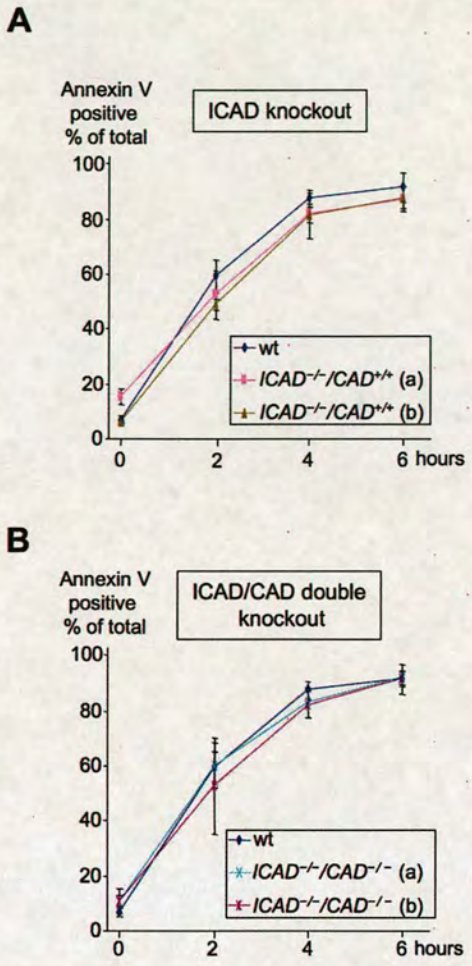

Fig. 4.5. Quantification of phosphatidylserine exposure on the outer leaflet of the plasma membrane of DT40 cells by Annexin V staining. This analysis was carried out for DT40 wt, *ICAD*$^{-/-}$ and *ICAD*$^{-/-}$/*CAD*$^{-/-}$ double knockout cell lines upon induction of apoptosis with 10 μM etoposide. Samples were collected at 0, 2, 4 and 6 hours, stained with Annexin-V-FLUOS and analysed by flow cytometry. The number of Annexin V positive cells is indicated as a percentage of the total. **(A)** Annexin V staining for *ICAD*$^{-/-}$ knockout clones a and b. **(B)** Annexin V staining for *ICAD*$^{-/-}$/*CAD*$^{-/-}$ double knockout clones a and b. The same DT40 wt data are shown in both panels. Experiments were repeated at least three times. The standard deviation is indicated by error bars.

4.5. Oligonucleosomal DNA fragmentation and stage II DNA condensation are absent in DT40 knockout cells lacking ICAD or ICAD plus CAD

Oligonucleosomal DNA fragmentation was undetectable in the *ICAD*$^{-/-}$ knockout and *ICAD*$^{-/-}$/*CAD*$^{-/-}$ double knockout cells upon induction of apoptosis with etoposide (Fig. 4.6A lanes 4-15). In contrast, DNA fragmentation proceeded efficiently in wild type DT40 cells (Fig. 4.6A lanes 1-3). The *CAD*$^{-/-}$ knockout had previously been characterized in DT40 and shown to lack DNA fragmentation (Samejima et al., 2001).

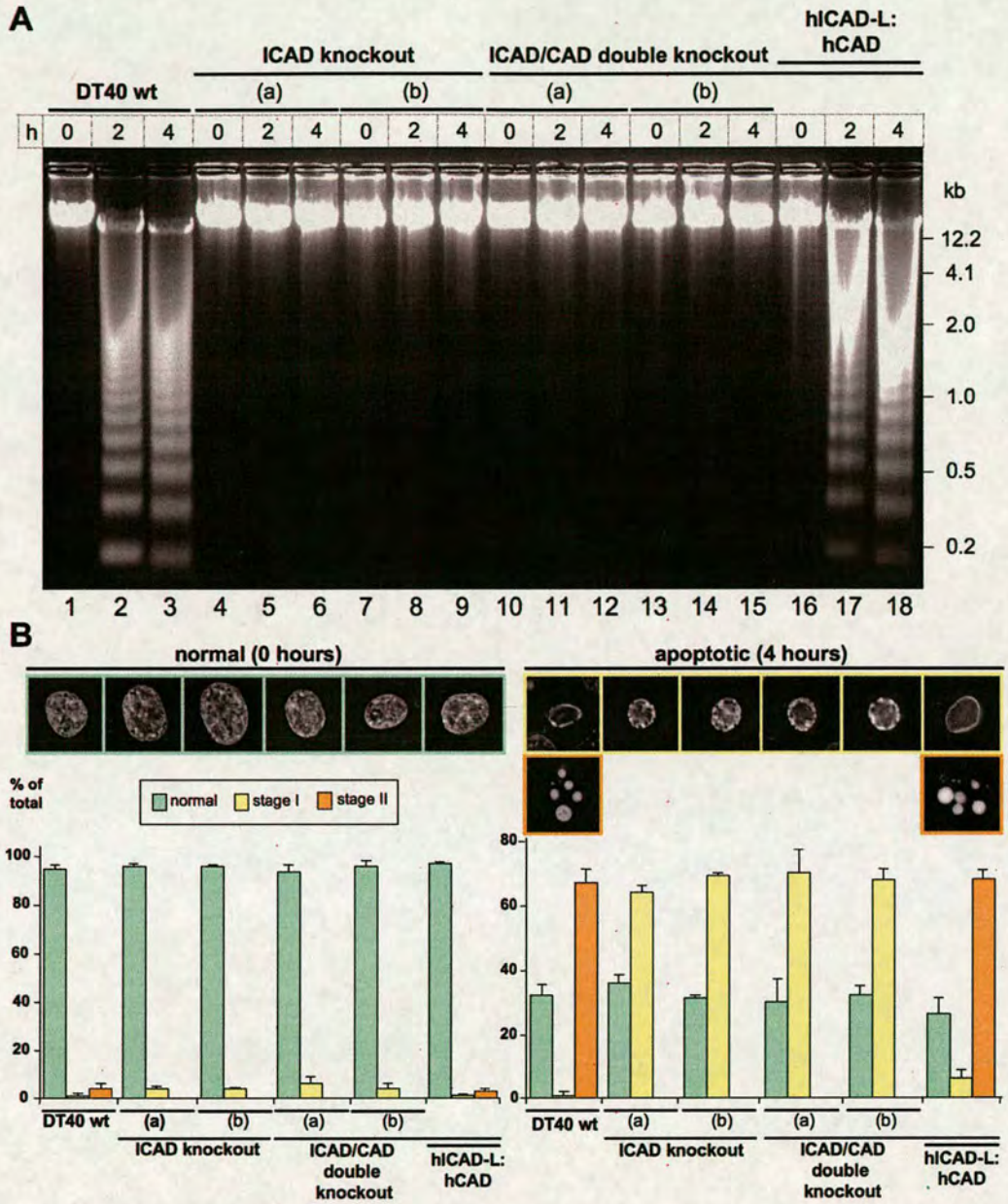

Fig. 4.6. DNA fragmentation and stage II chromatin condensation are absent in ICAD and ICAD/CAD double knockouts following induction of apoptosis by 10 μM etoposide. **(A)** DNA fragmentation. Genomic DNA samples were collected at 0, 2 and 4 hours. Two *ICAD*$^{-/-}$ knockout clones (a - lanes 4-6) and (b - lanes 7-9) and two *ICAD*$^{-/-}$/*CAD*$^{-/-}$ double knockout clones (a - lanes 10-12) and (b - lanes 13-15) were analysed. The stable cell line expressing hICAD-L:hCAD (lanes 16-18) was constructed by introduction of the human cDNAs into the *ICAD*$^{-/-}$/*CAD*$^{-/-}$ double knockout. **(B)** Images of cells before (0 hour) and after (4 hours) induction of apoptosis. DNA was stained with DAPI. The percentage of cells with normal, stage I and stage II chromatin condensation is indicated. Data represent a minimum of at least three independent experiments with over 300 cells counted for each.

The absence of oligonucleosomal DNA fragmentation in the ICAD knockout indicates that ICAD protein is absolutely required as a chaperone for synthesis of active CAD in DT40 cells. This is consistent with results obtained in certain cells from ICAD knockout mice (Zhang et al., 1998).

Chromatin condensation was also affected in *ICAD*$^{-/-}$ knockout and *ICAD*$^{-/-}$/*CAD*$^{-/-}$ double knockout cells (Fig. 4.6B). Stage II chromatin condensation was absent in both knockout cell lines upon induction of apoptosis. Only peripheral (stage I) chromatin condensation was observed. There were no significant differences in the pattern of DNA condensation in *ICAD*$^{-/-}$ knockout and *ICAD*$^{-/-}$/*CAD*$^{-/-}$ double knockout cells, both of which resembled the DT40 *CAD*$^{-/-}$ knockout, characterized previously (Samejima et al., 2001). The induction of apoptosis with etoposide for longer than 4 hours did not result in DNA fragmentation or stage II chromatin condensation in any of these knockout cell lines (data not shown). Therefore, CAD nuclease is required for stage II DNA condensation in DT40 cells, and stage I DNA condensation must be driven by another mechanism.

Interestingly, the phenotype of stage I chromatin condensation in the knockout cells differed slightly from the stage I condensation that is observed normally as the first step in apoptotic chromatin condensation (Fig. 4.6B). In the *ICAD*$^{-/-}$, *CAD*$^{-/-}$ and *ICAD*$^{-/-}$/*CAD*$^{-/-}$ knockout cell lines, terminal stage I condensed chromatin resembled small round balls distributed around the nuclear periphery. In contrast, stage I condensed chromatin in cells undergoing apoptotic chromatin condensation frequently resembles a smooth line of compact chromatin around the nuclear periphery.

4.6. Human ICAD and CAD proteins can rescue the DNA fragmentation phenotype of DT40 ICAD$^{-/-}$/CAD$^{-/-}$ cells.

To test whether ICAD/CAD function as an independent module for chromatin processing in apoptosis I used the *ICAD$^{-/-}$/CAD$^{-/-}$* double knockout cells to construct humanized DT40 cell lines expressing human ICAD and CAD (Tab. 4). DNA fragmentation and stage II chromatin condensation upon induction of apoptosis were completely rescued in *ICAD$^{-/-}$/CAD$^{-/-}$* double knockout cell lines (SC4.10) expressing hICAD-L and hCAD (Fig. 4.6A lines 16-18 and Fig. 4.6B). This humanized cell line provided the basis for our further studies of the role of ICAD-S in CAD regulation.

4.7 Discussion

ICAD/DFF45 and CAD/DFF40/CPAN together compromise a module that is responsible for the destruction of cellular DNA during classical apoptosis (Enari et al., 1998; Halenbeck et al., 1998; Liu et al., 1998; Liu et al., 1997; Sakahira et al., 1998). This module has been widely studied, but several key questions remain, such as the role of the ICAD splice variant ICAD-S *in vivo*, the role of other nucleases, such as endonuclease G, in DNA cleavage during apoptosis and the role of other molecules, including nucleophosmin/B23 and CIIA, as 'back-up' inhibitors of CAD *in vivo*. To address these questions, I constructed a humanized system in which the ICAD and CAD genes of chicken DT40 cells were deleted and the function of the ICAD/CAD module restored by the expression of wild type and variant forms of human ICAD and CAD.

Chicken DT40 cells lacking ICAD, CAD or both are deficient in DNA degradation and in the formation of apoptotic bodies during etoposide-induced apoptosis, but the other aspects of apoptosis appear to proceed with normal kinetics, as shown previously in DT40 $CAD^{-/-}$ (Samejima et al., 2001), mouse $ICAD^{-/-}$ (Zhang et al., 1999) and mouse $CAD^{-/-}$ knockouts (Kawane et al., 2003). In DT40 cells, chromatin condensation is arrested at stage I, with the condensed chromatin appearing as a necklace of small beads around the nuclear periphery. These results confirm that CAD activity is required for full apoptotic chromatin condensation (Samejima et al., 2001). It is possible that cleavage by CAD releases the DNA from local entanglements or associations with nuclear substructures that constrain the condensed DNA into bead-like domains in the absence of CAD activity. Interestingly, whatever these constraints must

be, they are located around the nuclear periphery, as even in the absence of CAD activity, no condensed DNA is detectible in the interior of apoptotic DT40 cell nuclei.

The formation of small, round ball structures in cells with absent CAD may be a specific feature of the factor responsible for the chromatin condensation up to stage I. AIF can contribute to chromatin condensation (Susin et al., 2000; Susin et al., 1999) and, therefore, could be responsible for the stage I phenotype in the cells with absent CAD. This hypothesis can also be supported by the fact the AIF is able to physically interact with DNA and to condense it *in vitro* (Vahsen et al., 2006). Moreover, AIF co-localizes with DNA during apoptosis (Ye et al., 2002). Such co-localisation is particularly evident during stage I chromatin condensation (Ye et al., 2002). In cells expressing the caspase-resistant ICAD mutant to prevent CAD activation, the depletion of AIF by RNAi or blocking antibody affected the phenotype of stage I chromatin condensation (Yuste et al., 2005), yet some chromatin condensation was still observed. Topoisomerase IIα can also contribute to chromatin condensation in HeLa nuclei (Durrieu et al., 2000). Its function in chromatin condensation during the induction of apoptosis with etoposide in DT40 cells may not be seen because etoposide is also a topoisomerase IIα inhibitor. The exact role of AIF, topoisomerase IIα or other factors possibly involved in stage I chromatin condensation remains to be tested.

DNA fragmentation was absent in the ICAD and ICAD/CAD double knockout after the induction of apoptosis. This data is consistent with the previous findings from the DT40 CAD knockout (Samejima et al., 2001), meaning that the phenotype is similar when either ICAD or CAD is absent. Endonuclease G could cause the oligonucleosomal DNA fragmentation in mouse fibroblasts (Li et al., 2001); for an alternative view, see

(Irvine et al., 2005). However, Endonuclease G does not appear to work in DT40 cells. Also, there are no other nucleases, for example, DNAseI (Oliveri et al., 2001) or DNAseII (Kawane et al., 2003), that can cause DNA fragmentation in DT40 cells if activated by the etoposide treatment. This, however, still does not exclude the possibility that some other protein with nuclease activity could be activated in DT40 by alternative apoptotic stimuli.

In addition, as part of my thesis research, the methodology for the recycling of drug resistance cassettes with mutant loxP sites by the transient transfection with Cre-recombinase was optimised for application in DT40 cells. Mutant loxP sites have been previously used in mouse embryonic stem cells and DT40 cells (Arakawa et al., 2001; Araki et al., 1997; Kanayama et al., 2005). The recycling of the loxP tagged sequences in DT40 cells, however, was achieved using MerCreMer, which is an N-terminal and C-terminal fusion of Cre-recombinase with Mer (mutated estrogen receptor) (Verrou et al., 1999). The drawback of this method is that it requires the establishment of a stable cell line expressing MerCreMer (Arakawa et al., 2001). Therefore, I decided to optimise the method used for transient transfection with Cre-recombinase in mouse fertilized eggs (Araki et al., 1995) for application in DT40 cells. The efficiency of the loxP cassette removal without any selection was within the range of 3.5-11%. This variability may be due to the transient transfection efficiency. The advantage of transient transfection is that it allows the isolation of stable cell lines expressing MerCreMer to be bypassed, therefore saving time and one of the valuable selection markers.

5. CAD role in cell death and a new technology for targeted protein cleavage *in vivo*

5.1 Introduction

The hypothesis that activation of CAD on its own can cause cell death makes this nuclease an attractive target for cancer therapy. I have therefore established a model system in DT40 cells to test the role of CAD in cell death (Fig. 5.1). To activate CAD artificially *in vivo* in the absence of apoptosis in order to show whether this is sufficient to kill cells, ICAD must be destroyed. ICAD, however, in addition to its inhibitor function for CAD, also performs a chaperone function during translation that is absolutely necessary for CAD to achieve an active conformation (Enari et al., 1998). Therefore, the destruction of ICAD must be initiated in living cells that have already made CAD protein in the presence of active ICAD. To target ICAD for destruction, the protein must somehow be modified to make it susceptible to an artificial signal for its destruction. This must be done in a cell line with knockouts of the endogenous ICAD and CAD genes to prevent the interference of the endogenous proteins with the newly introduced CAD and modified ICAD genes. Site-specific proteases have been considered for destruction of artificially engineered ICAD protein with recognition sites for specific protease.

Proteolytic enzymes have a wide range of specificities of target protein cleavage. The ones which are site-specific can either be involved in physiological processes in an organism or perform a function during viral infection (Babe and Craik, 1997; Krausslich and Wimmer, 1988; Seidah and Chretien, 1997). Among physiological site-specific enzymes used for proteolysis *in vitro* are activated blood coagulation factor X (Nagai and Thogersen, 1984), α-thrombin (Chang, 1985) and enterokinase (LaVallie et al.,

1993). However, all these proteases have also been reported to cleave unspecifically (Choi et al., 2001; Jenny et al., 2003), in part due to their short recognition sequences, which are five amino acids or less. The shorter the cleavage recognition site, the greater the likelihood that it can be encountered in another protein.

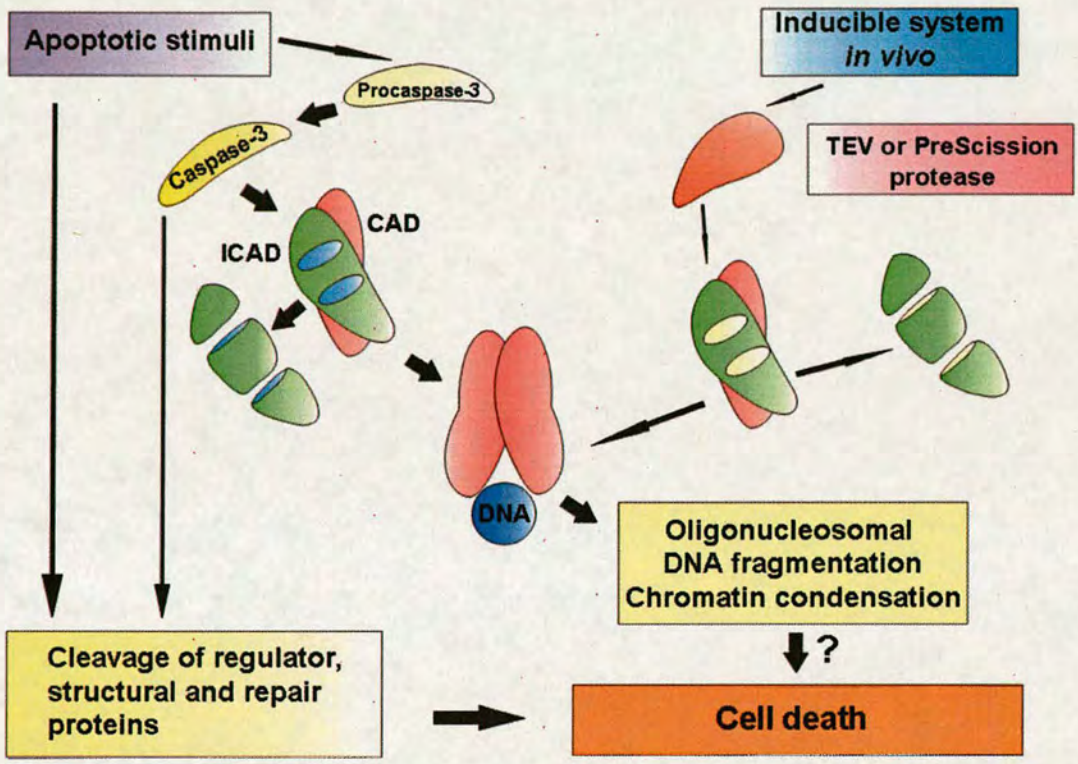

Fig. 5.1. Model system to test whether CAD activation can kill the cell. Apoptotic stimuli cause the activation of multiple pathways leading to cell death through cleavage of regulator, structural and repair proteins. The model system has been designed to test if one of such pathways involves CAD nuclease. ICAD protein was artificially engineered to incorporate either two TEV or two PreScission protease recognition sites instead of two caspase-3 sites. TEV protease or PreScission protease, under the control of inducible system in DT40 ICAD/CAD double knockout, can be used to initiate the cleavage of ICAD protein containing protease recognition sites. That would identify whether specific activation of CAD caused by cleavage of its inhibitor can cause cell death in the absence of apoptotic stimuli.

By contrast, several viral proteases are characterised by stringent sequence specificity (Babe and Craik, 1997). A wide range of viruses can use proteases to enable specific post-translational modifications of their polyprotein products (Krausslich and Wimmer, 1988). At present, TEV (tobacco etch virus) from Invitrogen and PreScission (GE Healthcare) are the only well characterized commercially available site-specific proteases with stringent specificity for their recognition site. TEV and PreScission proteases recognise seven and eight amino acid sites, respectively (Carrington and Dougherty, 1988; Walker et al., 1994). However, both of these enzymes can still cleave their recognition sequences in the presence of certain amino acid variations at some positions within the recognition sequence. TEV and PreScission proteases are extensively used for site-specific protein cleavage *in vitro* (Parks et al., 1994; Walker et al., 1994). In addition, TEV protease was reported to work *in vivo* in *E. coli* (Ehrmann et al., 1997; Mondigler and Ehrmann, 1996) and yeast cells (Smith and Kohorn, 1991; Uhlmann et al., 2000; Yang et al., 2005). There is, however, no published application of any protease for site-specific protein cleavage in vertebrate cells, as far as I am aware. Therefore, one of the aims of my PhD project was to develop a novel technology for site-specific protein cleavage *in vivo*.

5.2 Introduction of TEV protease cleavage sites into human ICAD-L

TEV protease was isolated from a plant pathogen, tobacco etch virus (Carrington and Dougherty, 1987). Mutational analysis identified the seven amino acid sites (Fig. 5.2) efficiently recognized by TEV protease (Carrington et al., 1988; Carrington and Dougherty, 1988). To test the application of TEV protease cleavage in DT40 cells,

hICAD-L protein was artificially modified to introduce two TEV protease cleavage sites in place of the two caspase-3 cleavage sites whose cleavage releases active CAD in apoptosis (Fig. 5.2).

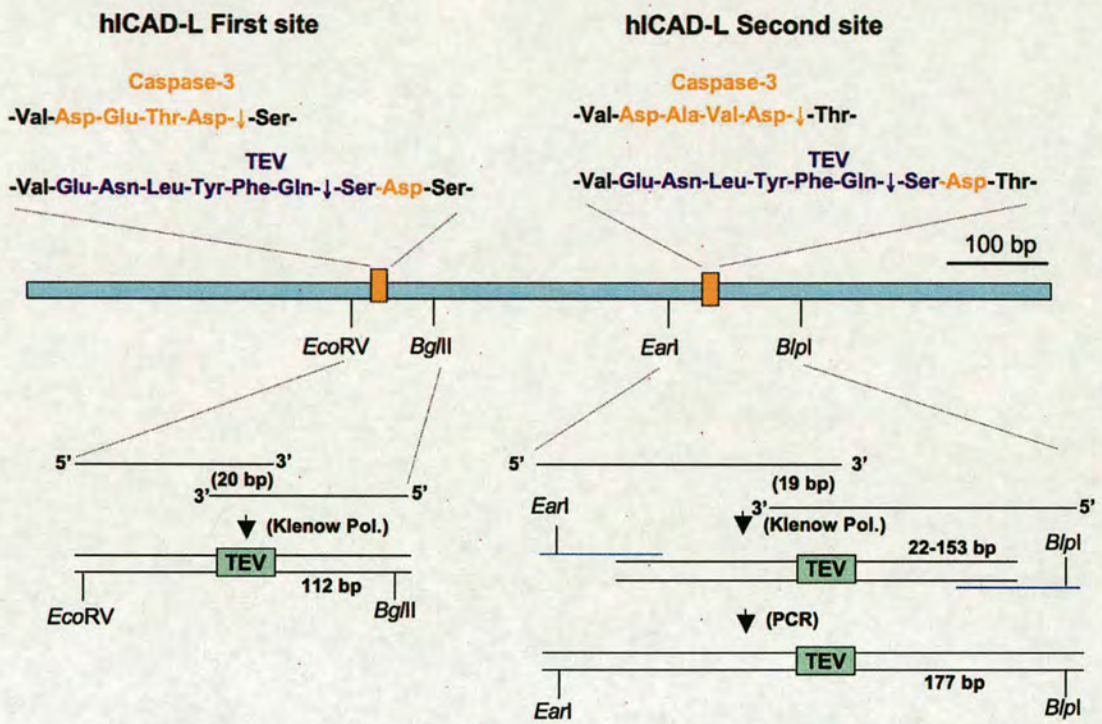

Fig. 5.2. Strategy for replacement of two caspase-3 sites in hICAD-L protein with two TEV protease sites. Caspase-3 has two four amino acid recognition sites in hICAD-L. These sites were replaced by two seven amino acid TEV protease recognition sites. For the first caspase-3 recognition site, a double stranded DNA fragment encoding the TEV protease recognition site was synthesized using Klenow polymerase from two long DNA oligos and then introduced into the hICAD-L cDNA by replacement cloning. A similar approach for the second TEV recognition site yielded only a partial fragment. The desired fragment was obtained by extension using PCR with a long primer, then introduced into the hICAD-L cDNA by replacement cloning.

First, ICAD-L protein was modified by site-directed mutagenesis to introduce an *Eco*RV site, which allowed replacement cloning (construct AA5.1). The mutation did not result in any change of the hICAD-L amino acid sequence. Next, the first TEV site was synthesized using long primers and introduced into hICAD-L by replacement

cloning (construct AA5.2). Then, the second TEV protease cleavage site was synthesized using a similar strategy (construct AA5.4). However, the insertion fragment for the second TEV protease cleavage site was longer than the first one (Fig. 5.2), and the expected full-length product was not obtained. To get the full-length product for replacement cloning required further extension using the PCR reaction with a long primers encoding the missing portions of the sequence (construct AA5.5). As a result, the second TEV protease cleavage site was introduced into the ICAD-L protein (construct AA5.6).

5.3 TEV protease cleaves hICAD-L^{2TEV} and activates hCAD *in vitro*.

To test whether TEV protease can cleave hICAD-L^{2TEV} *in vitro*, cell-free extracts were made from the stable cell line (SC 5.2) expressing hICAD-L^{2TEV}:hCAD. hCAD expression in these cells was confirmed by RT-PCR (Fig. 5.3A). TEV protease was added to the extracts and the reaction was incubated at 37°C for two hours (Fig. 5.3B and C). As a result, the hICAD-L^{2TEV} protein was cleaved by TEV protease *in vitro*. ICAD N-terminal antibody was used to confirm that the cleavage of the first TEV protease site occurred (Fig. 5.3B). The antibody recognises a 13 kDa band, which is the result of hICAD-L^{2TEV} protein cleavage with TEV protease. It was then confirmed that the second TEV protease site was cleaved in the hICAD-L^{2TEV} protein. ICAD C-terminal antibody was used for this purpose (Fig 5.3C). Again, a 10 kDa cleavage product of hICAD-L^{2TEV} protein was detected as a result of TEV protease cleavage of the hICAD-L^{2TEV} second TEV protease site. In both cases, there was no full-length hICAD-L^{2TEV} fragment left.

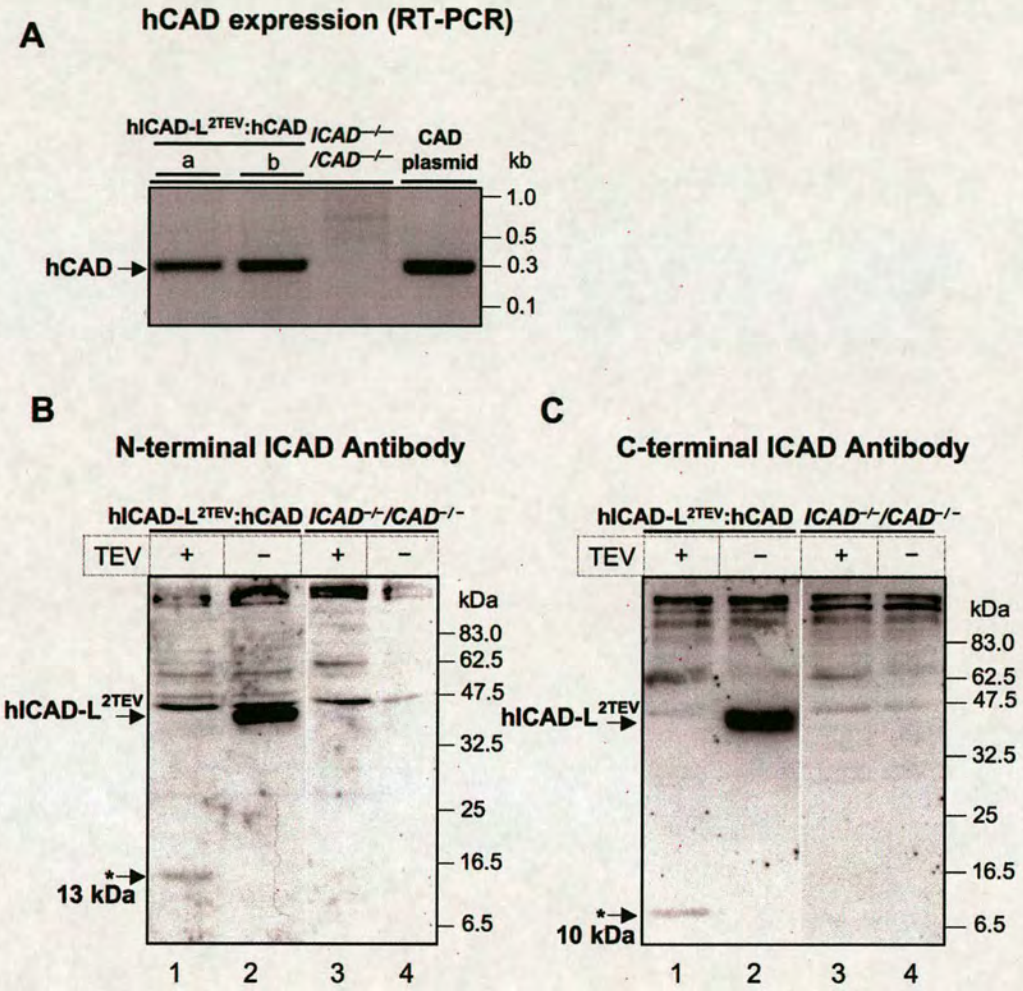

Fig. 5.3. hICAD-L^{2TEV} is cleaved *in vitro*. A stable cell line expressing hICAD-L^{2TEV}:hCAD in DT40 ICAD/CAD double knockout was analysed for hICAD-L^{2TEV} cleavage. **(A)** A hCAD fragment was amplified in RT-PCR reaction. **(B)** Cell-free extract was prepared from the stable cell line. The cleavage of the first **(B)** and second **(C)** TEV sites in hICAD-L^{2TEV} by TEV protease was confirmed, using ICAD N-terminal and C-terminal antibodies, respectively. The hICAD-L^{TEV} cleavage product is marked by an asterisk.

One important question was whether the CAD protease released from the hICAD-L^{2TEV} was catalytically active. Therefore, plasmid DNA was added to the reaction mixture of the hICAD-L^{2TEV} cleavage with TEV protease (Fig 5.4). The

reaction was performed separately in the presence and absence of caspase-3, as there could potentially be other proteins in the cell extract cleavable by caspase-3, which might normally inhibit CAD activation in non-apoptotic cytoplasm. Interestingly, after hICAD-L^{2TEV} cleavage, CAD was activated and degraded the plasmid DNA (Fig. 5.4 lanes 1-2, 5-6). This means that the hICAD-L^{2TEV} protein can also efficiently work as a chaperone and produce active CAD capable of performing the DNA fragmentation reaction. Moreover, the presence or absence of caspase-3 did not make any difference for the reaction.

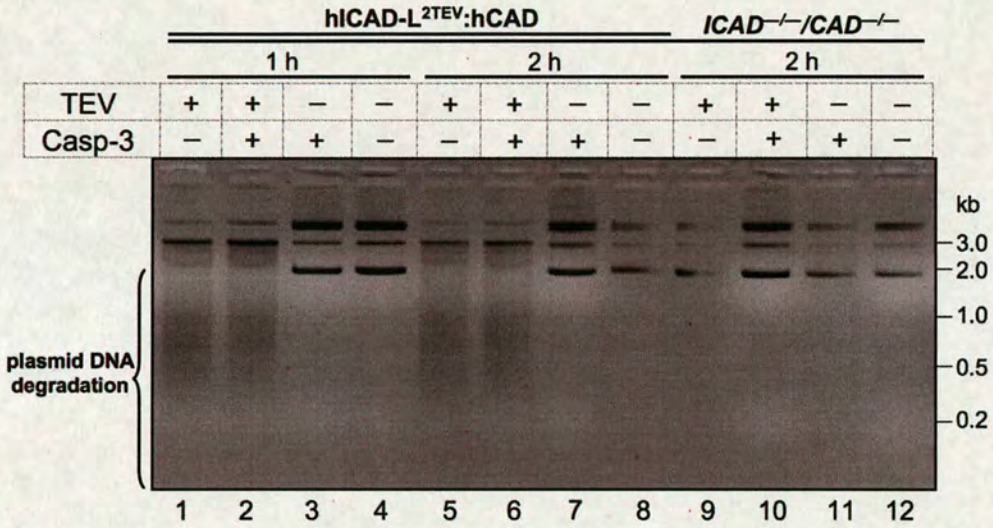

Fig. 5.4. hCAD is activated after hICAD-L^{2TEV} cleavage by TEV protease *in vitro*. Extracts were prepared from stable cell lines expressing hICAD-L^{2TEV}:hCAD (lanes 1-8) in the *ICAD*$^{-/-}$/*CAD*$^{-/-}$ double knockout (lanes 9-12) background. Plasmid DNA was added to each reaction mixture, either alone or with TEV protease, caspase-3, or both. Plasmid DNA was degraded in reactions where hCAD was released as a result of hICAD cleavage. The reaction was performed for one or two hours at 37°C.

5.4 TEV protease is expressed, but does not cleave hICAD-L^{2TEV} protein *in vivo*.

The Tet-On system was used to induce TEV protease *in vivo* (Fig. 5.5A). This system is composed of a reverse tetracycline-controlled transactivator (rtTA) and a promoter sequence containing tetracycline (tet) operators (Gossen et al., 1995). rtTA is a modification of tTA, which consists of Tet Repressor and the activating domain of virion protein 16 of herpes simplex virus (Gossen and Bujard, 1992). Tet repressor normally binds the tet operator in the absence of tetracycline. In the rtTA, a mutation in the Tet repressor reverses that property so that Tet repressor binds to tet operator only when tetracycline is present (Gossen et al., 1995). Therefore, the addition of tetracycline stimulates the binding of rtTA to the tet operator and induces the transcription of the desired gene. Doxycycline (Dox), a member of the tetracycline antibiotic group, was used to induce the Tet-On system in DT40 cells, as Dox is a more efficient inducer for the system than tetracycline (Gossen et al., 1995).

Stable cell lines were constructed expressing TEV protease with two SV40 NLS under the control of the Tet-On system, rtTA, hICAD-L^{2TEV} and hCAD. First, stable cell lines expressing hCAD and rtTA were selected (SC 5.1). hICAD-L^{2TEV} was then introduced into these cell lines (SC 5.2). Finally, TEV protease was introduced under the control of the Tet-On system (SC 5.3). TEV protease expression was induced by adding doxycycline to two SC 5.3 cell lines. As TEV protease has a N-terminal Myc tag, its presence after the induction of Dox was recognised on the Western Blot (Fig. 5.5B).

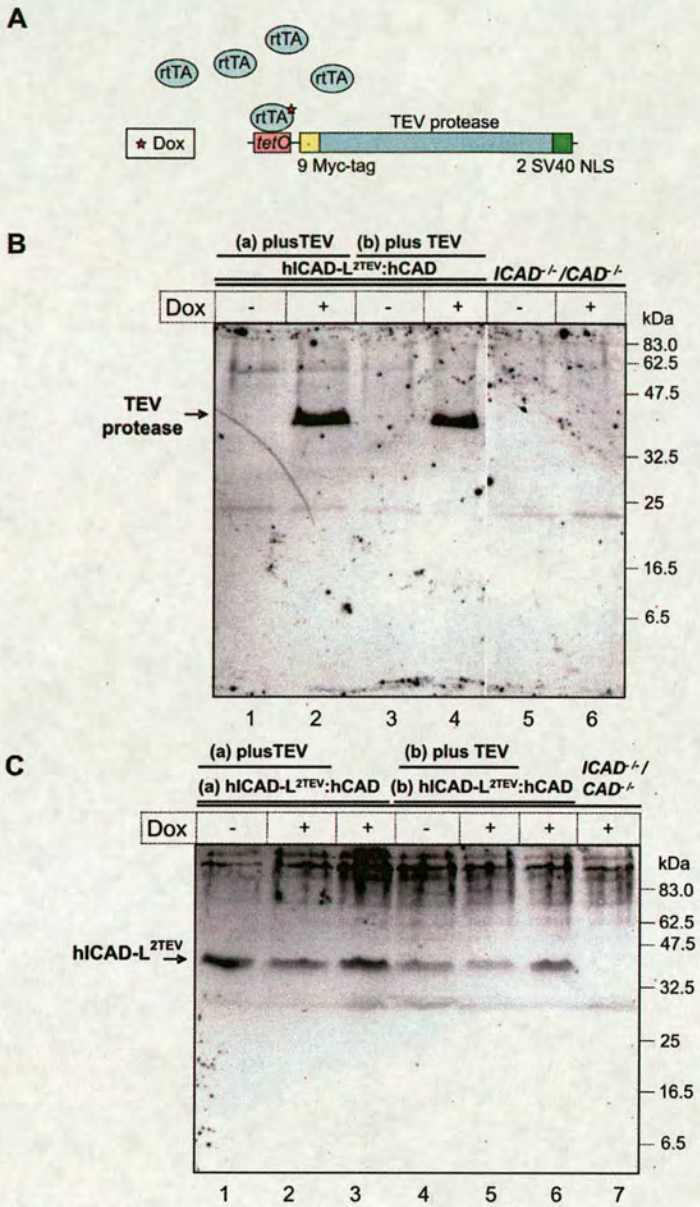

Fig. 5.5. TEV protease is expressed, but does not cleave hICAD-L^{2TEV} protein *in vivo*. Stable cell lines were constructed expressing hICAD-L^{2TEV}:hCAD in the DT40 ICAD/CAD double knockout. In addition, the TEV protease and rtTA for its regulation with the Tet-On system were expressed in two cell lines (a and b). **(A)** The diagram of the Tet-On system function. The expression of TEV protease was controlled by tet operator. rtTA binds to tet operator and activates the transcription only when Dox is added. TEV protease has nine copies of Myc tag on its N-terminus and two SV40 NLS on its C-terminus. **(B)** TEV protease was induced by addition of Dox in two independent cell lines (a and b). TEV protease expression was detected with Myc-tag antibody, which recognizes the Myc-tag located on the N-terminal part of TEV protease. **(C)** The level of expressed hICAD-L^{2TEV} protein amount was monitored with ICAD antibody.

Importantly, the DT40 cells did not die when TEV protease was induced in the model system. It was then checked whether hICAD-L^{2TEV} had been cleaved (Fig. 5.5C), but the hICAD-L^{2TEV} band was unaltered after the induction of TEV protease. Therefore, in contrast to the *in vitro* experiment, TEV protease does not destroy the hICAD-L^{2TEV} protein *in vivo*.

5.5 Mutant TEV protease is only partly active in DT40 cells

As TEV protease was able to perform hICAD-L^{2TEV} cleavage *in vitro* but not *in vivo*, the problem could be in the activity of TEV protease in DT40 cells. Interestingly, one of the studies reported that a mutant version of TEV protease is significantly more efficient than the normal version (Kapust et al., 2001). This was achieved by a mutation that prevents the natural self-cleavage of TEV protease and its resultant progressive inactivation. The mutant version of TEV protease was also reported to be more efficiently catalytically active. As there appeared to be a problem with TEV protease activity in my study, I decided to examine whether the mutant TEV protease could cleave hICAD-L^{2TEV} *in vivo*.

The mutant TEV protease (Kapust et al., 2001) was supplemented with two SV40 NLS on its C-terminus in a PCR reaction (construct 5.16). This was necessary to target TEV protease to the nucleus. The mutant TEV protease was in a fusion with MBP (Maltose-Binding Protein), which promotes TEV protease folding. MBP was previously shown to work as a chaperone in a fusion with other proteins (Kapust and Waugh, 1999). Once TEV protease is synthesised, MBP is removed after TEV cleaves itself off

the MBP-TEV construct using the internal TEV protease recognition site between two proteins (Fig. 5.6A).

The stable cell line (SC 5.4) was assembled expressing mutant TEV protease under control of the inducible Tet-On system in the hICAD-L^{2TEV}:hCAD, rtTA cell line. The mutant TEV protease was induced by adding Dox and the cells were analysed for mutant TEV protease induction and hICAD-L^{2TEV} cleavage (Fig. 5.6).

However, hICAD-L^{2TEV} was not cleaved after the induction of the mutant TEV protease with Dox *in vivo*. hICAD-L^{2TEV} was also not cleaved by endogenous mutant TEV protease during the incubation of lysed cell-free extracts *in vitro* which could have potentially allowed mutant TEV protease to cleave hICAD-L^{2TEV}. Under these conditions TEV would be expected to cleave hICAD-L^{2TEV} even if they were mislocalised in different subcellular compartments *in vivo*. However, hICAD-L^{2TEV} was cleaved when an exogenous TEV protease was added to the reaction mixture, indicating that its two TEV sites are accessible to the protease.

Interestingly, the TEV protease was able to self-cleave off the MBP *in vivo* (Fig. 5.6C lane 3). This was achieved through the cleavage of the TEV protease site between MBP and mutant TEV protease *in vivo*. However, the activity of TEV protease was still insufficient to cleave the hICAD-L^{2TEV} protein *in vivo*.

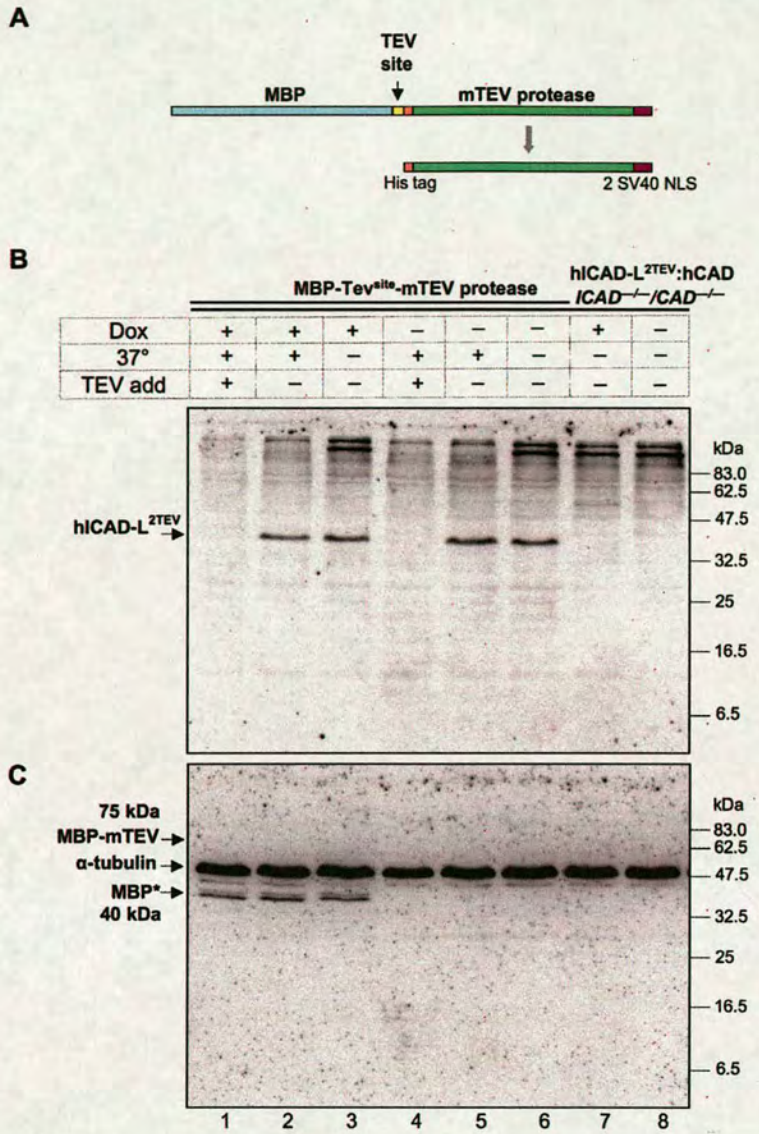

Fig. 5.6. Mutant TEV protease is partly active in DT40 cells but insufficiently to cleave hICAD-L^{2TEV}. **(A)** Diagram of the MBP – mutant TEV protease construct. The construct consists of MBP (Maltose-Binding Protein), followed by the TEV recognition site and mutant (m) TEV protease. Once synthesized, mTEV protease uses the TEV site to cleave itself from the MBP. The released mTEV protease has His tag on its N-terminal and two SV40 NLS on its C-terminal. **(B)** Extracts were prepared from stable cell lines expressing MBP-mTEV protease together with rtTA for its regulation (lanes 1-6) and hICAD-L^{2TEV}:hCAD (lanes 1-8) in the *ICAD*$^{-/-}$/*CAD*$^{-/-}$ double knockout background. The expression of MBP-mTEV was induced by the addition of Dox for 24 hours before cell extract preparation (lanes 1-3). In addition, TEV protease was added to the cell-free extracts *in vitro* (lanes 1 and 4) and the reactions were performed at 37°C for two hours (lanes 1-2 and 4-5). **(C)** The cleavage of the MBP-mTEV construct was detected with MBP antibody (lanes 1-3). MBP cleavage product is marked by an asterisk. The estimated size of full-length uncleaved MBP-mTEV product is 75 kDa.

5.6 Introduction of PreScission protease cleavage sites into hICAD-L

The expression of TEV protease *in vivo* did not result in successful cleavage of the hICAD-L^{2TEV} protein. Therefore, it was decided to change the strategy and to design an alternative way to achieve hICAD-L cleavage.

PreScission protease is one of the most site-specific proteases (Cordingley et al., 1990; Walker et al., 1994). It is a fusion protein derived from GST (glutathione S-transferase) and human rhinovirus 3C protease (Leong et al., 1992), and was designed for the *in vitro* cleavage of GST affinity tags from the purified proteins. In addition, the GST tag in PreScission protease allows the removal of the enzyme from the reaction mixture after cleavage. PreScission protease is used for protein cleavage *in vitro*. However, there is as yet no report of artificially engineered model systems for *in vivo* cleavage with PreScission protease. 3C protease, from which PreScission protease is derived, is able to perform the cleavage of the viral polyprotein precursor during viral infection of human cells. Therefore, an artificial model system for site-specific *in vivo* protein cleavage with PreScission protease could have a potential application in human and vertebrate cells, including DT40. I decided to determine whether PreScission protease can be used for *in vivo* cleavage of target proteins by testing it on a model system involving human ICAD-L with two PreScission sites (hICAD-L^{2PRE}) and hCAD.

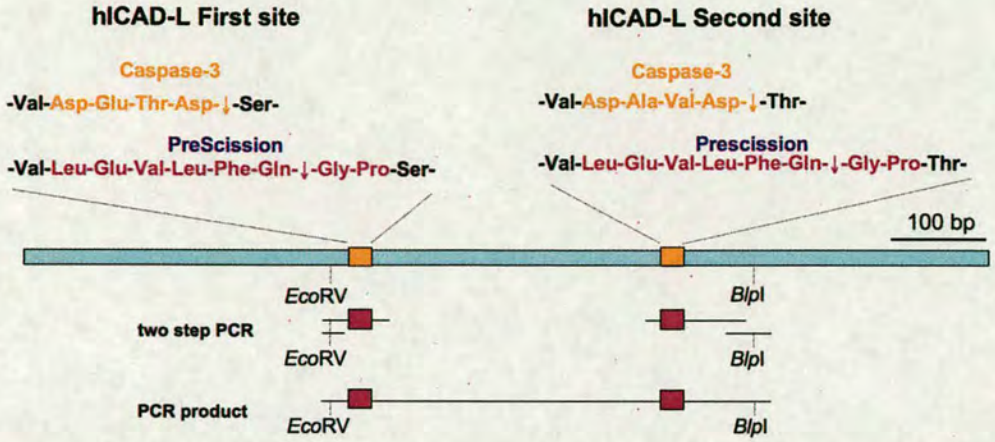

Fig. 5.7. Strategy for replacement of two caspase-3 sites in hICAD-L protein with two PreScission protease sites. Two caspase-3 sites in hICAD-L protein were replaced by two eight amino acid PreScission protease recognition sites. The fragment of hICAD-L protein containing two PreScission protease sites was amplified in a two-step PCR reaction. In the first step, a fragment was amplified using oligos encoding PreScission protease recognition sites. In the second step, in the same PCR reaction, the fragment was further extended to allow replacement cloning using *Eco*RV and *Blp*I sites. The desired fragment was then introduced into the hICAD-L cDNA.

To do this, two caspase-3 recognition sites in the hICAD-L protein were replaced with two PreScission protease recognition sites (Fig. 5.7). The hICAD-L^{2PRE} protein was engineered using a strategy based on that used to create the hICAD-L^{2TEV} protein. Long primers containing sequences encoding PreScission protease recognition sites were used in a PCR reaction to amplify the DNA fragment of ICAD-L protein between cleavage sites together with some flanking sequences. Next, the PCR reaction was continued to extend the 3' part of hICAD-L protein to reach the *Blp*I site (construct 5.24). This allowed replacement cloning of the amplified fragment into hICAD-L protein using *Eco*RV and *Blp*I sites. As a result, the hICAD-L^{2PRE} protein was constructed (construct 5.25).

5.7 New technology for targeted protein cleavage *in vivo* with PreScission protease.

To test whether PreScission protease can cleave hICAD-L^{2PRE} protein *in vivo*, it was decided to establish stable cell lines expressing both the hICAD-L^{2PRE} protein and PreScission protease at the same time under constitutive expression. These stable cell lines were constructed starting with the ICAD/CAD double knockout, so there was no CAD present to be activated. Five stable cell lines were isolated after transfection of the constructs encoding hICAD-L^{2PRE} and PreScission protease; all five showed detectable PreScission protease expression, which was confirmed by RT-PCR (Fig. 5.8A). hICAD-L^{2PRE} mRNA was expressed in three (SC 5.5) out of five of these stable cell lines, and these cell lines were chosen for further analysis. Surprisingly, although these cell lines expressed both PreScission protease and hICAD-L^{2PRE} mRNA, there was no detectable level of the hICAD-L^{2PRE} protein (Fig 5.8B).

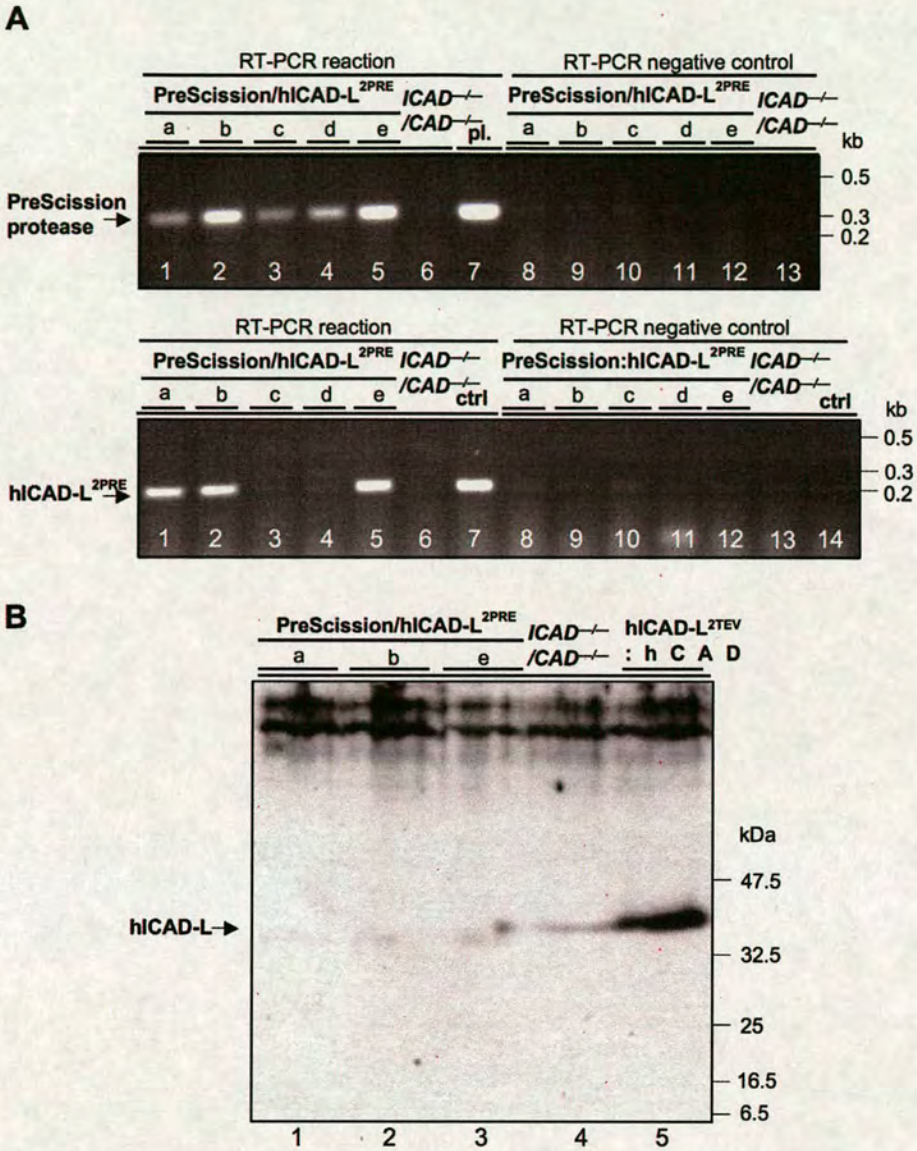

Fig. 5.8. Analysis of stable cell lines expressing PreScission protease and hICAD-L^{2PRE}. **(A)** PreScission protease and hICAD-L^{2PRE} expression was confirmed by RT-PCR. Top panel: Five clones (a, b, c, d, e) were tested for PreScission protease expression (lanes 1-5). Also, ICAD/CAD double knockout (lane 6) and plasmid DNA encoding the PreScission protease gene (lane 7) were used for the reaction. The RT-PCR negative control (lanes 8-13) did not have reverse transcriptase added to synthesize cDNA from RNA. Bottom panel: The same clones were tested for hICAD-L^{2PRE} expression. The stable cell line expressing hICAD-L^{2TEV} (lane 7 and 14) was used as a control for hICAD-L amplification. **(B)** Analysis of hICAD-L expression by immunoblotting in stable cell lines (a, b, e) expressing PreScission protease and hICAD-L^{2PRE} (lanes 1-3), ICAD/CAD double knockout (lane 4) and a cell line expressing hICAD-L^{2TEV}:hCAD (lane 5). ICAD protein was detected with ICAD N-terminal antibody.

To further investigate the stable cell line (SC 5.5b) expressing PreScission protease, it was transiently transfected with the hICAD-L^{2PRE} construct to express increased level of hICAD-L^{2PRE} protein (Fig 5.9A). Transient transfection was performed by nucleofection, which is characterized by a high transfection efficiency and consequently often achieves a high expression level (Martinet et al., 2003). The cell line had the hICAD-L^{2PRE} protein expressed after the transient transfection. Interestingly there were two fragments 12 kDa and 26 kDa corresponding to the predicted size of the cleaved fragments of hICAD-L^{2PRE} protein (Fig. 5.9). Notably, the size of one fragment was 12 kDa, which corresponds to the N-terminal fragment of ICAD-L protein formed after the cleavage of the first site. Another hICAD-L^{2PRE} fragment detected with ICAD N-terminal antibody, had a size 26 kDa. According to the diagram (Fig. 5.9C), this might correspond to the N-terminal fragment of hICAD-L^{2PRE} protein where the second, but not the first, site is cleaved. Finally, in this experiment, proteasome inhibitor MG132 was used to prevent the protein degradation. The cell extracts from the analysed cell lines were also incubated *in vitro* to stimulate the possible additional cleavage of hICAD-L^{2PRE} by PreScission protease.

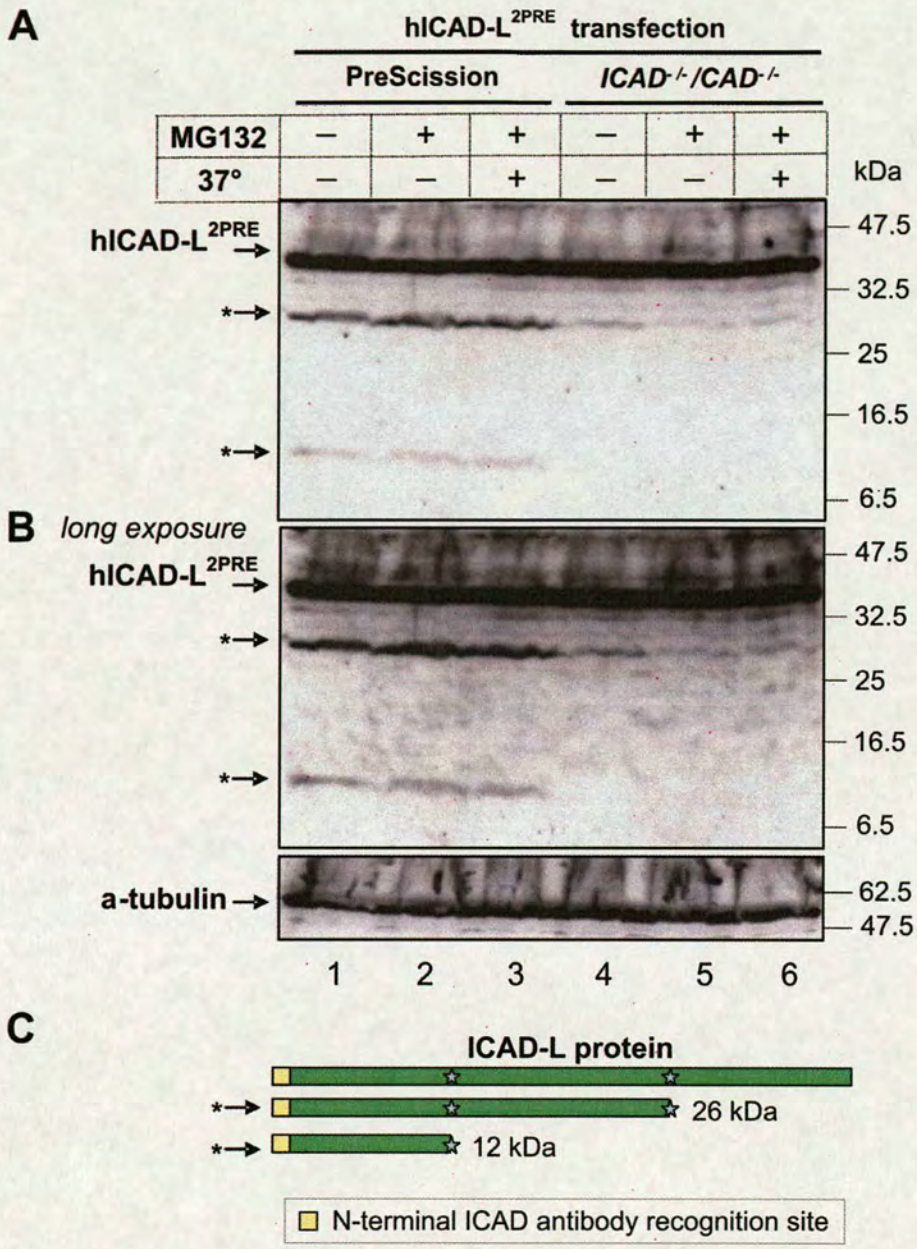

Fig. 5.9. PreScission protease cleaves hICAD-L^{2PRE} *in vivo*.
(A) Transient transfection of hICAD-L^{2PRE} into stable cell line expressing PreScission protease (lanes 1-3) or ICAD/CAD double knockout (lanes 4-6). The cell lines were also treated with proteosome inhibitor MG132 for 6 hours before sample collection (lanes 2 and 5) or cell extracts were incubated *in vitro* for 2 hours at 37° C in the presence of MG132 (lanes 3 and 6). hICAD-L^{2PRE} was detected with ICAD N-terminal antibody. hICAD-L^{2PRE} cleavage product is marked by an asterisk. **(B)** Shows a longer exposure of this blot. **(C)** Diagram of ICAD-L protein showing the predicted size of PreScission cleavage products that could potentially be recognised by ICAD N-terminal antibody.

5.8 Transient transfection of PreScission protease into hICAD-L^{2PRE}:hCAD stable cell lines.

To determine whether CAD can kill the cell once it is activated after cleavage of the hICAD-L^{2PRE} protein with PreScission protease, two stable cell lines (SC 5.7) were constructed expressing the hICAD-L^{2PRE} protein and hCAD. The PreScission protease-expressing vector was transfected into these cell lines by nucleofection. As a control, the cell lines were transfected with the vector alone. At one and two days after nucleofection, the number of living cells was measured by the trypan blue exclusion method. The percent difference in viability between cells transfected with PreScission protease and the vector alone (PreScission protease transfection/vector alone transfection×100) is shown in Fig. 5.10. The percentage of living cells transfected with PreScission protease was always lower when compared to those transfected with vector alone. At 0 hour, equal amounts of cells were added to the transfection with PreScission protease or the vector alone. Transfection of cultures with PreScission protease resulted in cell death, including the ICAD/CAD double knockout where no targets of PreScission protease are predicted to be present. However, the degree of cell death was consistently higher in hICAD-L^{2PRE}:CAD cell lines than for the ICAD/CAD double knockout cell line. This was statistically significant at 24 hours after transfection.

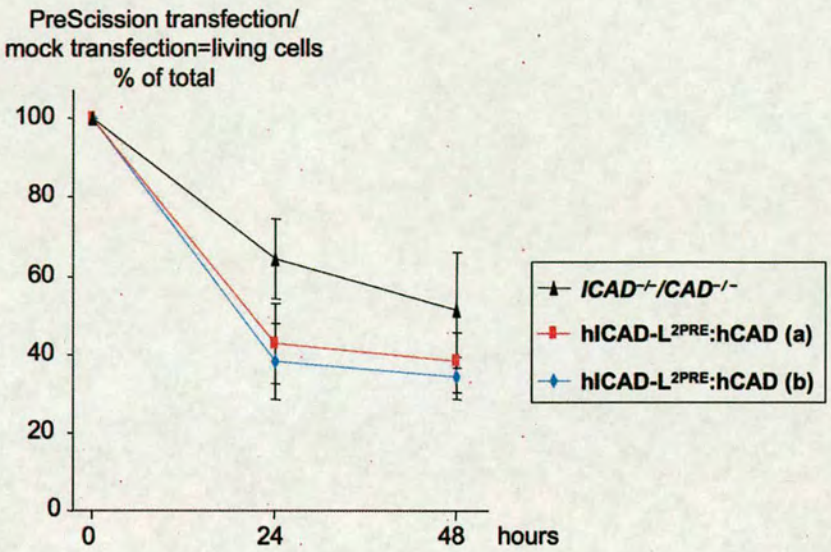

Fig. 5.10. Stable cell lines expressing hICAD-L^{2PRE}:hCAD are more susceptible to cell death after transient transfection with PreScission protease than *ICAD*$^{-/-}$/*CAD*$^{-/-}$ cells. Plasmid expressing PreScission protease or vector alone (mock transfection) were transfected into stable cell lines (a and b) expressing hICAD-L^{2PRE}:hCAD in the ICAD/CAD double knockout background. The number of living cells was calculated in both transfections at 24 and 48 hours using the trypan blue exclusion method. The number at 0 hour is estimated. The difference in the number of living cells observed after transfection with PreScission protease and mock transfection is indicated as a percentage of the total in the graph.

5.9 Discussion

To test whether CAD activation can kill the cell, several model systems were constructed using ICAD that could be cleaved with TEV and PreScission proteases. The PreScission protease was used here for the first time in order to test its applicability as a tool for site-specific protein cleavage *in vivo*.

To demonstrate CAD's ability to cause cell death in the absence of initial apoptosis, I decided to cleave its inhibitor ICAD, modified to incorporate two TEV sites. It is known that TEV protease needs to have efficient access to its cleavage site target to perform the reaction (Ehrmann et al., 1997). Therefore, it was necessary to confirm whether TEV protease could access its cleavage sites in the hICAD-L^{2TEV} protein. In fact, both TEV recognition sites in hICAD-L^{2TEV} were cleaved by TEV protease *in vitro*. This resulted in CAD activation *in vitro*, as detected by the degradation of plasmid DNA. Therefore, the artificially designed hICAD-L^{2TEV} protein was functional and able to work as both a chaperone and inhibitor for CAD.

Achieving CAD activation *in vivo*, however, proved to be a much more difficult task. TEV protease was induced *in vivo* and efficiently expressed, but the expressed protease either lacked the ability to cleave the hICAD-L^{2TEV} protein, or did not cleave it at significant levels. The later would be particularly important if hICAD-L^{2TEV}/hCAD ratio was high. Then, more TEV activity would be necessary to cleave the inhibitor pool before CAD could be activated. In addition, I can not exclude the possibility that some low level cleavage of hICAD-L^{2TEV} protein by TEV protease may occur and thus results in the variability of protein amount in Fig. 5.5. Alternatively, the variability may be due

to the differences in sample loading. In any case, the complete hICAD-L^{2TEV} protein cleavage and the cell death that could be the result of it, did not occur *in vivo* thus requiring the development of alternative approaches to destroy the protein. The lack of protein cleavage was not due to inaccessibility of the sites due to the three-dimensional structure of the hICAD-L^{2TEV} protein, as TEV protease could cleave hICAD-L^{2TEV} *in vitro*. In cells, however, TEV protease and hICAD-L^{2TEV} could potentially be located in different sub-cellular compartments. To avoid this situation, TEV and mutant TEV protease were targeted to the nucleus with two SV40 NLS. It must also be noted that the version of TEV protease with two SV40 NLS sequences was the same as that used in yeast studies (Uhlmann et al., 2000) in which the TEV protease with added NLS was localised in the nucleus. As hICAD-L^{2TEV} has its own NLS, both proteins would be predicted to target to the nucleus using their localisation signals.

Another possible reason why TEV protease did not work *in vivo* is that it might lack sufficient activity to cleave hICAD-L^{2TEV} *in vivo*. Although TEV protease has been used in yeast cells and *E. coli* for site-specific protein cleavage *in vivo* (Ehrmann et al., 1997; Mondigler and Ehrmann, 1996; Smith and Kohorn, 1991; Uhlmann et al., 2000; Yang et al., 2005), I am unaware of reports of its successful application in vertebrate cells. This is somewhat surprising, considering that there are numerous experiments for which it might be reasonable to extend the use of TEV protease cleavage technology from yeast to vertebrate model systems.

I decided to try to solve the potential problem posed by the lack of TEV protease activity by using a mutant TEV protease, which was reported to be more stable and catalytically active than the normal version (Kapust et al., 2001). However, cleavage of

the hICAD-L^{2TEV} protein still did not occur *in vivo* when this mutant TEV protease was expressed. As in the previous case with normal TEV protease, hICAD-L^{2TEV} protein was cleaved only *in vitro* when exogenous TEV protease was added. Importantly, mutant TEV protease expressed *in vivo* was not able to cleave the hICAD-L^{2TEV} protein even in lysed cell-free extracts, where cellular compartmentalisation barriers that could potentially prevent access to hICAD-L^{2TEV} protein would be absent. Interestingly, TEV protease was able to self-cleave off the MBP *in vivo*, so it must have had some activity in DT40 cells. That activity, however, was not enough to cleave the hICAD-L^{2TEV} protein *in vivo*. One possibility is that TEV protease expressed *in vivo* is somehow inactivated – e.g. by phosphorylation or binding of an inhibitor.

At present, I am unaware of any model system available for site-specific protein cleavage in vertebrate cells. As a result, there is no system to be used to test whether CAD activation outside of apoptosis can trigger cell death. As TEV protease originates in a plant virus (Carrington and Dougherty, 1987), its performance has been evolutionally optimised to work in plant cells. This is possibly one of the reasons why TEV protease does not work efficiently in DT40 cells. By contrast, PreScission protease originates in human rhinovirus (Cordingley et al., 1989; Hanecak et al., 1982) and thus has been evolutionally adapted to work in human cells. Therefore, it has the potential to be used for site-specific protein cleavage in vertebrate cells.

In the present study, I obtained evidence suggesting for the first time that PreScission protease can cleave a target protein *in vivo*. PreScission protease appeared to cleave the hICAD-L^{2PRE} protein *in vivo* in a stable cell line expressing the enzyme. Moreover, the isolation of a stable cell line expressing PreScission protease indicates

that DT40 cells can tolerate the enzyme, at least when it is not overexpressed. After transient transfection of the hICAD-L^{2PRE} protein into a stable cell line expressing PreScission protease, fragments corresponding to the size of the predicted cleaved products of the hICAD-L^{2PRE} protein were detected. That the levels of the cleaved product were significantly less than that of a full-length hICAD-L^{2PRE} protein could potentially be explained if the cleavage could be inefficient for an as yet unknown reason. Alternatively, it is possible that the cleaved product of hICAD-L^{2TEV} might be rapidly degraded *in vitro*. In stable cell lines expressing hICAD-L:hCAD, it was not possible to detect the cleaved product of the hICAD-L protein after its caspase-3 cleavage *in vivo*. It is possible that hICAD-L^{2PRE} protein expression in the nucleofection experiment was so robust that relatively large amounts of its cleaved fragment were produced, permitting its detection.

Once PreScission had been demonstrate to apparently cleave hICAD-L^{2PRE} *in vivo*, I attempted to construct an inducible Tet-On system with PreScission protease based on the hICAD-L^{2PRE}:hCAD stable cell line. However, I was unable to isolate cell clones expressing PreScission protease using the system that had worked previously to induce TEV protease (data not shown). This could possibly be due to a basal level of expression in the Tet-On system without induction (Sipo et al., 2006). Such expression could produce enough PreScission protease for hICAD-L^{2PRE} cleavage and hCAD activation. If that resulted in cell death, such clones would die in the selection process.

As an alternative, transiently transfected PreScission protease could be used to induce hICAD-L^{2PRE} cleavage in these cells. In fact, transiently transfection of PreScission protease does result in a decrease in the viability of DT40 cell lines,

particularly those expressing hICAD-L^{2PRE}:hCAD. Nucleofection can result in the high level of expression of the transfected protein (Martinet et al., 2003). Such high levels of PreScission protease might be toxic to DT40 cells. Although, PreScission protease is a site-specific protease, but it might cleave sequences resembling its recognition site with reduced efficiency. Such side effects could potentially be important when there is an overexpression of the PreScission protease. Interestingly, after PreScission protease transfection, the number of living cells expressing hICAD-L^{2PRE}:hCAD was less than that seen following transfection of double knockout cells. These data were statistically significant at 24 hours in two independent cell lines. Therefore, although I recognise that considerable amount of work remain to be done, I hypothesize based on these preliminary observations that CAD nuclease can contribute to cell death after its inhibitor hICAD-L^{2PRE} protein is cleaved by PreScission protease.

6. The role of ICAD-S *in vivo*

6.1 Introduction.

There are two forms of ICAD protein in cells, ICAD-L/DFF-45 and ICAD-S/DFF35 (Enari et al., 1998; Gu et al., 1999; Sakahira et al., 1998), that result from alternative splicing of a single pre-mRNA (Kawane et al., 1999). Most studies have focused on ICAD-L, and the function of ICAD-S remains obscure. ICAD-S does not appear to function as a chaperone for CAD folding, since it does not support the production of active CAD if it is expressed in $ICAD^{-/-}$ mouse MEFs (Nagase et al., 2003). Nevertheless, ICAD-S was able to work as an inhibitor for CAD *in vitro* (Gu et al., 1999; Sakahira et al., 1999). ICAD-S in rat neurons prevents CAD activation (Chen et al., 2000). No ICAD-L protein, however, was detected in this system, making it unclear just how CAD had been chaperoned, how ICAD-S had become associated with CAD, and what its specific function in the cell was. Furthermore, tissue-specific differences in the quantity of ICAD-L and ICAD-S have been observed (Chen et al., 2000; Kawane et al., 1999), and recent studies show that the ratio of ICAD-L and ICAD-S can be regulated in a single cell type (Li et al., 2005).

In the experiments described here, I used the chicken ICAD knockout and the ICAD/CAD double knockouts to identify the function of ICAD-S *in vivo*.

6.2 Analysing chicken ICAD ORF for alternative splice forms and constructing chicken ICAD-L and ICAD-S.

The chicken ICAD genomic region was isolated by Dr Kumiko Samejima and sequenced by Matthew A. Sims at GlaxoSmithKline. Dr Samejima performed the identification of the chicken ICAD ORF and the analysis of the ICAD exon/intron boundaries for the genomic sequence. The chicken ICAD protein has six exons and five

introns (Fig. 6.1). A cICAD-L mRNA is formed from the six ICAD exons. Studies done in human, rat and mouse model systems also identify a shorter version of the ICAD protein ICAD-S (Chen et al., 2000; Enari et al., 1998; Gu et al., 1999; Sakahira et al., 1998). The formation of the ICAD-S transcript in mice happens by alternative splicing when intron 5 is left unspliced from the initial transcript (Kawane et al., 1999). A stop codon in intron 5 stops the ICAD-S mRNA translation forming a shorter version of ICAD protein.

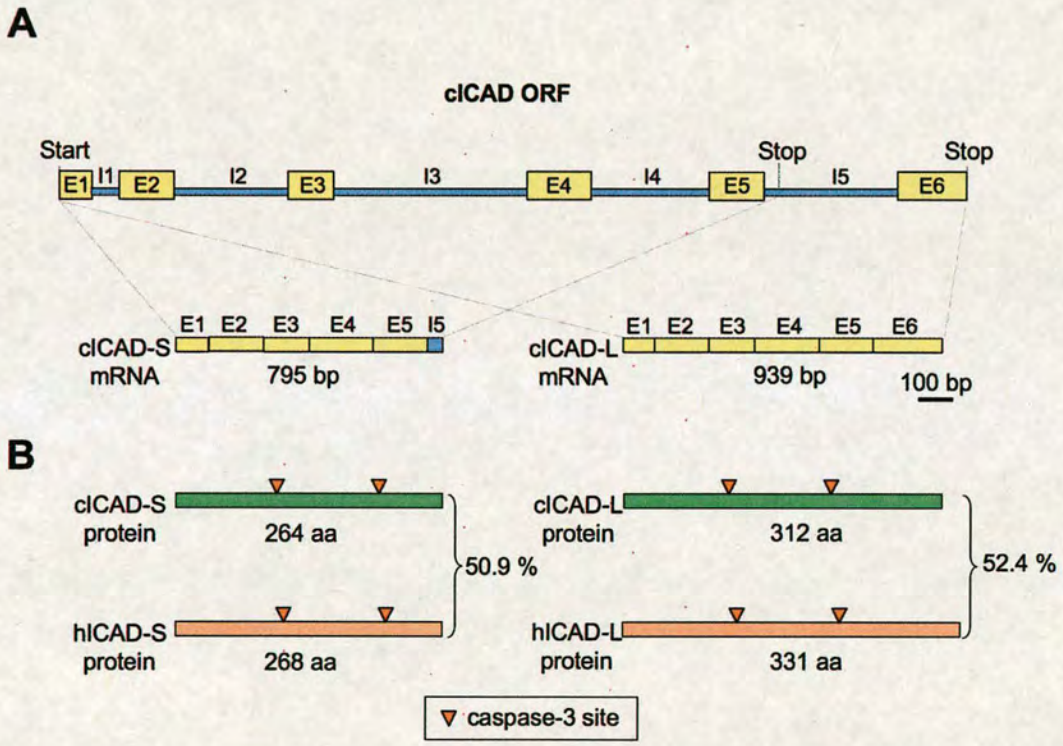

Fig. 6.1. Diagram of the chicken ICAD ORF and ICAD alternative splice forms synthesized from it. Chicken ICAD ORF consists of six exons and five introns. cICAD-L is synthesized from six exons. The cICAD-S alternative splice form is synthesized from the first five exons and the part of the fifth intron before the intrinstic stop codon. cICAD-L and cICAD-S proteins have two caspase-3 cleavage sites. The percentage of the amino acid sequence identity between chicken and human splice forms is indicated.

The possibility of alternative splicing of the ICAD transcript in chickens was analysed using chicken ICAD ORF, and the stop codon was identified in chicken ICAD intron 5. Therefore, alternative splicing of cICAD-S can happen in DT40 cells in a way similar to that of mouse cells. While this work was in progress, data confirming the occurrence of the two ICAD splice forms ICAD-S and ICAD-L in DT40 cells was published (Li et al., 2005). Therefore, it was decided to engineer chicken ICAD-L and ICAD-S proteins and proceed directly to the analysis of their function.

Chicken ICAD-L (construct AA6-2) was engineered from an incomplete cICAD-L cDNA isolated by Dr. Samejima using long primers to introduce the missing sequences. cICAD-S (construct AA6-8) was engineered in a PCR reaction from the cICAD-L cDNA. The 3' end of cICAD-S, which is different to that of cICAD-L, was introduced via a long primer sequence based on the cICAD genomic region sequencing data.

6.3 Chicken ICAD-S function in DT40 cells.

Once chicken ICAD-L and ICAD-S were isolated, I decided to identify their function in DT40 cells. It was particularly interesting to characterise the function of the ICAD-S splice form, as almost no data is available for its function *in vivo*. To identify the function of ICAD-S, I took advantage of the ICAD and ICAD/CAD double knockouts, as they allowed any splice form to be expressed in the absence of the endogenous ICAD protein.

Stable cell lines expressing chicken ICAD-S were isolated in the ICAD knockout (SC6.4). These stable cell lines were analysed for the presence of DNA fragmentation after the induction of apoptosis with 10 μM etoposide (Fig. 6.2). There was no DNA fragmentation in any of these cell lines. Thus, their phenotype resembled that of the ICAD knockout. By contrast, the DNA fragmentation progressed normally in DT40 wt cells exposed to the drug. The expression of chicken ICAD-S mRNA was analysed in the isolated stable cell lines (Fig 6.2). It was expressed in three cell lines (Fig. 6.2B lanes 1-3) and absent from one (Fig. 6.2B lane 4). None of these cell lines, however, was able to develop detectable DNA fragmentation. As a positive control, the total RNA of the DT40 wt was used. Amplification was also carried from plasmid DNA with the cICAD-S gene. In both cases, there was a band corresponding to the fragment of cICAD-S that was amplified using these specific primers. The amplified ICAD-S band in DT40 wt was significantly weaker than in the stable cell lines. There was another band observed in amplifications of DT40 wt RNA with a higher yield. This was absent in the negative control where no reverse transcriptase was added, and may potentially represent another splice form of the ICAD protein. I then attempted to amplify a longer fragment of chicken cDNA, but the amplification of long cDNA fragments with different ICAD cDNA primers was not successful. In general, it was only possible to efficiently isolate small fragments of chicken ICAD cDNA by RT-PCR.

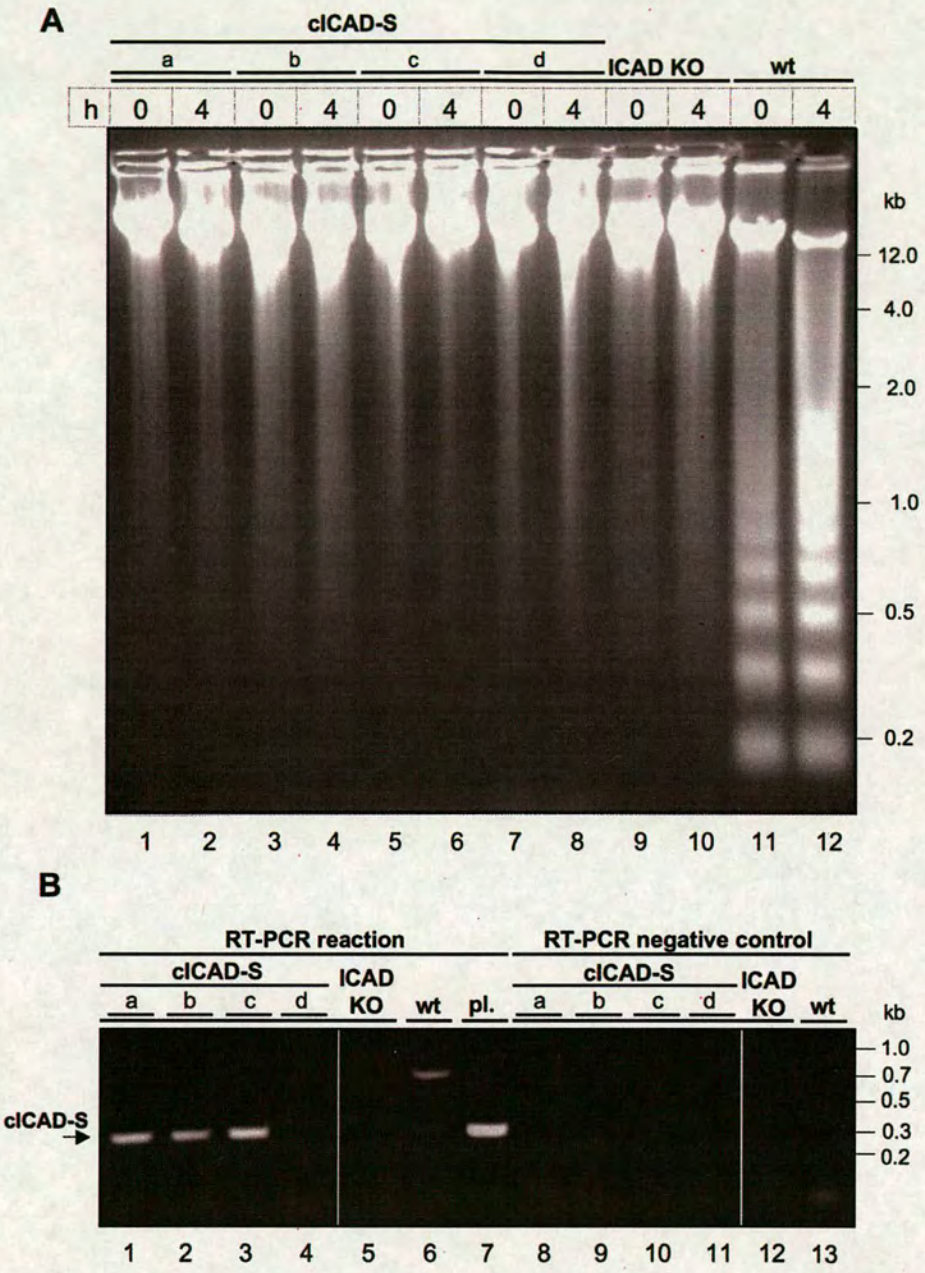

Fig. 6.2. DNA fragmentation is absent in stable cell lines expressing cICAD-S in the chicken ICAD knockout. **(A)** DNA fragmentation. Genomic DNA samples were collected at 0 and 4 hours after the induction of apoptosis with 10 μM etoposide. Four stable cell lines selected for the presence of cICAD-S plasmids were tested (a, b, c and d). ICAD knockout was used as a negative control and DT40 wt as a positive control. **(B)** RT-PCR reaction to detect the expression of cICAD-S in the analysed cell lines. The primers used for RT-PCR reactions were designed to amplify only a part of the cICAD-S cDNA. The RT-PCR negative control was a reaction in which no reverse transcriptase was added during the first-strand synthesis.

As there was no DNA fragmentation in cells expressing only cICAD-S, it was necessary to confirm that the long version of chicken ICAD protein – cICAD-L together with chicken CAD – can perform the function of reconstructing DNA fragmentation in the ICAD/CAD double knockout. I originally planned to construct a stable cell line containing chicken ICAD-L tagged with a C-terminal triple tandem purification tag (S-tag-TEVsite-SBP-tag-His – SATH-tag) for the purification of the interacting proteins (Fig. 6.3A). S-tag is a fragment of RNAse A that binds with high affinity during protein purification to another component of RNAse A, S-protein (Karpeisky et al., 1994). The SBP (Streptavidin Binding Peptide) tag has a high affinity for streptavidin (Keefe et al., 2001), another useful property for protein purification. The TEV site between S-tag and SBP could be used to cleave the tagged protein off the streptavidin beads. Finally, the His-tag can provide an additional step for tandem protein purification (Terpe, 2003).

The ICAD/CAD double knockout was transfected with cICAD-L-SATH-tag and cCAD plasmids and stable cell lines were selected (e.g. SC6.5), then tested for DNA fragmentation upon induction of apoptosis with 10 μM etoposide (Fig. 6.3B). DNA fragmentation was observed in the cICAD-L-SATH:cCAD stable cell line (Fig. 6.3B), but not the double knockout cells. Therefore, cICAD-L protein tagged with C-terminal SATH tag is functional in DT40 cells.

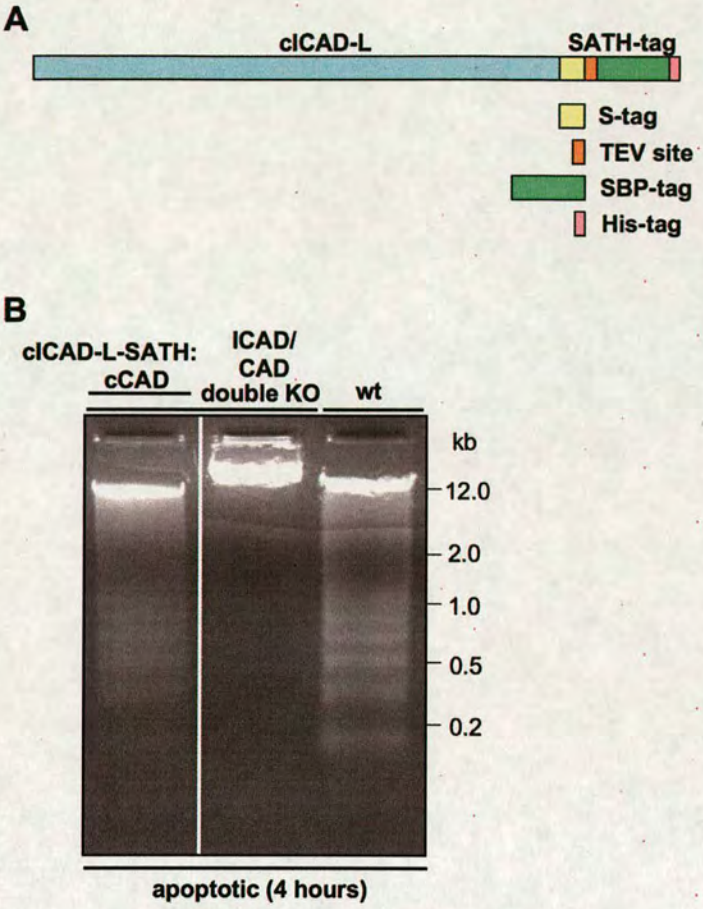

Fig. 6.3. DNA fragmentation is present in a cICAD-L-SATH:cCAD stable cell line constructed starting with the ICAD/CAD double knockout. **(A)** Diagram of the cICAD-L-SATH tag construct. The C-terminal SATH tag consists of an S-tag, TEV protease site, SBP (Straptavidin Binding Peptide) and His-tag. **(B)** Genomic DNA samples from cICAD-L-SATH:cCAD and the control stable cell line were collected four hours after the induction of apoptosis with etoposide.

6.4 Human ICAD-S also does not work as a folding chaperone for CAD *in vivo*.

Since human ICAD-L plus CAD could reconstitute the DNA destruction system in DT40 *ICAD*$^{-/-}$/*CAD*$^{-/-}$ double knockout cells and there are antibodies available for the detection of human proteins, I decided to ask whether a similar rescue could be obtained using hICAD-S in place of hICAD-L. After the induction of apoptosis by etoposide, hICAD-S was cleaved in these (SC6.3) cells (Fig. 6.4A lanes 1-3), but no DNA fragmentation could be detected in these cell lines (Fig. 6.4A lanes 1-3). Furthermore,

chromatin condensation did not proceed beyond stage I, with small balls of chromatin distributed around the nuclear periphery (Fig. 6.4B). Therefore, hICAD-S cannot replace hICAD-L as a chaperone *in vivo* for the folding of active CAD.

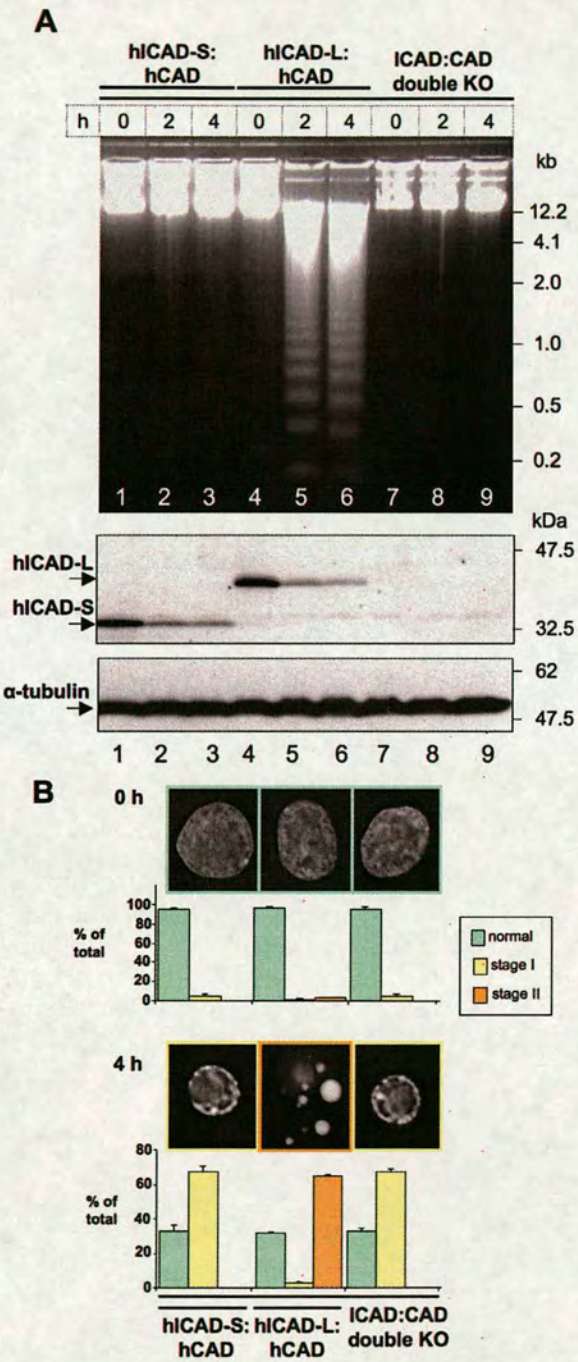

Fig. 6.4. hICAD-L but not hICAD-S supports the production of active hCAD *in vivo*. **(A)** Apoptosis was induced by 10 μM etoposide in stable cell lines expressing hICAD-S:hCAD (lanes 1-3) and hICAD-L:hCAD (lanes 4-6) in the chicken $ICAD^{-/-}$:$CAD^{-/-}$ background. (upper) Genomic DNA was isolated at 0, 2 and 4 hours after induction of apoptosis. (lower) The cleavage of hICAD-S and hICAD-L was detected with hICAD N-terminal antibody. **(B)** Images of cells before and after induction of apoptosis (0 and 4 hours). Stage II chromatin condensation was absent in cells expressing hICAD-S:hCAD and present in cells expressing hICAD-L:hCAD. Data represent a minimum of at least three independent experiments with over 300 cells counted for each.

6.5 ICAD-S inhibits CAD *in vivo*.

Importantly, ICAD is essential not only for the folding of active CAD, but also for its subsequent inactivation until an appropriate apoptotic stimulus is detected. I therefore used the humanized cell system to test whether ICAD-S can fill this second role as an inhibitor of CAD *in vivo*. To do this, I constructed a form of hICAD-S that was resistant to cleavage by caspases, but could be cleaved at the same sites by the viral TEV protease. I then introduced ICAD-S^{2TEV} into the humanized DT40 cells in which endogenous chicken ICAD and CAD had been replaced with hICAD-L and hCAD (Fig. 6.5A lanes 1-9). In these cell lines (SC6.1), hICAD-L acts as a folding chaperone and inhibitor for hCAD. Treatment of these cell lines with etoposide resulted in activation of the intrinsic pathway of apoptosis, leading to caspase activation and cleavage of hICAD-L but not hICAD-S^{2TEV} (Fig. 6.5A lanes 1-9). Thus, if hICAD-S^{2TEV} can bind and inhibit hCAD *in vivo* these cells should fail to show any activation of CAD nuclease.

Indeed, after induction of apoptosis in the humanized cells expressing hICAD-S^{2TEV} hCAD activation was prevented (Fig. 6.5A lanes 1-9). In clones expressing high levels of hICAD-S^{2TEV} no evidence DNA fragmentation or apoptotic body formation was observed (Fig. 6.5A lanes 1-3, Fig 6.5B). More variable results were obtained in cell clones expressing lower levels of hICAD-S^{2TEV}. In one stable cell line expressing lower levels of hICAD-S^{2TEV}, no DNA fragmentation was observed (Fig. 6.5A lanes 4-6). In a second hICAD-S^{2TEV}-expressing clone, low levels of DNA fragmentation could be observed (Fig. 6.5A lanes 7-9) and apoptotic bodies were formed, albeit ~three-fold less efficiently than in the "wild type" humanized cells expressing only hICAD-L plus

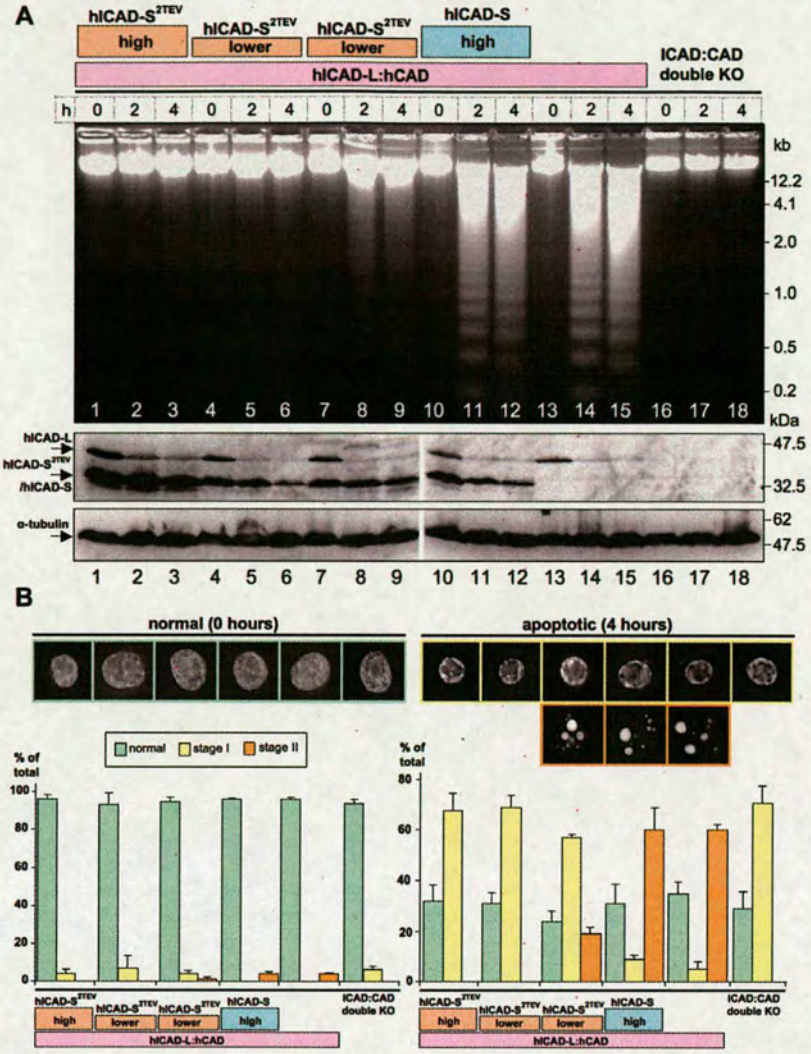

Fig. 6.5. ICAD-S can inhibit CAD *in vivo*. Stable cell lines expressing different levels of hICAD-S^{2TEV} were constructed starting with the humanized cell line expressing hICAD-L:hCAD in the *ICAD*$^{-/-}$/*CAD*$^{-/-}$ double knockout. **(A)** Genomic DNA was isolated at 0, 2 and 4 hours after induction of apoptosis (top). The status of hICAD-L and hICAD-S^{2TEV} was monitored by immunoblotting. hICAD-L but not hICAD-S^{2TEV} was cleaved by caspase *in vivo* during the induction of apoptosis. One of the cell lines had a high level of hICAD-S^{2TEV} (lanes 1-3) Two other cell lines had a lower level of hICAD-S^{2TEV} (lanes 4-9). A cell line expressing high level of caspase-cleavable hICAD-S was used as a control (lanes 10-12). **(B)** Images of cells before and after induction of apoptosis (0 and 4 hours). DNA was stained with DAPI. Histograms show the percentage of cells with normal, stage I and stage II chromatin condensation. The experiment was done at least three times with over 300 cells counted for each independent experiment.

hCAD (Fig. 6.5B). There was no obvious difference in the levels of hICAD-S^{2TEV} protein in these two cell lines so the explanation for the difference is not clear. Importantly, in all cell lines expressing higher levels of hICAD-S^{2TEV}, hCAD activation was completely abolished.

6.6 TEV protease cleaves ICAD-S^{2TEV} *in vitro* and releases active CAD

An *in vitro* experiment confirmed that both hICAD-L and hICAD-S can efficiently perform the function of inhibiting hCAD and that cleavage of both inhibitors is required for hCAD activation. In this experiment, I prepared extracts from humanized DT40 cells (SC6.1) in which endogenous ICAD and CAD had been replaced by hICAD-S^{2TEV} plus hICAD-L plus hCAD (Fig. 6.6 lanes 1-4). In those extracts, added caspase-3 selectively cleaves ICAD-L but not ICAD-S^{2TEV}, whilst added TEV selectively cleaves ICAD-S^{2TEV} but not ICAD-L. Using this system, I observed CAD activation only when both caspase-3 and TEV were added to the extracts (Fig. 6.6 lane 4).

In a control experiment, I prepared extract from a stable cell line (SC4.10) expressing hICAD-L plus hCAD. In that extract, plasmid DNA was degraded when caspase-3 was added to the reaction mixture, but not when TEV protease was added (Fig. 6.6 lanes 5-8). This confirms the well known activation of hCAD following hICAD-L cleavage by caspase-3.

To test whether the replacement of caspase-3 sites with TEV protease sites affected the ability of ICAD-L to act as a folding chaperone function for production of active CAD I constructed stable cell lines (SC5.2) expressing hICAD-L^{2TEV} plus hCAD in the absence of endogenous ICAD and CAD. When cell-free extracts from those cell

lines were analysed *in vitro*, the addition of TEV protease was found to release active CAD, leading to the cleavage of plasmid DNA (Fig. 6.6 lanes 11-12). Therefore, replacing the two caspase cleavage sites of hICAD-L protein with TEV sites did not affect its chaperone and inhibitor function. Furthermore, this experiment reveals for the first time that under non-apoptotic conditions, specific cleavage of ICAD, is the only requirement for CAD activation in cell-free extracts.

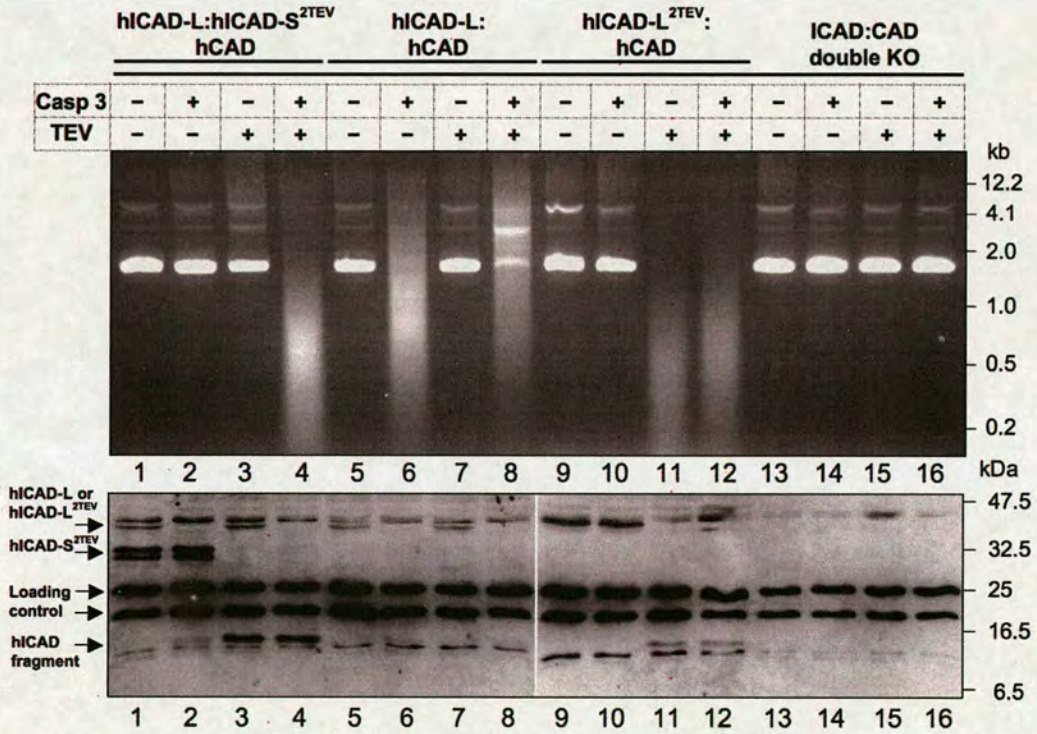

Fig. 6.6. hCAD is activated *in vitro* after the cleavage of hICAD in non-apoptotic extracts. Extracts were prepared from stable cell lines expressing hICAD-S^{2TEV}:hICAD-L:hCAD (lanes 1-4), hICAD-L:hCAD (lanes 5-8) and hICAD-L^{2TEV}:CAD (lanes 9-12) in the *ICAD*$^{-/-}$/*CAD*$^{-/-}$ double knockout (lanes 13-16) background. Plasmid DNA was added to each reaction mixture either alone, or together with caspase-3, TEV protease or both. Plasmid DNA was degraded in reactions where hCAD was released as a result of hICAD cleavage.

As a final control, when either caspase-3 or TEV protease was added to cell-free extracts prepared from *ICAD*$^{-/-}$/*CAD*$^{-/-}$ double knockout cells, no plasmid DNA

degradation was observed. Therefore, neither protease is activating another latent nuclease, such as endonuclease G, in the cell-free extracts.

6.8 Discussion.

ICAD splice forms ICAD-L and ICAD-S are ubiquitously present in human, mouse, rat and chicken cells (Chen et al., 2000; Kawane et al., 1999; Li et al., 2005). Interestingly, while the ICAD-L splice form has been extensively studied, the function of ICAD-S remains elusive.

I constructed a humanized system by expressing hICAD-L and hCAD cDNAs in chicken DT40 cells lacking the entire ORFs for ICAD and CAD. In those cells, normal DNA degradation and chromatin condensation were observed following addition of etoposide. In this system, hICAD-S was unable to replace hICAD-L, thereby confirming an earlier observation that ICAD-S is unable to function as a chaperone to promote the folding of active CAD (Nagase et al., 2003).

To test the role of ICAD-S as an inhibitor of CAD *in vivo* and *in vitro*, I created an allele of ICAD-S in which the two caspase cleavage sites had been replaced by TEV protease cleavage sites (ICAD-S^{2TEV}). When ICAD-S was expressed at high levels in the humanized DT40 cells (ICAD/CAD double knockout expressing hICAD-L and hCAD) it was able to completely abolish both DNA cleavage and stage II chromatin condensation following the addition of etoposide. Thus, ICAD-S^{2TEV} can bind to CAD, which has been liberated following the cleavage of ICAD-L and inhibit its nuclease activity.

The results of this experiment were confirmed using an *in vitro* assay in which cell-free extracts expressing various combinations of hICAD-L, hICAD-L^{2TEV}, hICAD-S, hICAD-S^{2TEV} and hCAD were treated either with active caspase-3, with TEV

protease, or both and examined for the activation of CAD nuclease. These experiments showed clearly that either ICAD-L or ICAD-S can fully inhibit CAD activity, and that providing CAD has been translated in the presence of ICAD-L, cleavage of ICAD by either protease can release active CAD.

I originally designed this system to examine whether cleavage of ICAD in a non-apoptotic context *in vivo* would result in CAD activation and cell death. This approach used as a model experiments in which expression of TEV in budding yeast was used to cleave cohesin component Scc1/Mcd1 and release cells into anaphase (Uhlmann et al., 2000). However, after almost two years of attempts using multiple vector systems for the expression of nuclear and cytoplasmic TEV protease in DT40 cells, I was able to express TEV but could never demonstrate any cleavage of ICAD-L^{2TEV}. I do not know the reason for this lack of TEV cleavage in living DT40 cells, but it is unlikely to result from inaccessibility of the TEV sites, as both ICAD-L^{2TEV} and ICAD-S^{2TEV} were efficiently cleaved in cell-free extracts by exogenous TEV.

This system could also be used to ask whether DT40 cells contain other activities that can inhibit CAD, should ICAD-L be removed. It has been proposed that nucleophosmin/B23 (Ahn et al., 2005) and CIIA (Cho et al., 2003) can fulfil this role. These inhibitors have been proposed to modulate CAD function either in normal cells or during apoptosis. Inhibiting CAD could be one of several functions of B23 that would be expected to be lost once B23 is cleaved by caspase-3 in apoptosis (Chou and Yung, 2001). In contrast, the cleavage of CIIA has not been reported in apoptosis.

To address the importance of these or any other possible alternative inhibitors of CAD function, I expressed a caspase-resistant ICAD-L^{2TEV}/CAD module in DT40 cells

lacking endogenous CAD and ICAD. ICAD-L^{2TEV} is competent as a folding chaperone for CAD, and active nuclease was released following its cleavage with exogenous TEV, providing the first example of caspase-independent CAD activation and confirming that ICAD cleavage is sufficient to activate CAD. B23 and CIIA lack consensus cleavage sites for TEV, and DT40 cells expressing TEV appear to grow normally (AVA, unpublished). It therefore appears that DT40 cell-free extracts lack other proteins that can replace ICAD as inhibitors of CAD.

These studies suggest a possible role for ICAD-S as a "buffer" of inhibitor to stop the sporadic loss or cleavage of ICAD-L from resulting in destruction of the genomic DNA. This is possible because ICAD-S acts as an inhibitor, but not a chaperone for CAD. ICAD-L cannot act as such a "buffer" since it also acts as a chaperone to promote the folding of active CAD. As a result, expression of higher levels of ICAD would simply raise the possibility of folding larger levels of active CAD. ICAD-L and ICAD-S are ubiquitously expressed during the mouse development (Zhang et al., 1999). The ratio of ICAD-S and ICAD-L varies in different tissues and organs (Chen et al., 2000; Kawane et al., 1999), and can be regulated at the level of alternative splicing (Li et al., 2005). Interestingly, in some tissues that are destined for long-term existence such as neurons, only ICAD-S is detected and not ICAD-L (Chen et al., 2000) (for contrasting results in human brain tissues see (Masuoka et al., 2001)).

My study leads to a view of the ICAD/CAD module as a three-part system with ICAD-L acting both as activator and inhibitor of CAD, whilst ICAD-S is held in reserve as a "buffer" that prevents accidental activation of CAD. The humanized DT40 cell system described here should provide a useful asset for future studies of the role and

regulation of the ICAD/CAD module in DNA degradation and chromatin condensation during apoptosis.

7. Conclusions

To investigate the role of CAD in cell death and the function of ICAD-S *in vivo*, ICAD and ICAD/CAD double knockouts were constructed in DT40 cells. The results of my PhD studies have led to the following conclusions and findings:

1. *ICAD and ICAD/CAD double knockouts are characterised by the absence of DNA fragmentation and stage II chromatin condensation.* This data confirms the previous findings that CAD is absolutely required for DNA fragmentation in DT40 cells. ICAD is a mandatory chaperone for CAD, and therefore DNA fragmentation is absent even in ICAD knockouts with an intact CAD gene. In addition, CAD is required for the final stage II chromatin condensation that involves the formation of distinct apoptotic bodies.

2. *A method for the removal of loxP-neo-loxP and loxP-puro-loxP cassettes with transient transfection of Cre-recombinase was developed for use in DT40 cells.* A method to remove drug-resistance cassettes that had been integrated into the genome flanked by mutant loxP sites was developed for DT40 cells. Marker gene removal after transient transfection with a vector encoding Cre-recombinase was highly efficient and did not require specific selection.

3. *Human ICAD and CAD proteins work as a module in the DT40 ICAD/CAD double knockout.* Introduction of human ICAD-L and CAD proteins into the DT40 (chicken) ICAD/CAD double knockout completely restored the DNA fragmentation and chromatin condensation phenotype. Therefore, these proteins can function as a module sufficient for DNA fragmentation and chromatin condensation during apoptosis.

4. *TEV protease technology for* in vivo *protein cleavage is not applicable in DT40 cells.* Both TEV and mutant TEV protease proved to be unable to perform the

cleavage of hICAD-L^{2TEV} in DT40 cells. That was particularly surprising and disappointing, as substrate cleavage was efficiently performed *in vitro* using exogenous TEV protease. This excludes the possibility that the three-dimensional structure of the artificially engineered hICAD-L^{2TEV} protein interfered with the cleavage.

5. *A novel technology for* in vivo *protein cleavage with PreScission protease has been developed in DT40 cells with potential application throughout vertebrate cells.* The development of a new technology for site-specific protein cleavage with PreScission protease in vertebrate cells is a significant advancement of the tools available in cell biology for the study of protein function *in vivo*. This can be applied to identify the roles and mechanisms of action of a wide range of proteins if they are modified to have the PreScission protease cleavage site and then destroyed by protease cleavage. This method can be used to study protein function in cell lines through the depletion of the endogenous protein by genetic knockout or RNAi.

6. *Preliminary data suggests CAD activation may lead to cell death as a result of likely hICAD-L^{2PRE} cleavage with PreScission protease.* In the particular case of the application of PreScission protease technology to the model system to test the role of CAD in cell death, preliminary data from transient transfection experiments suggests that CAD activation may be sufficient to kill cells. A new model system with PreScission protease under tight regulation must be developed *in vivo* to confirm this data.

7. *Neither chicken nor human ICAD-S works as a chaperone for CAD.* ICAD-S was not able to support the production of active CAD. Therefore, unlike ICAD-L, ICAD-S does not have chaperone function *in vivo*.

8. *ICAD-S works as an inhibitor for CAD* in vivo *and* in vitro. ICAD-S is able to efficiently prevent CAD activation *in vivo* after ICAD-L cleavage. In addition, the cleavage of both ICAD-S and ICAD-L is required for CAD activation *in vitro*. Therefore, my study leads to a view of the ICAD/CAD module as a three-part system with ICAD-L acting both as activator and inhibitor of CAD, whilst ICAD-S is held in reserve as a 'buffer' that prevents accidental activation of CAD.

8. Future directions

The data and stable cell lines obtained during my PhD project suggest the following follow-up investigations:

1. *ICAD/CAD double knockouts provide a model system to study the initial stages of chromatin condensation in the absence of ICAD and CAD.* Stage II DNA condensation is abolished in the ICAD/CAD double knockout. However, the stage I chromatin condensation is still present in the absence of CAD, and results in the formation of a necklace ring of small beads around the nuclear periphery. It would be interesting to identify the driving forces leading to the formation of this phenotype. As AIF is one of the factors contributing to DNA condensation, one possibility for studying the involvement of AIF in stage I condensation phenotype would be to deplete it with RNAi or genetic knockout in the ICAD/CAD double knockout and DT40 wild-type. This could provide a particular insight into the order and relative contribution of AIF and CAD action during apoptotic chromatin condensation.

2. *Study of ICAD-S:ICAD-L:CAD module function in the context of its localisation in cells.* As both ICAD splice forms can inhibit CAD *in vivo*, it would be particularly interesting to determine the intracellular localisation of all the components before and after the induction of apoptosis, as well as their associations with each other. The stable cell line expressing CAD tagged with tandem purification tag could be used for this purpose. The tagged CAD protein could be used for the purification of associated proteins either from cytoplasmic or nuclear fractions. This would allow the identification of the particular ICAD splice forms associated with CAD in these compartments before and after the induction of apoptosis. Moreover, the system might allow the identification by mass spectrometry analysis of other proteins associated with

CAD or the ICAD:CAD complex. In addition, if ICAD-L and ICAD-S were also separately tagged, the subcellular localisation of all three components could be traced by fluorescence microscopy.

3. *New technology for site-specific protein cleavage with PreScission protease* in vivo *and inducing CAD activation* in vivo. To further develop the new technology for site-specific protein cleavage with PreScission protease, it is necessary to establish an inducible model system with tight regulation for expression of the protease. PreScission protease is able to cleave its target when expressed, and therefore, expression system with tight regulation is required. One such system is the T-REx (Invitrogen), in which the expression of the desired protein product is prevented by the TetR repressor, positioned on the *tet* operator, thus preventing transcription. Expression is initiated when TetR is removed from the operator following binding of its inducer doxycycline. T-REx system contains two *tet* operators to accommodate two TetR for tighter regulation of PreScission protease regulation, until induced by Dox. The development of the PreScission protease inducible system would provide direct evidence that CAD activation after hICAD-L^{2PRE} cleavage can cause cell death.

If CAD activated in the absence of apoptosis can degrade the cellular DNA *in vivo* and kill the cell, this would suggest a possible approach to killing cancer cells through DNA cleavage. This could be done by discovering small molecular compounds that disrupt interactions between CAD and ICAD. Subsequent studies would address the possibilities of specifically targeting such compounds to cancer cells. Compounds capable of acting in such a way could then be used as anticancer drugs. Because CAD is situated at the end of the apoptotic signalling pathway, if it could be directly activated to

kill the cell, it might not be subject to control by the complex apoptosis regulation machinery.

9. References

Acehan, D., Jiang, X., Morgan, D.G., Heuser, J.E., Wang, X., and Akey, C.W. (2002). Three-dimensional structure of the apoptosome: implications for assembly, procaspase-9 binding, and activation. Molecular Cell *9*, 423-432.

Adams, J.M., and Cory, S. (1998). The Bcl-2 protein family: arbiters of cell survival. Science (New York, NY *281*, 1322-1326.

Ahn, J.Y., Liu, X., Cheng, D., Peng, J., Chan, P.K., Wade, P.A., and Ye, K. (2005). Nucleophosmin/B23, a nuclear PI(3,4,5)P(3) receptor, mediates the antiapoptotic actions of NGF by inhibiting CAD. Molecular Cell *18*, 435-445.

Arakawa, H., Lodygin, D., and Buerstedde, J.M. (2001). Mutant loxP vectors for selectable marker recycle and conditional knock-outs. BMC Biotechnology *1*, 7.

Araki, K., Araki, M., Miyazaki, J., and Vassalli, P. (1995). Site-specific recombination of a transgene in fertilized eggs by transient expression of Cre recombinase. Proc Natl Acad Sci U S A *92*, 160-164.

Araki, K., Araki, M., and Yamamura, K. (1997). Targeted integration of DNA using mutant lox sites in embryonic stem cells. Nucleic Acids Research *25*, 868-872.

Ashkenazi, A., and Dixit, V.M. (1998). Death receptors: signaling and modulation. Science (New York, NY *281*, 1305-1308.

Babe, L.M., and Craik, C.S. (1997). Viral proteases: evolution of diverse structural motifs to optimize function. Cell *91*, 427-430.

Basanez, G., Sharpe, J.C., Galanis, J., Brandt, T.B., Hardwick, J.M., and Zimmerberg, J. (2002). Bax-type apoptotic proteins porate pure lipid bilayers through a mechanism sensitive to intrinsic monolayer curvature. The Journal of Biological Chemistry *277*, 49360-49365.

Bayascas, J.R., Yuste, V.J., Sole, C., Sanchez-Lopez, I., Segura, M.F., Perera, R., and Comella, J.X. (2004). Characterization of splice variants of human caspase-activated DNase with CIDE-N structure and function. FEBS Letters *566*, 234-240.

Ben-Yehudah, A., Aqeilan, R., Robashkevich, D., and Lorberboum-Galski, H. (2003). Using apoptosis for targeted cancer therapy by a new gonadotropin releasing hormone-DNA fragmentation factor 40 chimeric protein. Clin Cancer Res *9*, 1179-1190.

Boatright, K.M., Renatus, M., Scott, F.L., Sperandio, S., Shin, H., Pedersen, I.M., Ricci, J.E., Edris, W.A., Sutherlin, D.P., Green, D.R., *et al.* (2003). A unified model for apical caspase activation. Molecular Cell *11*, 529-541.

Boix, J., Llecha, N., Yuste, V.J., and Comella, J.X. (1997). Characterization of the cell death process induced by staurosporine in human neuroblastoma cell lines. Neuropharmacology *36*, 811-821.

Boldin, M.P., Varfolomeev, E.E., Pancer, Z., Mett, I.L., Camonis, J.H., and Wallach, D. (1995). A novel protein that interacts with the death domain of Fas/APO1 contains a sequence motif related to the death domain. The Journal of Biological Chemistry *270*, 7795-7798.

Boulares, A.H., Zoltoski, A.J., Yakovlev, A., Xu, M., and Smulson, M.E. (2001). Roles of DNA fragmentation factor and poly(ADP-ribose) polymerase in an amplification phase of tumor necrosis factor-induced apoptosis. The Journal of Biological Chemistry *276*, 38185-38192.

Bursch, W. (2001). The autophagosomal-lysosomal compartment in programmed cell death. Cell Death and Differentiation *8*, 569-581.

Cain, K., Bratton, S.B., Langlais, C., Walker, G., Brown, D.G., Sun, X.M., and Cohen, G.M. (2000). Apaf-1 oligomerizes into biologically active approximately 700-kDa and inactive approximately 1.4-MDa apoptosome complexes. The Journal of Biological Chemistry *275*, 6067-6070.

Cande, C., Cecconi, F., Dessen, P., and Kroemer, G. (2002). Apoptosis-inducing factor (AIF): key to the conserved caspase-independent pathways of cell death? Journal of Cell Science *115*, 4727-4734.

Cande, C., Vahsen, N., Kouranti, I., Schmitt, E., Daugas, E., Spahr, C., Luban, J., Kroemer, R.T., Giordanetto, F., Garrido, C., *et al.* (2004). AIF and cyclophilin A cooperate in apoptosis-associated chromatinolysis. Oncogene *23*, 1514-1521.

Cannon, J.S., Hamzeh, F., Moore, S., Nicholas, J., and Ambinder, R.F. (1999). Human herpesvirus 8-encoded thymidine kinase and phosphotransferase homologues confer sensitivity to ganciclovir. J Virol *73*, 4786-4793.

Carlile, G.W., Smith, D.H., and Wiedmann, M. (2004). Caspase-3 has a nonapoptotic function in erythroid maturation. Blood *103*, 4310-4316.

Carrington, J.C., Cary, S.M., and Dougherty, W.G. (1988). Mutational analysis of tobacco etch virus polyprotein processing: cis and trans proteolytic activities of polyproteins containing the 49-kilodalton proteinase. J Virol *62*, 2313-2320.

Carrington, J.C., and Dougherty, W.G. (1987). Small Nuclear Inclusion Protein Encoded by a Plant Potyvirus Genome Is a Protease. J Virol *61*, 2540-2548.

Carrington, J.C., and Dougherty, W.G. (1988). A viral cleavage site cassette: identification of amino acid sequences required for tobacco etch virus polyprotein processing. Proc Natl Acad Sci U S A *85*, 3391-3395.

Chang, D.W., Xing, Z., Capacio, V.L., Peter, M.E., and Yang, X. (2003). Interdimer processing mechanism of procaspase-8 activation. The EMBO Journal *22*, 4132-4142.

Chang, J.Y. (1985). Thrombin specificity. Requirement for apolar amino acids adjacent to the thrombin cleavage site of polypeptide substrate. European Journal of Biochemistry / FEBS *151*, 217-224.

Chen, D., Stetler, R.A., Cao, G., Pei, W., O'Horo, C., Yin, X.M., and Chen, J. (2000). Characterization of the rat DNA fragmentation factor 35/Inhibitor of caspase-activated DNase (Short form). The endogenous inhibitor of caspase-dependent DNA fragmentation in neuronal apoptosis. The Journal of Biological Chemistry *275*, 38508-38517.

Chen, M., Orozco, A., Spencer, D.M., and Wang, J. (2002). Activation of initiator caspases through a stable dimeric intermediate. The Journal of Biological Chemistry *277*, 50761-50767.

Cheng, E.H., Wei, M.C., Weiler, S., Flavell, R.A., Mak, T.W., Lindsten, T., and Korsmeyer, S.J. (2001). BCL-2, BCL-X(L) sequester BH3 domain-only molecules preventing BAX- and BAK-mediated mitochondrial apoptosis. Molecular Cell *8*, 705-711.

Chinnaiyan, A.M., O'Rourke, K., Tewari, M., and Dixit, V.M. (1995). FADD, a novel death domain-containing protein, interacts with the death domain of Fas and initiates apoptosis. Cell *81*, 505-512.

Cho, S.G., Kim, J.W., Lee, Y.H., Hwang, H.S., Kim, M.S., Ryoo, K., Kim, M.J., Noh, K.T., Kim, E.K., Cho, J.H., *et al.* (2003). Identification of a novel antiapoptotic protein that antagonizes ASK1 and CAD activities. J Cell Biol *163*, 71-81.

Choi, S.I., Song, H.W., Moon, J.W., and Seong, B.L. (2001). Recombinant enterokinase light chain with affinity tag: expression from Saccharomyces cerevisiae and its utilities in fusion protein technology. Biotechnology and Bioengineering *75*, 718-724.

Chou, C.C., and Yung, B.Y. (2001). Increased stability of nucleophosmin/B23 in anti-apoptotic effect of ras during serum deprivation. Mol Pharmacol *59*, 38-45.

Cipolat, S., Rudka, T., Hartmann, D., Costa, V., Serneels, L., Craessaerts, K., Metzger, K., Frezza, C., Annaert, W., D'Adamio, L., *et al.* (2006). Mitochondrial rhomboid PARL regulates cytochrome c release during apoptosis via OPA1-dependent cristae remodeling. Cell *126*, 163-175.

Clarke, P.G. (1990). Developmental cell death: morphological diversity and multiple mechanisms. Anatomy and Embryology *181*, 195-213.

Cohen, G.M. (1997). Caspases: the executioners of apoptosis. The Biochemical Journal *326 (Pt 1)*, 1-16.

Cordingley, M.G., Callahan, P.L., Sardana, V.V., Garsky, V.M., and Colonno, R.J. (1990). Substrate requirements of human rhinovirus 3C protease for peptide cleavage in vitro. The Journal of Biological Chemistry *265*, 9062-9065.

Cordingley, M.G., Register, R.B., Callahan, P.L., Garsky, V.M., and Colonno, R.J. (1989). Cleavage of small peptides in vitro by human rhinovirus 14 3C protease expressed in Escherichia coli. J Virol *63*, 5037-5045.

Creagh, E.M., Conroy, H., and Martin, S.J. (2003). Caspase-activation pathways in apoptosis and immunity. Immunological Reviews *193*, 10-21.

Cregan, S.P., Fortin, A., MacLaurin, J.G., Callaghan, S.M., Cecconi, F., Yu, S.W., Dawson, T.M., Dawson, V.L., Park, D.S., Kroemer, G., *et al.* (2002). Apoptosis-inducing factor is involved in the regulation of caspase-independent neuronal cell death. J Cell Biol *158*, 507-517.

Crompton, M. (1999). The mitochondrial permeability transition pore and its role in cell death. The Biochemical Journal *341 (Pt 2)*, 233-249.

Da, L., Li, D., Yokoyama, K.K., Li, T., and Zhao, M. (2006). Dual promoters control the cell-specific expression of the human cell death-inducing DFF45-like effector B gene. The Biochemical Journal *393*, 779-788.

Danesch, U., Hoeck, W., and Ringold, G.M. (1992). Cloning and transcriptional regulation of a novel adipocyte-specific gene, FSP27. CAAT-enhancer-binding protein (C/EBP) and C/EBP-like proteins interact with sequences required for differentiation-dependent expression. The Journal of Biological Chemistry *267*, 7185-7193.

Daugas, E., Susin, S.A., Zamzami, N., Ferri, K.F., Irinopoulou, T., Larochette, N., Prevost, M.C., Leber, B., Andrews, D., Penninger, J., *et al.* (2000). Mitochondrio-nuclear translocation of AIF in apoptosis and necrosis. Faseb J *14*, 729-739.

De Marchi, U., Campello, S., Szabo, I., Tombola, F., Martinou, J.C., and Zoratti, M. (2004). Bax does not directly participate in the Ca(2+)-induced permeability transition of isolated mitochondria. The Journal of Biological Chemistry *279*, 37415-37422.

Degterev, A., Boyce, M., and Yuan, J. (2003). A decade of caspases. Oncogene *22*, 8543-8567.

Desbarats, J., Birge, R.B., Mimouni-Rongy, M., Weinstein, D.E., Palerme, J.S., and Newell, M.K. (2003). Fas engagement induces neurite growth through ERK activation and p35 upregulation. Nature Cell Biology *5*, 118-125.

Deveraux, Q.L., Roy, N., Stennicke, H.R., Van Arsdale, T., Zhou, Q., Srinivasula, S.M., Alnemri, E.S., Salvesen, G.S., and Reed, J.C. (1998). IAPs block apoptotic events induced by caspase-8 and cytochrome c by direct inhibition of distinct caspases. The EMBO Journal *17*, 2215-2223.

Du, C., Fang, M., Li, Y., Li, L., and Wang, X. (2000). Smac, a mitochondrial protein that promotes cytochrome c-dependent caspase activation by eliminating IAP inhibition. Cell *102*, 33-42.

Durrieu, F., Samejima, K., Fortune, J.M., Kandels-Lewis, S., Osheroff, N., and Earnshaw, W.C. (2000). DNA topoisomerase IIalpha interacts with CAD nuclease and is involved in chromatin condensation during apoptotic execution. Curr Biol *10*, 923-926.

Earnshaw, W.C., Martins, L.M., and Kaufmann, S.H. (1999). Mammalian caspases: structure, activation, substrates, and functions during apoptosis. Annual Review of Biochemistry *68*, 383-424.

Eckhart, L., Fischer, H., and Tschachler, E. (2007). Phylogenomics of caspase-activated DNA fragmentation factor. Biochemical and Biophysical Research Communications *356*, 293-299.

Ehrmann, M., Bolek, P., Mondigler, M., Boyd, D., and Lange, R. (1997). TnTIN and TnTAP: mini-transposons for site-specific proteolysis in vivo. Proc Natl Acad Sci U S A *94*, 13111-13115.

Ellis, H.M., and Horvitz, H.R. (1986). Genetic control of programmed cell death in the nematode C. elegans. Cell *44*, 817-829.

Ellis, L., Clauser, E., Morgan, D.O., Edery, M., Roth, R.A., and Rutter, W.J. (1986). Replacement of insulin receptor tyrosine residues 1162 and 1163 compromises insulin-stimulated kinase activity and uptake of 2-deoxyglucose. Cell *45*, 721-732.

Enari, M., Sakahira, H., Yokoyama, H., Okawa, K., Iwamatsu, A., and Nagata, S. (1998). A caspase-activated DNase that degrades DNA during apoptosis, and its inhibitor ICAD. Nature *391*, 43-50.

Erdtmann, L., Franck, N., Lerat, H., Le Seyec, J., Gilot, D., Cannie, I., Gripon, P., Hibner, U., and Guguen-Guillouzo, C. (2003). The hepatitis C virus NS2 protein is an inhibitor of CIDE-B-induced apoptosis. The Journal of Biological Chemistry *278*, 18256-18264.

Eskelinen, E.L. (2005). Maturation of autophagic vacuoles in Mammalian cells. Autophagy *1*, 1-10.

Fadok, V.A., Voelker, D.R., Campbell, P.A., Cohen, J.J., Bratton, D.L., and Henson, P.M. (1992). Exposure of phosphatidylserine on the surface of apoptotic lymphocytes triggers specific recognition and removal by macrophages. J Immunol *148*, 2207-2216.

Festjens, N., Vanden Berghe, T., and Vandenabeele, P. (2006). Necrosis, a well-orchestrated form of cell demise: signalling cascades, important mediators and concomitant immune response. Biochimica et Biophysica Acta *1757*, 1371-1387.

Fischer, H., Koenig, U., Eckhart, L., and Tschachler, E. (2002). Human caspase 12 has acquired deleterious mutations. Biochemical and Biophysical Research Communications *293*, 722-726.

Fischer, H., Rossiter, H., Ghannadan, M., Jaeger, K., Barresi, C., Declercq, W., Tschachler, E., and Eckhart, L. (2005). Caspase-14 but not caspase-3 is processed during the development of fetal mouse epidermis. Differentiation; Rresearch in Biological Diversity *73*, 406-413.

Fischer, U., Janicke, R.U., and Schulze-Osthoff, K. (2003). Many cuts to ruin: a comprehensive update of caspase substrates. Cell Death and Differentiation *10*, 76-100.

Frezza, C., Cipolat, S., Martins de Brito, O., Micaroni, M., Beznoussenko, G.V., Rudka, T., Bartoli, D., Polishuck, R.S., Danial, N.N., De Strooper, B., *et al.* (2006). OPA1 controls apoptotic cristae remodeling independently from mitochondrial fusion. Cell *126*, 177-189.

Fukushima, K., Kikuchi, J., Koshiba, S., Kigawa, T., Kuroda, Y., and Yokoyama, S. (2002). Solution structure of the DFF-C domain of DFF45/ICAD. A structural basis for the regulation of apoptotic DNA fragmentation. J Mol Biol *321*, 317-327.

Ghosh, S., and Karin, M. (2002). Missing pieces in the NF-kappaB puzzle. Cell *109 Suppl*, S81-96.

Golks, A., Brenner, D., Fritsch, C., Krammer, P.H., and Lavrik, I.N. (2005). c-FLIPR, a new regulator of death receptor-induced apoptosis. The Journal of Biological Chemistry *280*, 14507-14513.

Golks, A., Brenner, D., Krammer, P.H., and Lavrik, I.N. (2006). The c-FLIP-NH2 terminus (p22-FLIP) induces NF-kappaB activation. The Journal of Experimental Medicine *203*, 1295-1305.

Gossen, M., and Bujard, H. (1992). Tight control of gene expression in mammalian cells by tetracycline-responsive promoters. Proc Natl Acad Sci U S A *89*, 5547-5551.

Gossen, M., Freundlieb, S., Bender, G., Muller, G., Hillen, W., and Bujard, H. (1995). Transcriptional activation by tetracyclines in mammalian cells. Science (New York, NY *268*, 1766-1769.

Gregory, C.D., and Devitt, A. (2004). The macrophage and the apoptotic cell: an innate immune interaction viewed simplistically? Immunology *113*, 1-14.

Grimsley, C., and Ravichandran, K.S. (2003). Cues for apoptotic cell engulfment: eat-me, don't eat-me and come-get-me signals. Trends Cell Biol *13*, 648-656.

Gross, A., McDonnell, J.M., and Korsmeyer, S.J. (1999a). BCL-2 family members and the mitochondria in apoptosis. Genes & Development *13*, 1899-1911.

Gross, A., Yin, X.M., Wang, K., Wei, M.C., Jockel, J., Milliman, C., Erdjument-Bromage, H., Tempst, P., and Korsmeyer, S.J. (1999b). Caspase cleaved BID targets mitochondria and is required for cytochrome c release, while BCL-XL prevents this release but not tumor necrosis factor-R1/Fas death. The Journal of Biological Chemistry *274*, 1156-1163.

Gu, J., Dong, R.P., Zhang, C., McLaughlin, D.F., Wu, M.X., and Schlossman, S.F. (1999). Functional interaction of DFF35 and DFF45 with caspase-activated DNA fragmentation nuclease DFF40. The Journal of Biological Chemistry *274*, 20759-20762.

Guo, Y., Srinivasula, S.M., Druilhe, A., Fernandes-Alnemri, T., and Alnemri, E.S. (2002). Caspase-2 induces apoptosis by releasing proapoptotic proteins from mitochondria. The Journal of Biological Chemistry *277*, 13430-13437.

Hacker, G. (2000). The morphology of apoptosis. Cell Tissue Res *301*, 5-17.

Halenbeck, R., MacDonald, H., Roulston, A., Chen, T.T., Conroy, L., and Williams, L.T. (1998). CPAN, a human nuclease regulated by the caspase-sensitive inhibitor DFF45. Curr Biol *8*, 537-540.

Hanecak, R., Semler, B.L., Anderson, C.W., and Wimmer, E. (1982). Proteolytic processing of poliovirus polypeptides: antibodies to polypeptide P3-7c inhibit cleavage at glutamine-glycine pairs. Proc Natl Acad Sci U S A *79*, 3973-3977.

Hartman, S.C., and Mulligan, R.C. (1988). Two dominant-acting selectable markers for gene transfer studies in mammalian cells. Proc Natl Acad Sci U S A *85*, 8047-8051.

Hengartner, M.O. (2000). The biochemistry of apoptosis. Nature *407*, 770-776.

Hingorani, K., Szebeni, A., and Olson, M.O. (2000). Mapping the functional domains of nucleolar protein B23. The Journal of Biological Chemistry *275*, 24451-24457.

Hsu, H., Huang, J., Shu, H.B., Baichwal, V., and Goeddel, D.V. (1996a). TNF-dependent recruitment of the protein kinase RIP to the TNF receptor-1 signaling complex. Immunity *4*, 387-396.

Hsu, H., Shu, H.B., Pan, M.G., and Goeddel, D.V. (1996b). TRADD-TRAF2 and TRADD-FADD interactions define two distinct TNF receptor 1 signal transduction pathways. Cell *84*, 299-308.

Hsu, H., Xiong, J., and Goeddel, D.V. (1995). The TNF receptor 1-associated protein TRADD signals cell death and NF-kappa B activation. Cell *81*, 495-504.

Hu, W.H., Johnson, H., and Shu, H.B. (2000). Activation of NF-kappaB by FADD, Casper, and caspase-8. The Journal of Biological Chemistry *275*, 10838-10844.

Hu, Y., Yao, J., Liu, Z., Liu, X., Fu, H., and Ye, K. (2005). Akt phosphorylates acinus and inhibits its proteolytic cleavage, preventing chromatin condensation. The EMBO Journal *24*, 3543-3554.

Inohara, N., Koseki, T., Chen, S., Wu, X., and Nunez, G. (1998). CIDE, a novel family of cell death activators with homology to the 45 kDa subunit of the DNA fragmentation factor. The EMBO Journal *17*, 2526-2533.

Irmler, M., Thome, M., Hahne, M., Schneider, P., Hofmann, K., Steiner, V., Bodmer, J.L., Schroter, M., Burns, K., Mattmann, C., *et al.* (1997). Inhibition of death receptor signals by cellular FLIP. Nature *388*, 190-195.

Irvine, R.A., Adachi, N., Shibata, D.K., Cassell, G.D., Yu, K., Karanjawala, Z.E., Hsieh, C.L., and Lieber, M.R. (2005). Generation and characterization of endonuclease G null mice. Mol Cell Biol *25*, 294-302.

Jacobson, M.D., Weil, M., and Raff, M.C. (1997). Programmed cell death in animal development. Cell *88*, 347-354.

Janicke, R.U., Ng, P., Sprengart, M.L., and Porter, A.G. (1998). Caspase-3 is required for alpha-fodrin cleavage but dispensable for cleavage of other death substrates in apoptosis. The Journal of Biological Chemistry *273*, 15540-15545.

Jenny, R.J., Mann, K.G., and Lundblad, R.L. (2003). A critical review of the methods for cleavage of fusion proteins with thrombin and factor Xa. Protein Expression and Purification *31*, 1-11.

Joselin, A.P., Schulze-Osthoff, K., and Schwerk, C. (2006). Loss of Acinus inhibits oligonucleosomal DNA fragmentation but not chromatin condensation during apoptosis. The Journal of Biological Chemistry *281*, 12475-12484.

Joza, N., Susin, S.A., Daugas, E., Stanford, W.L., Cho, S.K., Li, C.Y., Sasaki, T., Elia, A.J., Cheng, H.Y., Ravagnan, L., *et al.* (2001). Essential role of the mitochondrial apoptosis-inducing factor in programmed cell death. Nature *410*, 549-554.

Kanayama, N., Todo, K., Reth, M., and Ohmori, H. (2005). Reversible switching of immunoglobulin hypermutation machinery in a chicken B cell line. Biochemical and Biophysical Research Communications *327*, 70-75.

Kapust, R.B., Tozser, J., Fox, J.D., Anderson, D.E., Cherry, S., Copeland, T.D., and Waugh, D.S. (2001). Tobacco etch virus protease: mechanism of autolysis and rational design of stable mutants with wild-type catalytic proficiency. Protein Engineering *14*, 993-1000.

Kapust, R.B., and Waugh, D.S. (1999). Escherichia coli maltose-binding protein is uncommonly effective at promoting the solubility of polypeptides to which it is fused. Protein Sci *8*, 1668-1674.

Karin, M., and Lin, A. (2002). NF-kappaB at the crossroads of life and death. Nature Immunology *3*, 221-227.

Karpeisky, M., Senchenko, V.N., Dianova, M.V., and Kanevsky, V. (1994). Formation and properties of S-protein complex with S-peptide-containing fusion protein. FEBS Letters *339*, 209-212.

Kawane, K., Fukuyama, H., Adachi, M., Sakahira, H., Copeland, N.G., Gilbert, D.J., Jenkin, N.A., and Nagata, S. (1999). Structure and promoter analysis of murine CAD and ICAD genes. Cell Death and Differentiation *6*, 745-752.

Kawane, K., Fukuyama, H., Yoshida, H., Nagase, H., Ohsawa, Y., Uchiyama, Y., Okada, K., Iida, T., and Nagata, S. (2003). Impaired thymic development in mouse embryos deficient in apoptotic DNA degradation. Nature Immunology *4*, 138-144.

Keefe, A.D., Wilson, D.S., Seelig, B., and Szostak, J.W. (2001). One-step purification of recombinant proteins using a nanomolar-affinity streptavidin-binding peptide, the SBP-Tag. Protein Expression and Purification *23*, 440-446.

Kerr, J.F. (1971). Shrinkage necrosis: a distinct mode of cellular death. J Pathol *105*, 13-20.

Kerr, J.F., Wyllie, A.H., and Currie, A.R. (1972). Apoptosis: a basic biological phenomenon with wide-ranging implications in tissue kinetics. Br J Cancer *26*, 239-257.

Kischkel, F.C., Hellbardt, S., Behrmann, I., Germer, M., Pawlita, M., Krammer, P.H., and Peter, M.E. (1995). Cytotoxicity-dependent APO-1 (Fas/CD95)-associated proteins form a death-inducing signaling complex (DISC) with the receptor. The EMBO Journal *14*, 5579-5588.

Kischkel, F.C., Lawrence, D.A., Tinel, A., LeBlanc, H., Virmani, A., Schow, P., Gazdar, A., Blenis, J., Arnott, D., and Ashkenazi, A. (2001). Death receptor recruitment of endogenous caspase-10 and apoptosis initiation in the absence of caspase-8. The Journal of Biological Chemistry *276*, 46639-46646.

Klionsky, D.J., and Emr, S.D. (2000). Autophagy as a regulated pathway of cellular degradation. Science (New York, NY *290*, 1717-1721.

Koenig, U., Eckhart, L., and Tschachler, E. (2001). Evidence that caspase-13 is not a human but a bovine gene. Biochemical and Biophysical Research Communications *285*, 1150-1154.

Koh, D.W., Dawson, T.M., and Dawson, V.L. (2005). Mediation of cell death by poly(ADP-ribose) polymerase-1. Pharmacol Res *52*, 5-14.

Koopman, G., Reutelingsperger, C.P., Kuijten, G.A., Keehnen, R.M., Pals, S.T., and van Oers, M.H. (1994). Annexin V for flow cytometric detection of phosphatidylserine expression on B cells undergoing apoptosis. Blood *84*, 1415-1420.

Korsmeyer, S.J., Wei, M.C., Saito, M., Weiler, S., Oh, K.J., and Schlesinger, P.H. (2000). Pro-apoptotic cascade activates BID, which oligomerizes BAK or BAX into pores that result in the release of cytochrome c. Cell Death and Differentiation *7*, 1166-1173.

Krammer, P.H. (2000). CD95's deadly mission in the immune system. Nature *407*, 789-795.

Krausslich, H.G., and Wimmer, E. (1988). Viral proteinases. Annual Review of Biochemistry *57*, 701-754.

Kreuz, S., Siegmund, D., Scheurich, P., and Wajant, H. (2001). NF-kappaB inducers upregulate cFLIP, a cycloheximide-sensitive inhibitor of death receptor signaling. Mol Cell Biol *21*, 3964-3973.

Krueger, A., Baumann, S., Krammer, P.H., and Kirchhoff, S. (2001). FLICE-inhibitory proteins: regulators of death receptor-mediated apoptosis. Mol Cell Biol *21*, 8247-8254.

Lamkanfi, M., Declercq, W., Kalai, M., Saelens, X., and Vandenabeele, P. (2002). Alice in caspase land. A phylogenetic analysis of caspases from worm to man. Cell Death and Differentiation *9*, 358-361.

Lassus, P., Opitz-Araya, X., and Lazebnik, Y. (2002). Requirement for caspase-2 in stress-induced apoptosis before mitochondrial permeabilization. Science (New York, NY *297*, 1352-1354.

LaVallie, E.R., Rehemtulla, A., Racie, L.A., DiBlasio, E.A., Ferenz, C., Grant, K.L., Light, A., and McCoy, J.M. (1993). Cloning and functional expression of a cDNA encoding the catalytic subunit of bovine enterokinase. The Journal of Biological Chemistry *268*, 23311-23317.

Lavrik, I., Golks, A., and Krammer, P.H. (2005). Death receptor signaling. Journal of Cell Science *118*, 265-267.

Lavrik, I.N., Golks, A., Riess, D., Bentele, M., Eils, R., and Krammer, P.H. (2007). Analysis of CD95 Threshold Signaling: triggering of (CD95 (Fas/Apo-1) at low concentrations primarily results in survival signalling. The Journal of Biological Chemistry *282*, 13664-13671.

Lechardeur, D., Drzymala, L., Sharma, M., Zylka, D., Kinach, R., Pacia, J., Hicks, C., Usmani, N., Rommens, J.M., and Lukacs, G.L. (2000). Determinants of the nuclear localization of the heterodimeric DNA fragmentation factor (ICAD/CAD). J Cell Biol *150*, 321-334.

Leong, L.E.-C., Walker, P.A., and G., P.A. (1992). Efficient expression and purification of a protease from the common cold virus, human rhinovirus type 14. Journal of Crystal Growth *122*, 246-252.

Letai, A., Bassik, M.C., Walensky, L.D., Sorcinelli, M.D., Weiler, S., and Korsmeyer, S.J. (2002). Distinct BH3 domains either sensitize or activate mitochondrial apoptosis, serving as prototype cancer therapeutics. Cancer Cell *2*, 183-192.

Levine, B., and Klionsky, D.J. (2004). Development by self-digestion: molecular mechanisms and biological functions of autophagy. Developmental Cell *6*, 463-477.

Levine, B., and Yuan, J. (2005). Autophagy in cell death: an innocent convict? The Journal of Clinical Investigation *115*, 2679-2688.

Li, H., Zhu, H., Xu, C.J., and Yuan, J. (1998a). Cleavage of BID by caspase 8 mediates the mitochondrial damage in the Fas pathway of apoptosis. Cell *94*, 491-501.

Li, J.H., Rosen, D., Ronen, D., Behrens, C.K., Krammer, P.H., Clark, W.R., and Berke, G. (1998b). The regulation of CD95 ligand expression and function in CTL. J Immunol *161*, 3943-3949.

Li, L.Y., Luo, X., and Wang, X. (2001). Endonuclease G is an apoptotic DNase when released from mitochondria. Nature *412*, 95-99.

Li, P., Nijhawan, D., Budihardjo, I., Srinivasula, S.M., Ahmad, M., Alnemri, E.S., and Wang, X. (1997). Cytochrome c and dATP-dependent formation of Apaf-1/caspase-9 complex initiates an apoptotic protease cascade. Cell *91*, 479-489.

Li, X., Wang, J., and Manley, J.L. (2005). Loss of splicing factor ASF/SF2 induces G2 cell cycle arrest and apoptosis, but inhibits internucleosomal DNA fragmentation. Genes & Development *19*, 2705-2714.

Liang, L., Zhao, M., Xu, Z., Yokoyama, K.K., and Li, T. (2003). Molecular cloning and characterization of CIDE-3, a novel member of the cell-death-inducing DNA-fragmentation-factor (DFF45)-like effector family. The Biochemical Journal *370*, 195-203.

Liu, Q.L., Kishi, H., Ohtsuka, K., and Muraguchi, A. (2003). Heat shock protein 70 binds caspase-activated DNase and enhances its activity in TCR-stimulated T cells. Blood *102*, 1788-1796.

Liu, X., Li, P., Widlak, P., Zou, H., Luo, X., Garrard, W.T., and Wang, X. (1998). The 40-kDa subunit of DNA fragmentation factor induces DNA fragmentation and chromatin condensation during apoptosis. Proc Natl Acad Sci U S A *95*, 8461-8466.

Liu, X., Zou, H., Slaughter, C., and Wang, X. (1997). DFF, a heterodimeric protein that functions downstream of caspase-3 to trigger DNA fragmentation during apoptosis. Cell *89*, 175-184.

Liu, X., Zou, H., Widlak, P., Garrard, W., and Wang, X. (1999). Activation of the apoptotic endonuclease DFF40 (caspase-activated DNase or nuclease). Oligomerization and direct interaction with histone H1. The Journal of Biological Chemistry *274*, 13836-13840.

Lorenzo, H.K., and Susin, S.A. (2004). Mitochondrial effectors in caspase-independent cell death. FEBS Letters *557*, 14-20.

Lucken-Ardjomande, S., and Martinou, J.C. (2005). Newcomers in the process of mitochondrial permeabilization. Journal of Cell Science *118*, 473-483.

Lugovskoy, A.A., Zhou, P., Chou, J.J., McCarty, J.S., Li, P., and Wagner, G. (1999). Solution structure of the CIDE-N domain of CIDE-B and a model for CIDE-N/CIDE-N interactions in the DNA fragmentation pathway of apoptosis. Cell *99*, 747-755.

Lui, J.C., and Kong, S.K. (2006). Erythropoietin activates caspase-3 and downregulates CAD during erythroid differentiation in TF-1 cells - a protection mechanism against DNA fragmentation. FEBS Lett *580*, 1965-1970.

Martinet, W., Schrijvers, D.M., and Kockx, M.M. (2003). Nucleofection as an efficient nonviral transfection method for human monocytic cells. Biotechnology Letters *25*, 1025-1029.

Martinon, F., and Tschopp, J. (2004). Inflammatory caspases: linking an intracellular innate immune system to autoinflammatory diseases. Cell *117*, 561-574.

Martins, L.M. (2002). The serine protease Omi/HtrA2: a second mammalian protein with a Reaper-like function. Cell Death and Differentiation *9*, 699-701.

Martins, L.M., Iaccarino, I., Tenev, T., Gschmeissner, S., Totty, N.F., Lemoine, N.R., Savopoulos, J., Gray, C.W., Creasy, C.L., Dingwall, C., *et al.* (2002). The serine protease Omi/HtrA2 regulates apoptosis by binding XIAP through a reaper-like motif. The Journal of Biological Chemistry *277*, 439-444.

Masuoka, J., Shiraishi, T., Ichinose, M., Mineta, T., and Tabuchi, K. (2001). Expression of ICAD-l and ICAD-S in human brain tumor and its cleavage upon activation of apoptosis by anti-Fas antibody. Jpn J Cancer Res *92*, 806-812.

McCarty, J.S., Toh, S.Y., and Li, P. (1999a). Multiple domains of DFF45 bind synergistically to DFF40: roles of caspase cleavage and sequestration of activator domain of DFF40. Biochemical and Biophysical Research Communications *264*, 181-185.

McCarty, J.S., Toh, S.Y., and Li, P. (1999b). Study of DFF45 in its role of chaperone and inhibitor: two independent inhibitory domains of DFF40 nuclease activity. Biochemical and Biophysical Research Communications *264*, 176-180.

McIlroy, D., Sakahira, H., Talanian, R.V., and Nagata, S. (1999). Involvement of caspase 3-activated DNase in internucleosomal DNA cleavage induced by diverse apoptotic stimuli. Oncogene *18*, 4401-4408.

Medema, J.P., Scaffidi, C., Kischkel, F.C., Shevchenko, A., Mann, M., Krammer, P.H., and Peter, M.E. (1997). FLICE is activated by association with the CD95 death-inducing signaling complex (DISC). The EMBO Journal *16*, 2794-2804.

Meylan, E., and Tschopp, J. (2005). The RIP kinases: crucial integrators of cellular stress. Trends in Biochemical Sciences *30*, 151-159.

Mihara, M., Erster, S., Zaika, A., Petrenko, O., Chittenden, T., Pancoska, P., and Moll, U.M. (2003). p53 has a direct apoptogenic role at the mitochondria. Molecular Cell *11*, 577-590.

Milhas, D., Cuvillier, O., Therville, N., Clave, P., Thomsen, M., Levade, T., Benoist, H., and Segui, B. (2005). Caspase-10 triggers Bid cleavage and caspase cascade activation in FasL-induced apoptosis. The Journal of Biological Chemistry *280*, 19836-19842.

Mitamura, S., Ikawa, H., Mizuno, N., Kaziro, Y., and Itoh, H. (1998). Cytosolic nuclease activated by caspase-3 and inhibited by DFF-45. Biochemical and Biophysical Research Communications *243*, 480-484.

Mizuta, R., Mizuta, M., Araki, S., Shiokawa, D., Tanuma, S., and Kitamura, D. (2006). Action of apoptotic endonuclease DNase gamma on naked DNA and chromatin substrates. Biochemical and Biophysical Research Communications *345*, 560-567.

Mondigler, M., and Ehrmann, M. (1996). Site-specific proteolysis of the Escherichia coli SecA protein in vivo. Journal of Bacteriology *178*, 2986-2988.

Muzio, M., Chinnaiyan, A.M., Kischkel, F.C., O'Rourke, K., Shevchenko, A., Ni, J., Scaffidi, C., Bretz, J.D., Zhang, M., Gentz, R., *et al.* (1996). FLICE, a novel FADD-homologous ICE/CED-3-like protease, is recruited to the CD95 (Fas/APO-1) death--inducing signaling complex. Cell *85*, 817-827.

Muzio, M., Stockwell, B.R., Stennicke, H.R., Salvesen, G.S., and Dixit, V.M. (1998). An induced proximity model for caspase-8 activation. The Journal of Biological Chemistry *273*, 2926-2930.

Nagai, K., and Thogersen, H.C. (1984). Generation of beta-globin by sequence-specific proteolysis of a hybrid protein produced in Escherichia coli. Nature *309*, 810-812.

Nagase, H., Fukuyama, H., Tanaka, M., Kawane, K., and Nagata, S. (2003). Mutually regulated expression of caspase-activated DNase and its inhibitor for apoptotic DNA fragmentation. Cell Death and Differentiation *10*, 142-143.

Nagata, S. (1997). Apoptosis by death factor. Cell *88*, 355-365.

Nagata, S. (2000). Apoptotic DNA fragmentation. Exp Cell Res *256*, 12-18.

Nagata, S., Nagase, H., Kawane, K., Mukae, N., and Fukuyama, H. (2003). Degradation of chromosomal DNA during apoptosis. Cell Death and Differentiation *10*, 108-116.

Nicholson, D.W., and Thornberry, N.A. (1997). Caspases: killer proteases. Trends in Biochemical Sciences *22*, 299-306.

Ohtsuka, T., Ryu, H., Minamishima, Y.A., Macip, S., Sagara, J., Nakayama, K.I., Aaronson, S.A., and Lee, S.W. (2004). ASC is a Bax adaptor and regulates the p53-Bax mitochondrial apoptosis pathway. Nature Cell Biology *6*, 121-128.

Okada, H., Suh, W.K., Jin, J., Woo, M., Du, C., Elia, A., Duncan, G.S., Wakeham, A., Itie, A., Lowe, S.W., *et al.* (2002). Generation and characterization of Smac/DIABLO-deficient mice. Mol Cell Biol *22*, 3509-3517.

Oliveri, M., Daga, A., Cantoni, C., Lunardi, C., Millo, R., and Puccetti, A. (2001). DNase I mediates internucleosomal DNA degradation in human cells undergoing drug-induced apoptosis. Eur J Immunol *31*, 743-751.

Otera, H., Ohsakaya, S., Nagaura, Z., Ishihara, N., and Mihara, K. (2005). Export of mitochondrial AIF in response to proapoptotic stimuli depends on processing at the intermembrane space. The EMBO Journal *24*, 1375-1386.

Otomo, T., Sakahira, H., Uegaki, K., Nagata, S., and Yamazaki, T. (2000). Structure of the heterodimeric complex between CAD domains of CAD and ICAD. Nature Structural Biology *7*, 658-662.

Park, C., Sakamaki, K., Tachibana, O., Yamashima, T., Yamashita, J., and Yonehara, S. (1998). Expression of fas antigen in the normal mouse brain. Biochemical and Biophysical Research Communications *252*, 623-628.

Parks, T.D., Leuther, K.K., Howard, E.D., Johnston, S.A., and Dougherty, W.G. (1994). Release of proteins and peptides from fusion proteins using a recombinant plant virus proteinase. Analytical Biochemistry *216*, 413-417.

Parrish, J., Li, L., Klotz, K., Ledwich, D., Wang, X., and Xue, D. (2001). Mitochondrial endonuclease G is important for apoptosis in C. elegans. Nature *412*, 90-94.

Pistritto, G., Jost, M., Srinivasula, S.M., Baffa, R., Poyet, J.L., Kari, C., Lazebnik, Y., Rodeck, U., and Alnemri, E.S. (2002). Expression and transcriptional regulation of caspase-14 in simple and complex epithelia. Cell Death and Differentiation *9*, 995-1006.

Ravagnan, L., Gurbuxani, S., Susin, S.A., Maisse, C., Daugas, E., Zamzami, N., Mak, T., Jaattela, M., Penninger, J.M., Garrido, C., *et al.* (2001). Heat-shock protein 70 antagonizes apoptosis-inducing factor. Nature Cell Biology *3*, 839-843.

Rich, T., Allen, R.L., and Wyllie, A.H. (2000). Defying death after DNA damage. Nature *407*, 777-783.

Rusten, T.E., Lindmo, K., Juhasz, G., Sass, M., Seglen, P.O., Brech, A., and Stenmark, H. (2004). Programmed autophagy in the Drosophila fat body is induced by ecdysone through regulation of the PI3K pathway. Developmental Cell *7*, 179-192.

Saelens, X., Festjens, N., Vande Walle, L., van Gurp, M., van Loo, G., and Vandenabeele, P. (2004). Toxic proteins released from mitochondria in cell death. Oncogene *23*, 2861-2874.

Sahara, S., Aoto, M., Eguchi, Y., Imamoto, N., Yoneda, Y., and Tsujimoto, Y. (1999). Acinus is a caspase-3-activated protein required for apoptotic chromatin condensation. Nature *401*, 168-173.

Sakahira, H., Enari, M., and Nagata, S. (1998). Cleavage of CAD inhibitor in CAD activation and DNA degradation during apoptosis. Nature *391*, 96-99.

Sakahira, H., Enari, M., and Nagata, S. (1999). Functional differences of two forms of the inhibitor of caspase-activated DNase, ICAD-L, and ICAD-S. The Journal of Biological Chemistry *274*, 15740-15744.

Sakahira, H., Iwamatsu, A., and Nagata, S. (2000). Specific chaperone-like activity of inhibitor of caspase-activated DNase for caspase-activated DNase. The Journal of Biological Chemistry *275*, 8091-8096.

Sakahira, H., and Nagata, S. (2002). Co-translational folding of caspase-activated DNase with Hsp70, Hsp40, and inhibitor of caspase-activated DNase. The Journal of Biological Chemistry *277*, 3364-3370.

Sakahira, H., Takemura, Y., and Nagata, S. (2001). Enzymatic active site of caspase-activated DNase (CAD) and its inhibition by inhibitor of CAD. Arch Biochem Biophys *388*, 91-99.

Salvesen, G.S., and Dixit, V.M. (1999). Caspase activation: the induced-proximity model. Proc Natl Acad Sci U S A *96*, 10964-10967.

Sambrook, J.J., and, and Russell, D.W.D.W. (2001). Molecular cloning: a laboratory manual. (Cold Spring Harbor, N.Y., Cold Spring Harbor Laboratory Press).

Samejima, K., and Earnshaw, W.C. (1998). ICAD/DFF regulator of apoptotic nuclease is nuclear. Exp Cell Res *243*, 453-459.

Samejima, K., and Earnshaw, W.C. (2000). Differential localization of ICAD-L and ICAD-S in cells due to removal of a C-terminal NLS from ICAD-L by alternative splicing. Exp Cell Res *255*, 314-320.

Samejima, K., Tone, S., and Earnshaw, W.C. (2001). CAD/DFF40 nuclease is dispensable for high molecular weight DNA cleavage and stage I chromatin condensation in apoptosis. The Journal of Biological Chemistry *276*, 45427-45432.

Savkur, R.S., and Olson, M.O. (1998). Preferential cleavage in pre-ribosomal RNA byprotein B23 endoribonuclease. Nucleic Acids Research *26*, 4508-4515.

Scaffidi, C., Fulda, S., Srinivasan, A., Friesen, C., Li, F., Tomaselli, K.J., Debatin, K.M., Krammer, P.H., and Peter, M.E. (1998). Two CD95 (APO-1/Fas) signaling pathways. The EMBO Journal *17*, 1675-1687.

Scaffidi, C., Schmitz, I., Zha, J., Korsmeyer, S.J., Krammer, P.H., and Peter, M.E. (1999). Differential modulation of apoptosis sensitivity in CD95 type I and type II cells. The Journal of Biological Chemistry *274*, 22532-22538.

Scholz, S.R., Korn, C., Gimadutdinow, O., Knoblauch, M., Pingoud, A., and Meiss, G. (2002). The effect of ICAD-S on the formation and intracellular distribution of a nucleolytically active caspase-activated DNase. Nucleic Acids Research *30*, 3045-3051.

Schroter, H., and Bode, J. (1982). The binding sites for large and small high-mobility-group (HMG) proteins. Studies on HMG-nucleosome interactions in vitro. European Journal of Biochemistry / FEBS *127*, 429-436.

Schuler, M., and Green, D.R. (2001). Mechanisms of p53-dependent apoptosis. Biochem Soc Trans *29*, 684-688.

Scorrano, L., Ashiya, M., Buttle, K., Weiler, S., Oakes, S.A., Mannella, C.A., and Korsmeyer, S.J. (2002). A distinct pathway remodels mitochondrial cristae and mobilizes cytochrome c during apoptosis. Developmental Cell *2*, 55-67.

Scorrano, L., Oakes, S.A., Opferman, J.T., Cheng, E.H., Sorcinelli, M.D., Pozzan, T., and Korsmeyer, S.J. (2003). BAX and BAK regulation of endoplasmic reticulum Ca2+: a control point for apoptosis. Science (New York, NY *300*, 135-139.

Seidah, N.G., and Chretien, M. (1997). Eukaryotic protein processing: endoproteolysis of precursor proteins. Current Opinion in Biotechnology *8*, 602-607.

Seth, R., Yang, C., Kaushal, V., Shah, S.V., and Kaushal, G.P. (2005). p53-dependent caspase-2 activation in mitochondrial release of apoptosis-inducing factor and its role in renal tubular epithelial cell injury. The Journal of Biological Chemistry *280*, 31230-31239.

Sharif-Askari, E., Alam, A., Rheaume, E., Beresford, P.J., Scotto, C., Sharma, K., Lee, D., DeWolf, W.E., Nuttall, M.E., Lieberman, J., *et al.* (2001). Direct cleavage of the human DNA fragmentation factor-45 by granzyme B induces caspase-activated DNase release and DNA fragmentation. The EMBO Journal *20*, 3101-3113.

Shin, D.H., Lee, E., Kim, H.J., Kim, S., Cho, S.S., Chang, K.Y., and Lee, W.J. (2002). Fas ligand mRNA expression in the mouse central nervous system. Journal of Neuroimmunology *123*, 50-57.

Shiokawa, D., and Tanuma, S. (1998). Molecular cloning and expression of a cDNA encoding an apoptotic endonuclease DNase gamma. The Biochemical Journal *332 (Pt 3)*, 713-720.

Sipo, I., Hurtado Pico, A., Wang, X., Eberle, J., Petersen, I., Weger, S., Poller, W., and Fechner, H. (2006). An improved Tet-On regulatable FasL-adenovirus vector system for lung cancer therapy. Journal of Molecular Medicine (Berlin, Germany) *84*, 215-225.

Smith, C.A., Farrah, T., and Goodwin, R.G. (1994). The TNF receptor superfamily of cellular and viral proteins: activation, costimulation, and death. Cell *76*, 959-962.

Smith, T.A., and Kohorn, B.D. (1991). Direct selection for sequences encoding proteases of known specificity. Proc Natl Acad Sci U S A *88*, 5159-5162.

Sprick, M.R., Rieser, E., Stahl, H., Grosse-Wilde, A., Weigand, M.A., and Walczak, H. (2002). Caspase-10 is recruited to and activated at the native TRAIL and CD95 death-inducing signalling complexes in a FADD-dependent manner but can not functionally substitute caspase-8. The EMBO Journal *21*, 4520-4530.

Susin, S.A., Daugas, E., Ravagnan, L., Samejima, K., Zamzami, N., Loeffler, M., Costantini, P., Ferri, K.F., Irinopoulou, T., Prevost, M.C., *et al.* (2000). Two distinct pathways leading to nuclear apoptosis. The Journal of Experimental Medicine *192*, 571-580.

Susin, S.A., Lorenzo, H.K., Zamzami, N., Marzo, I., Snow, B.E., Brothers, G.M., Mangion, J., Jacotot, E., Costantini, P., Loeffler, M., *et al.* (1999). Molecular characterization of mitochondrial apoptosis-inducing factor. Nature *397*, 441-446.

Susin, S.A., Zamzami, N., Castedo, M., Hirsch, T., Marchetti, P., Macho, A., Daugas, E., Geuskens, M., and Kroemer, G. (1996). Bcl-2 inhibits the mitochondrial release of an apoptogenic protease. The Journal of Experimental Medicine *184*, 1331-1341.

Suzuki, Y., Imai, Y., Nakayama, H., Takahashi, K., Takio, K., and Takahashi, R. (2001). A serine protease, HtrA2, is released from the mitochondria and interacts with XIAP, inducing cell death. Molecular Cell *8*, 613-621.

Szalai, G., Krishnamurthy, R., and Hajnoczky, G. (1999). Apoptosis driven by IP(3)-linked mitochondrial calcium signals. The EMBO Journal *18*, 6349-6361.

Szebeni, A., Herrera, J.E., and Olson, M.O. (1995). Interaction of nucleolar protein B23 with peptides related to nuclear localization signals. Biochemistry *34*, 8037-8042.

Szebeni, A., and Olson, M.O. (1999). Nucleolar protein B23 has molecular chaperone activities. Protein Sci *8*, 905-912.

Tartaglia, L.A., Ayres, T.M., Wong, G.H., and Goeddel, D.V. (1993). A novel domain within the 55 kd TNF receptor signals cell death. Cell *74*, 845-853.
Tartaglia, L.A., and Goeddel, D.V. (1992). Two TNF receptors. Immunology today *13*, 151-153.
Terpe, K. (2003). Overview of tag protein fusions: from molecular and biochemical fundamentals to commercial systems. Applied Microbiology and Biotechnology *60*, 523-533.

Thomas, D.A., Du, C., Xu, M., Wang, X., and Ley, T.J. (2000). DFF45/ICAD can be directly processed by granzyme B during the induction of apoptosis. Immunity *12*, 621-632.

Thomas, D.A., Scorrano, L., Putcha, G.V., Korsmeyer, S.J., and Ley, T.J. (2001). Granzyme B can cause mitochondrial depolarization and cell death in the absence of BID, BAX, and BAK. Proc Natl Acad Sci U S A *98*, 14985-14990.

Thome, M., Schneider, P., Hofmann, K., Fickenscher, H., Meinl, E., Neipel, F., Mattmann, C., Burns, K., Bodmer, J.L., Schroter, M., *et al.* (1997). Viral FLICE-inhibitory proteins (FLIPs) prevent apoptosis induced by death receptors. Nature *386*, 517-521.

Thompson, C.B. (1995). Apoptosis in the pathogenesis and treatment of disease. Science (New York, NY *267*, 1456-1462.

Thornberry, N.A., and Lazebnik, Y. (1998). Caspases: enemies within. Science (New York, NY *281*, 1312-1316.

Ting, A.T., Pimentel-Muinos, F.X., and Seed, B. (1996). RIP mediates tumor necrosis factor receptor 1 activation of NF-kappaB but not Fas/APO-1-initiated apoptosis. The EMBO Journal *15*, 6189-6196.

Toh, S.Y., Wang, X., and Li, P. (1998). Identification of the nuclear factor HMG2 as an activator for DFF nuclease activity. Biochemical and Biophysical Research Communications *250*, 598-601.

Tschopp, J., Irmler, M., and Thome, M. (1998). Inhibition of fas death signals by FLIPs. Current Opinion in Immunology *10*, 552-558.

Tsukada, M., and Ohsumi, Y. (1993). Isolation and characterization of autophagy-defective mutants of Saccharomyces cerevisiae. FEBS Letters *333*, 169-174.

Tu, S., McStay, G.P., Boucher, L.M., Mak, T., Beere, H.M., and Green, D.R. (2006). In situ trapping of activated initiator caspases reveals a role for caspase-2 in heat shock-induced apoptosis. Nature Cell Biology *8*, 72-77.

Turjanski, A.G., Vaque, J.P., and Gutkind, J.S. (2007). MAP kinases and the control of nuclear events. Oncogene *26*, 3240-3253.

Uegaki, K., Otomo, T., Sakahira, H., Shimizu, M., Yumoto, N., Kyogoku, Y., Nagata, S., and Yamazaki, T. (2000). Structure of the CAD domain of caspase-activated DNase and interaction with the CAD domain of its inhibitor. J Mol Biol *297*, 1121-1128.

Uhlmann, F., Wernic, D., Poupart, M.A., Koonin, E.V., and Nasmyth, K. (2000). Cleavage of cohesin by the CD clan protease separin triggers anaphase in yeast. Cell *103*, 375-386.

Vahsen, N., Cande, C., Dupaigne, P., Giordanetto, F., Kroemer, R.T., Herker, E., Scholz, S., Modjtahedi, N., Madeo, F., Le Cam, E., *et al.* (2006). Physical interaction of apoptosis-inducing factor with DNA and RNA. Oncogene *25*, 1763-1774.

Vaux, D.L., and Korsmeyer, S.J. (1999). Cell death in development. Cell *96*, 245-254.

Verhagen, A.M., Ekert, P.G., Pakusch, M., Silke, J., Connolly, L.M., Reid, G.E., Moritz, R.L., Simpson, R.J., and Vaux, D.L. (2000). Identification of DIABLO, a mammalian protein that promotes apoptosis by binding to and antagonizing IAP proteins. Cell *102*, 43-53.

Verrou, C., Zhang, Y., Zurn, C., Schamel, W.W., and Reth, M. (1999). Comparison of the tamoxifen regulated chimeric Cre recombinases MerCreMer and CreMer. Biological Chemistry *380*, 1435-1438.

Walker, P.A., Leong, L.E.-C., Ng, P.W.P., Tan, S.H., Waller, S., Murphy, D., and Porter, A.G. (1994). Efficient and rapid affinity purification of proteins using recombinant fusion proteases. Bio/technology *12*, 601-605.

Wang, J., Chun, H.J., Wong, W., Spencer, D.M., and Lenardo, M.J. (2001). Caspase-10 is an initiator caspase in death receptor signaling. Proc Natl Acad Sci U S A *98*, 13884-13888.

Wang, K., Yin, X.M., Chao, D.T., Milliman, C.L., and Korsmeyer, S.J. (1996). BID: a novel BH3 domain-only death agonist. Genes & Development *10*, 2859-2869.

Wei, M.C., Zong, W.X., Cheng, E.H., Lindsten, T., Panoutsakopoulou, V., Ross, A.J., Roth, K.A., MacGregor, G.R., Thompson, C.B., and Korsmeyer, S.J. (2001). Proapoptotic BAX and BAK: a requisite gateway to mitochondrial dysfunction and death. Science (New York, NY *292*, 727-730.

Widlak, P., Li, P., Wang, X., and Garrard, W.T. (2000). Cleavage preferences of the apoptotic endonuclease DFF40 (caspase-activated DNase or nuclease) on naked DNA and chromatin substrates. The Journal of Biological Chemistry *275*, 8226-8232.

Wilson, K.P., Black, J.A., Thomson, J.A., Kim, E.E., Griffith, J.P., Navia, M.A., Murcko, M.A., Chambers, S.P., Aldape, R.A., Raybuck, S.A., *et al.* (1994). Structure and mechanism of interleukin-1 beta converting enzyme. Nature *370*, 270-275.

Winding, P., and Berchtold, M.W. (2001). The chicken B cell line DT40: a novel tool for gene disruption experiments. Journal of Immunological Methods *249*, 1-16.

Wolf, B.B., Schuler, M., Echeverri, F., and Green, D.R. (1999). Caspase-3 is the primary activator of apoptotic DNA fragmentation via DNA fragmentation factor-45/inhibitor of caspase-activated DNase inactivation. The Journal of Biological Chemistry *274*, 30651-30656.

Wolter, K.G., Hsu, Y.T., Smith, C.L., Nechushtan, A., Xi, X.G., and Youle, R.J. (1997). Movement of Bax from the cytosol to mitochondria during apoptosis. J Cell Biol *139*, 1281-1292.

Woo, E.J., Kim, Y.G., Kim, M.S., Han, W.D., Shin, S., Robinson, H., Park, S.Y., and Oh, B.H. (2004). Structural mechanism for inactivation and activation of CAD/DFF40 in the apoptotic pathway. Molecular Cell *14*, 531-539.

Woo, M., Hakem, R., Soengas, M.S., Duncan, G.S., Shahinian, A., Kagi, D., Hakem, A., McCurrach, M., Khoo, W., Kaufman, S.A., *et al.* (1998). Essential contribution of caspase 3/CPP32 to apoptosis and its associated nuclear changes. Genes & Development *12*, 806-819.

Wood, E.R., and Earnshaw, W.C. (1990). Mitotic chromatin condensation in vitro using somatic cell extracts and nuclei with variable levels of endogenous topoisomerase II. J Cell Biol *111*, 2839-2850.

Wu, Y., Mehew, J.W., Heckman, C.A., Arcinas, M., and Boxer, L.M. (2001). Negative regulation of bcl-2 expression by p53 in hematopoietic cells. Oncogene *20*, 240-251.

Wyllie, A. (1998). Apoptosis. An endonuclease at last. Nature *391*, 20-21.

Wyllie, A.H. (1980). Glucocorticoid-induced thymocyte apoptosis is associated with endogenous endonuclease activation. Nature *284*, 555-556.

Wyllie, A.H., Kerr, J.F., and Currie, A.R. (1980). Cell death: the significance of apoptosis. Int Rev Cytol *68*, 251-306.

Yang, J., Liu, X., Bhalla, K., Kim, C.N., Ibrado, A.M., Cai, J., Peng, T.I., Jones, D.P., and Wang, X. (1997). Prevention of apoptosis by Bcl-2: release of cytochrome c from mitochondria blocked. Science (New York, NY *275*, 1129-1132.

Yang, X., Gregan, J., Lindner, K., Young, H., and Kearsey, S.E. (2005). Nuclear distribution and chromatin association of DNA polymerase alpha-primase is affected by TEV protease cleavage of Cdc23 (Mcm10) in fission yeast. BMC Molecular Biology *6*, 13.

Ye, H., Cande, C., Stephanou, N.C., Jiang, S., Gurbuxani, S., Larochette, N., Daugas, E., Garrido, C., Kroemer, G., and Wu, H. (2002). DNA binding is required for the apoptogenic action of apoptosis inducing factor. Nature Structural Biology *9*, 680-684.

Yi, X., Yin, X.M., and Dong, Z. (2003). Inhibition of Bid-induced apoptosis by Bcl-2. tBid insertion, Bax translocation, and Bax/Bak oligomerization suppressed. The Journal of Biological Chemistry *278*, 16992-16999.

Yu, S.W., Wang, H., Dawson, T.M., and Dawson, V.L. (2003). Poly(ADP-ribose) polymerase-1 and apoptosis inducing factor in neurotoxicity. Neurobiology of Disease *14*, 303-317.

Yu, S.W., Wang, H., Poitras, M.F., Coombs, C., Bowers, W.J., Federoff, H.J., Poirier, G.G., Dawson, T.M., and Dawson, V.L. (2002). Mediation of poly(ADP-ribose) polymerase-1-dependent cell death by apoptosis-inducing factor. Science (New York, NY *297*, 259-263.

Yuan, J., Shaham, S., Ledoux, S., Ellis, H.M., and Horvitz, H.R. (1993). The C. elegans cell death gene ced-3 encodes a protein similar to mammalian interleukin-1 beta-converting enzyme. Cell *75*, 641-652.

Yuste, V.J., Bayascas, J.R., Llecha, N., Sanchez-Lopez, I., Boix, J., and Comella, J.X. (2001). The absence of oligonucleosomal DNA fragmentation during apoptosis of IMR-5 neuroblastoma cells: disappearance of the caspase-activated DNase. The Journal of Biological Chemistry *276*, 22323-22331.

Yuste, V.J., Sanchez-Lopez, I., Sole, C., Moubarak, R.S., Bayascas, J.R., Dolcet, X., Encinas, M., Susin, S.A., and Comella, J.X. (2005). The contribution of apoptosis-inducing factor, caspase-activated DNase, and inhibitor of caspase-activated DNase to the nuclear phenotype and DNA degradation during apoptosis. The Journal of Biological Chemistry *280*, 35670-35683.

Zamzami, N., and Kroemer, G. (2003). Apoptosis: mitochondrial membrane permeabilization--the (w)hole story? Curr Biol *13*, R71-73.

Zeuner, A., Eramo, A., Peschle, C., and De Maria, R. (1999). Caspase activation without death. Cell Death and Differentiation *6*, 1075-1080.

Zhang, J., Dong, M., Li, L., Fan, Y., Pathre, P., Dong, J., Lou, D., Wells, J.M., Olivares-Villagomez, D., Van Kaer, L., *et al.* (2003a). Endonuclease G is required for early embryogenesis and normal apoptosis in mice. Proc Natl Acad Sci U S A *100*, 15782-15787.

Zhang, J., Lee, H., Lou, D.W., Bovin, G.P., and Xu, M. (2000). Lack of obvious 50 kilobase pair DNA fragments in DNA fragmentation factor 45-deficient thymocytes upon activation of apoptosis. Biochemical and Biophysical Research Communications *274*, 225-229.

Zhang, J., Liu, X., Scherer, D.C., van Kaer, L., Wang, X., and Xu, M. (1998). Resistance to DNA fragmentation and chromatin condensation in mice lacking the DNA fragmentation factor 45. Proc Natl Acad Sci U S A *95*, 12480-12485.

Zhang, J., Wang, X., Bove, K.E., and Xu, M. (1999). DNA fragmentation factor 45-deficient cells are more resistant to apoptosis and exhibit different dying morphology than wild-type control cells. The Journal of Biological Chemistry *274*, 37450-37454.

Zhang, J.H., Zhang, Y., and Herman, B. (2003b). Caspases, apoptosis and aging. Ageing Research Reviews *2*, 357-366.

Zhou, P., Lugovskoy, A.A., McCarty, J.S., Li, P., and Wagner, G. (2001). Solution structure of DFF40 and DFF45 N-terminal domain complex and mutual chaperone activity of DFF40 and DFF45. Proc Natl Acad Sci U S A *98*, 6051-6055.

Ziegler, U., and Groscurth, P. (2004). Morphological features of cell death. News Physiol Sci *19*, 124-128.

Zou, H., Henzel, W.J., Liu, X., Lutschg, A., and Wang, X. (1997). Apaf-1, a human protein homologous to C. elegans CED-4, participates in cytochrome c-dependent activation of caspase-3. Cell *90*, 405-413.

Zuliani, C., Kleber, S., Klussmann, S., Wenger, T., Kenzelmann, M., Schreglmann, N., Martinez, A., del Rio, J.A., Soriano, E., Vodrazka, P., *et al.* (2006). Control of neuronal branching by the death receptor CD95 (Fas/Apo-1). Cell Death and Differentiation *13*, 31-40.